A CONSTRUCTION OF H-REFLEX DETECTABLE INSTRUMENT AND THE RECORDING PROGRAM

JIRATN TANG-A-PHAN

A THESIS SUBMITTED IN PARTIAL FULFILLMENT
OF THE REQUIREMENTS FOR
THE DEGREE OF MASTER OF ENGINEERING
(BIOMEDICAL ENGINEERING)
FACULTY OF GRADUATE STUDIES
MAHIDOL UNIVERSITY
2004

ISBN 974-04-5521-2

Thesis
Entitled

A CONSTRUCTION OF H-REFLEX DETECTABLE INSTRUMENT AND THE RECORDING PROGRAM

Jiratn Tang-a-phan

Mr. Jiratn Tang-a-phan
Candidate

Assist. Prof. Warakorn Charoensuk,
Ph.D. (Electrical Engineering)
Major-advisor

Monthaporn Suteerawattananon

Assist. Prof. Monthaporn
Suteerawattananon,
Ph.D. (Physical Therapy)
Co-advisor

Decha Wilairat

Assist. Prof. Decha Wilairat,
M.Sc. (Electrical Engineering)
Co-advisor

Rassmidara Hoonsawat

Assoc.Prof.Rassmidara Hoonsawat,
Ph.D.
Dean
Faculty of Graduate Studies

Theeraporn Rubcumintara

Assist. Prof. Theeraporn Rubcumintara,
Ph.D. (Materials Engineering & Science)
Chair
Master of Engineering
Biomedical Engineering Program
Faculty of Engineering

Thesis
Entitled

A CONSTRUCTION OF H-REFLEX DETECTABLE INSTRUMENT AND THE RECORDING PROGRAM

was submitted to the Faculty of Graduate Studies, Mahidol University
for the Degree of Master of Engineering (Biomedical Engineering)
on
December 23, 2004

Jiratn Tang-a-phan
.....
Mr. Jiratn Tang-A-Phan
Candidate

.....
Assist. Prof. Warakorn Charoensuk,
Ph.D. (Electrical Engineering)
Chair

Kamontip Harnphadungkit
.....
Assoc. Prof. Kamontip Harnphadungkit,
M.D. Grad Dip Clin Sc (Rehab Med),
Dip Thai Brd Rehab Med.
Member

Monthaporn Suteerawattananon
.....
Assist. Prof. Monthaporn
Suteerawattananon,
Ph.D. (Physical Therapy)
Member

.....
Assist. Prof. Udom Thipayamontri,
Ph.D. (Physiology)
Member

Decha Wilairat
.....
Assist. Prof. Decha Wilairat,
M.Sc. (Electrical Engineering)
Member

.....
Assoc.Prof.Rassmidara Hoonsawat,
Ph.D.
Dean
Faculty of Graduate Studies
Mahidol University

.....
Assist. Prof. Piya Rattanasuwan,
M.Eng.
Dean
Faculty of Engineering
Mahidol University

ACKNOWLEDGEMENTS

The success of this thesis can be attributed to the extensive support and assistance from my major advisor, Assist. Prof. Warakorn Charoensuk and my co-advisor, Assist. Prof. Monthaporn Suteerawattananon and Assist. Prof. Decha Wilairat. I deeply thank them for their warm attention, expect guidance, valuable advice, English correction this thesis and supervision throughout. They were never lacking in kindness and support.

I am especially grateful to Assist. Prof. Wattana Jalayondeja and my co-advisor, Assist. Prof. Monthaporn Suteerawattananon, for their allowance to conduct the research in the Department of Orthopedic Surgery and Physical Therapy and their kindness in examining the research instrument, helpful guidance and support in testing my constructed device, and also providing suggestions for improvement.

I gratefully thank to Assoc. Prof. Kamontip Harnphadungkit, Department of Rehabilitation Medicine, for her kindness in examining the research instrument and providing suggestions for improvement, and for being the external examiner of the thesis defense.

I would like to thank Mr. Surachai Ngamrattanapaiboon and Mr. Pracha Yambangyang for their excellent assistance in collecting and printing data.

Special thanks are extended to all subjects who participation made this study possible. It is my pleasure to thank my family members, all of my friends, which I can not express all of them here but everyone is also in my mind, for their love, helpful and everything they have done for me.

Finally, I am grateful to my family for their financial support, entire care, and love. The usefulness of this thesis, I dedicate to my father, my mother and all the teachers who have taught me since my childhood.

Jiratn Tang-A-Phan

A CONSTUCTION OF H-REFLEX DETECTABLE INSTRUMENT AND THE RECORDING PROGRAM

JIRATN TANAG-A-PHAN 4337541 EGBE/M

M.Eng. (BIOMEDICAL ENGINEERING

THESIS ADVISORS: WARAKORN CHAROENSUK, Ph.D. (ELECTRICAL ENGINEERING), MONTHAPORN SUTEERAWATTANANON, Ph.D. (PHYSICAL THERAPY), DECHA WILAIRAT, M.Sc.

ABSTRACT

The purpose of this research is to design and construct a biomedical instrument, integrating both on electrical stimulator and data acquisition system, at an affordable cost. This instrument will be a basic prototype tool for further development associated with clinical diagnosis forms of reflex action and will serve as a fundamental diagnosis and prognosis instrument for testing/studying excitability of neuromuscular system and help in recovery studies of patients.

A construction of the stimulation, capture, and display device for the Hoffmann reflex (H-reflex) is presented here both practically and theoretically. The H-reflex is an electrical analogue of monosynaptic reflex in the spinal cord, and has applications in assessment of nervous system damage in stroke, spinal cord injury, Parkinson's disease, and other conditions. The system comprises a stimulation unit for evoking the H-reflex and a data acquisition part for acquiring response. This system has been designed and constructed to be an easy approach for eliciting and measuring the H-reflex. A constant-current stimulator for high-impedance loads using low-cost standard high-voltage components has been constructed to evoke the H-reflex response. This stimulator produces amplitude and pulsewidth within $0 \leq I_{skin} \leq 20$ mA and 0.1 ms $\leq T_{pulse} \leq 1.0$ ms, respectively. Pulse-repetition spans from 0.1 Hz to 1 Hz. Both pulsewidth and pulse-repetition are software controlled by LabVIEW program. The devices are incorporated into a computer designed for a reflex data acquisition system. Then, LabVIEW program is used for sending the appropriate commands to control acquirement, display and record of the H-reflex.

KEY WORDS: HOFFMANN REFLEX / H-REFLEX / CONSTANT-CURRENT STIMULATOR / DATA ACQUISITION / LabVIEW

124 P. ISBN 974-04-5521-2

การประดิษฐ์เครื่องมือกระตุ้น H-reflex และโปรแกรมแสดงสัญญาณ (A CONSTRUCTION OF H-REFLEX DETECTABLE INSTRUMENT AND THE RECORDING PROGRAM)

จิรัตน์ ตังอาพรรณ 4337541 EGBE/M

วศ.ม. (วิศวกรรมชีวการแพทย์)

คณะกรรมการควบคุมวิทยานิพนธ์ : วรากร เจริญสุข, Ph.D. (Electrical Engineering), มณฑภรณ์ สุธีรวัฒนานนท์, Ph.D. (Physical Therapy), เดชา วิไลรัตน์, M.Sc.

บทคัดย่อ

วัตถุประสงค์ของวิทยานิพนธ์นี้ เพื่อการออกแบบและสร้างเครื่องมือทางการแพทย์โดยรวมเครื่องมือการกระตุ้นไฟฟ้าและระบบการได้มาของข้อมูลเข้าด้วยกันในราคาที่พอซื้อหาได้ ซึ่งจะเป็นเครื่องมือต้นแบบพื้นฐานหนึ่งสำหรับการพัฒนาเพิ่มขึ้นในการวิเคราะห์รูปแบบต่าง ๆ ของ Reflex และยังเป็นประโยชน์กับการวินิฉัยและการทำนายเบื้องต้นสำหรับการทดสอบและศึกษาความไวต่อการกระตุ้นของระบบกล้ามเนื้อและระบบประสาท และยังช่วยในการศึกษาการฟื้นตัวของผู้ป่วยด้วย

การประดิษฐ์เครื่องมือสำหรับการกระตุ้น การจับสัญญาณ และการแสดงผลสัญญาณของ H-reflex ได้รับการนำเสนอในที่นี้ทั้งในทางทฤษฎีและปฏิบัติ สัญญาณ H-reflex เป็นผลตอบสนองทางไฟฟ้าหนึ่งของการส่งผ่านที่จุดประสานประสาททอดเดียวใน spinal cord สัญญาณนี้มีการประยุกต์ใช้ในการประเมินต่าง ๆ ในโรคทางระบบประสาท เช่น stroke, spinal injury หรือเงื่อนไขอื่น ๆ ที่เกี่ยวข้อง เครื่องมือที่ประดิษฐ์ขึ้นจะประกอบไปด้วยส่วนของการกระตุ้นและส่วนของระบบการได้มาของข้อมูล ทั้งสองส่วนนี้จะได้รับการออกแบบและสร้างเพื่อเป็นแนวทางที่ง่ายสำหรับการดึงและการวัดสัญญาณ H-reflex เครื่องกระตุ้นแบบปล่อยกระแสคงที่สำหรับโหลดที่มีอิมพิแดนซ์สูงด้วยการใช้ส่วนประกอบที่ประหยัดและมีมาตรฐานทั่วไปที่ทนแรงดันได้สูงได้รับการประดิษฐ์ขึ้นเพื่อปลุกสัญญาณ H-reflex ออกมา เครื่องกระตุ้นนี้จะปล่อยความเข้มกระแสในช่วง 0 ถึง 20 มิลลิแอมแปร์ และช่วงให้กระแสในช่วง 0.1 ถึง 1.0 มิลลิวินาที ความถี่ที่ใช้ในการกระตุ้นจะอยู่ในช่วง 0.1 ถึง 1.0 เฮิร์ตซ ทั้งนี้ช่วงที่ให้กระแสและความถี่จะถูกควบคุมผ่านทางซอฟแวร์ อุปกรณ์ต่าง ๆ จะถูกเชื่อมต่อกับคอมพิวเตอร์สำหรับการประมวลผลทางดิจิตอล หลังจากนั้นโปรแกรมจะถูกใช้สำหรับการส่งคำสั่งที่เหมาะสมไปควบคุมการได้รับ การแสดง และการบันทึกข้อมูลของสัญญาณ H-reflex

124 P. ISBN 974-04-5521-2

CONTENTS

CONTENTS (Continued)

LIST OF TABLES

LIST OF TABLES (Continued)

LIST OF FIGURES

LIST OF FIGURES (Continued)

LIST OF FIGURES (Continued)

LIST OF ABBREVIATIONS

1D	one-dimension
2D	two-dimension
A	Ampere
AAMI	Association for the Advancement of Medical Instrument
AC or a.c.	Alternating Current
Ac	Common mode of gain amplifier
ACH	Analog input channel
Ad	Differential mode of gain amplifier
A/D	Analogue to Digital
ADC	Analogue to Digital Converter
A/h or A/hr	Ampere per hour
B	the number of bits of the ADC
BF	Body Floating (IEC BF; < 100 μA, but ≤ 500 μA)
BIFET	Bipolar Field Effect Transistor
bit	binary digital equal to 0 or 1
BV	Breakdown Voltage
C	Capacitor
Ch	Channel
CMAPs	Compound Muscle Action Potentials
CMR	Common Mode Rejection
CMRR	Common Mode Rejection ratio
CNS	Central Nervous System
D	Diode
DAQ	Data Acquisition
dB	decibel
DC or d.c.	Direct Current
DIP	Dual-in-line Package
DMM	Digital Multimeter

LIST OF ABBREVIATIONS (Continued)

DVM	Digital Voltmeter
EEG	Electroencephalography
EMG	Electromyography
ENS	Electronic Neurostimulator
F	Farad
FNS	Functional Neuromuscular Stimulation
G	giga (10^9)
G program	Graphical programming language
GND	Ground
H-reflex	Hoffmann reflex
Hum	50 or 60 Hz noise
Hz	Hertz (frequency per second or cycle per second)
I	Current (amplitude unit)
IC	Integrated Circuit
IEC	International Electrical Commission, 1978
I/O	Input
ISA	Industry Standard Architecture
JFET	Junction Field Effect Transistor
k	kilo (10^3)
L_5	Lumbar root compression
La	Lead-acid
LabVIEW	Laboratory Virtual Instrument Engineering Workbench
Log or log	Logarithm
M	Mega (10^{-6})
m	milli (10^{-3}) or meters
MIO	Multifunction I/O
MOS	Metal-Oxide Semiconductor
MOSFET	Metal-Oxide Semiconductor Field Effect Transistor
M-wave	Motor direct response
n	nano (10^{-9})

LIST OF ABBREVIATIONS (Continued)

NI	National Instrument
Op-amp	Operational amplifier
O/P	Output
p	pico (10^{-12})
p-p	peak-to-peak
PWM	Pulse Width Modulation
R	Resistor
ref	reference
rms	root mean square
S	Sample
s	second
S_1	Sacral root compression
SD	Standard Deviation
subVI	subvirtual instrument
S/N	Signal-to-noise
T	Transformer
TTL	Transistor-transistor Logic
UMN	Upper Motor Neuron
V	Voltage or volts (amplitude unit)
Vi	Input Voltage
VIs	Virtual Instruments
V/I	Voltage to current converter
Vo	Output Voltage
VR	regulated voltage output
W	Watts
Z	Impedance
Zin	Input impedance

CHAPTER I
INTRODUCTION

1.1 Background

The electrophysical studies of reflexes for clinical uses in human body are increasing continuously now, because of these reflexes can point to physiological and pathophysiological states of a peripheral nerve and muscle system along with the studies of motor neuron excitability and electrodiagnosis pathways. The Hoffmann reflex, also called H-reflex, is an artificial elicited reflex response that is provided as an important clinical tool for testing the excitability of the neuromuscular system (1), and may also help in electrodiagnosis pathways. It is a biofeedback response of monosynaptic connection from Ia sensory fibers to spinal motor neurons in spinal cord concerned with nerve and sensory connection mechanism within the human nervous system. Its characteristics are frequently exploited for fundamental diagnosis and prognosis in medical conditions or neurological disorders such as root compression syndrome, neuropathy, upper motor neuron lesions, and related conditions (8).

The H-reflex measurement is elicited by applying a single electrical stimulus with any appropriate parameters into a peripheral nerve. The most commonly stimulated nerve is muscle spindle of sensory nerve fibers. Then, the recording electrode is placed to capture a reflex response from spinal cord traveling through motor nerve fiber. It can be brought to monitor for computer system. The result of reflex response known as the H-reflex will play an important role of excitability of neuromuscular mechanism and pathway of nerve fibers. These roles are clinically diagnosed and prognosticated to differentiate between normal and abnormal. The acquired H-reflex relies on the selective of the Group Ia afferent, which has an ending that spirals around the equatorial regions of both the nuclear chain and bag fibers, with electrical stimulating the Ia fibers in a peripheral nerve and recording this reflex in the homonymous muscle that can be measured in several parts of the body. Examples of these parts are gastrocnemius and soleus muscle, quadriceps femoris, tibialis anterior,

and muscle of the hand, foot, and forearm. In newborn infants and during the first year of life, H-reflex is elicited by stimulation of most nerves in the limb including ulnar nerve (2). In adults, H-reflex can be evoked only in the triceps surae muscle (the calf muscle) and flexor carpiradialis at rest. On the processes of this research, the H-reflex is examined in the popliteal fossa for stimulus and the soleus muscle for capture. It is believe that the H-reflex has been applied in many clinical situations. Therefore, it should be under investigation here. A novel approach of these studies is to design and construct suitable device for detection of H-reflex response.

The H-reflex detectable instrument is provided into two main modules including electronic neurostimulator (ENS), and data acquisition (DAQ) module. The design and construction of these modules are properly made following the features of response for convenience and efficiency in uses. In part of ENS module, it is emphasized in the characteristics of stimulating the sensory nerve fiber to evoke the biofeedback response from spinal cord with electrical stimulus parameters appropriately. These parameters include the frequency, duration time, and intensity of stimuli. The response is captured by the part of DAQ module that should be shown the correct waveform of H-reflex on the computer system for beginning clinical identification. In this module, the software is exploited to aim in signal analysis and to illustrate necessary parameters for clinical analysis.

1.2 Rationale and requirement

- Nowadays, a large number of people have problems about neuromuscular disorders and central nervous system (CNS) pool such as Spasticity, Parkinson's disease, and spinal cord injuries. These problems have tendency to increase in the future. The patients need to recover and rehabilitate the impaired neuromuscular system. The H-reflex is a measure of the level of excitability of the neuromuscular mechanism. Therefore, the H-reflex detectable instrument is designed and constructed to serve as fundamental diagnosis and prognostic of this mechanism in rehabilitation studies for the patients.

- The useable equipment to probe H response for hospitals in Thailand is still so much required and is also not widely used, because of the H-reflex studies lack for research in clinical suitable use. Most physical therapists and electromyographer in

these hospitals used electromyography (EMG) to measure quantities of the peripheral nerve and muscle pathologies that have complication and difficulty to diagnose patterns of EMG signals. Also, mostly used EMG is only the study of activities of muscle that is difficult for the study of reflex in man. Consequently, the design and construction of H-reflex detectable instrument is need in this research for clinical use which add efficiency to these patterns in analysis about behavior of muscle and nerve system and increased requirement in use of physical therapists, electromyographer and also patients.

- A recent device for H-reflex is mostly available in type of constant-voltage stimulator. This stimulator does not assure a current intensity as the delivered current changes with the characteristic of the electrode/skin load, which affect to elicit the H-reflex response. The constant-current stimulator is performed since the charge transferred per stimulus is constant.

- This research is also an approach to decrease a cost of medical equipments imported from foreign countries that can supply the need in the country.

- This research is also a basic prototype tool for developments to concern with novel diagnostic forms of spinal reflex of neuron system in the future.

1.3 Objective of thesis

- To study on the design and construction of H-reflex detectable instrument for fundamental diagnosis in the excitability of the neuromuscular system.

- To understand the behavior of muscle contraction and nerve phenomena in human.

- To capture and elicit H-reflex response to suit for clinical diagnosis and prognosis.

- The components are locally available used in Thailand.

- Having portable size and low cost.

- To substitute and support requirement of clinical uses for biomedical instruments.

1.4 Specification

1.4.1 General requirement

a) Ability

The H-reflex detectable instrument can evoke the H-reflex response and also activate the direct motor response (M-wave) together with measuring the both responses to the computer system. There are the part of preamplifier and filters for amplifying the real response and filtering the noise signal, respectively. Using the data acquisition plug-in board combine with the LabVIEW software for acquirement, display, analysis and store the data in the form of digital format. This helps to increase the efficiency of process and monitor of signal. The parameters composed amplitude, shape, and latency of both responses are displayed, analyzed, and stored by the LabVIEW program. Furthermore, the LabVIEW program sends appropriate instructions to generate a timing signal for controlling the pulsed stimulation of stimulator.

b) Reliability

- Be able to display H-reflex and M-wave that are normal or abnormal on the real time computer system correctly, including amplitude, shape, and latency.

- Be able to display correctly when comparing with the commercial equipment or standard device.

- Be able to display H-reflex and M-wave clearly without distortion.

- Be able to generate the electrical intensity of stimulus appropriately and safely.

- Be able to control frequency and duration of stimulation precisely and accurately as desired.

c) Cost and size

The H-reflex detectable instrument will be at reasonable cost by using the standard materials which are simple found inside the country. This aims to reduce the capital of import from the foreign country. This instrument is also considerate to size and body shape for convenience and efficiency that have been developed in small size but also easy use and full efficiency.

d) Safety

Because of the H-reflex detectable instrument is composed of nerved stimulation part with electrical intensity and power supply, these parts are isolated ground out from the subject by using isolated transformer and there are the protect circuits such as fuse, current and voltage limit aiming in guard the hazard that may be taken place from short circuit.

1.4.2 General specification

a) The power output of stimulation is constant current; the electrical intensity is adjustable in range from 0 to 20 mA, frequency adjustable from 0.1 to 1.0 Hz, and duration adjustable from 0.1 to 1.0 ms.

(b) The shape output of neurostimulator is rectangular pulse waveform.

(c) There is the trigger output for synchronous mode.

(d) Use the bipolar stimulating surface electrodes for activation, and the recording surface electrode disc for measurement including ground electrode.

(e) There is the amplifier and filter both hardware and software.

(f) Use the data acquisition (DAQ) plug-in device and the Laboratory Virtual Engineering Workbench (LabVIEW) program for acquiring, analyzing, and storing the data in digital format.

(g) It is not complicated to operate, and leakage current is low.

(h) Using rechargeable batteries with low voltage and use AC line power supply the device with isolation transformer into a charger circuit. The input subject is isolated from earth.

1.4.3 Specific specification

a) Neurostimulator

- Constant current power output.
- Rectangular pulse waveform.
- Power output adjustable 0-20 mA, Duration adjustable 0.1-1.0 ms (software selected), and Frequency adjustable 0.1-1.0 Hz (software selected).
- Triggering output for synchronous mode.
- Current and voltage limit circuit protection.

b) Preamplifier

- Differential inputs by using recording surface electrode discs.
- Input impedance ≥ 20 MΩ, and floating input amplifier.
- Common mode rejection ratio (CMRR) ≥ 100 dB.
- Sensitivity: can be lowest detected of 3 μV rms (10 μVp-p).
- Input bandwidth for frequency response of 2 Hz – 10 kHz.
- 4 steps of amplifier gain are ×1, × 10, ×100, and ×1000.

c) Filter

- Analog filter in pattern of Butterworth model.
- Low pass filter in the second order of Butterworth filter at frequency cutoff of 10 kHz.
- Notch filter at 50 Hz (Hum).

d) Electrode

- Surface stimulation in pattern of bipolar stimulating electrode with 6 mm diameter pads on 25 mm centers.
- Stainless steel ground electrode, 32 mm disc, 76 cm PVC coated connecting lead terminating in a touchproof plug.
- Silver/silver chloride disc recording electrodes with 9 mm diameter disc.

e) Data acquisition device (DAQ device)

- The data acquisition model use NI 6061E (AT-MIO-64E-3).
- 500 kS/s sampling rate, 12-bit resolution, up to 64 single-ended analog inputs.
- ±0.05 to ±10 V input range.
- Two 12-bit analog outputs.
- 8 digital I/O lines (5V/TTL); two 24-bit counter/timers.
- Analog and digital triggering.
- Available for ISA bus.

d) Accessories of DAQ device

- SCB-100 shielded I/O connector blocks.
- SH100100 shielded cable.
- Very low noise signal termination for connecting to 100-pin E-series DAQ device.

CHAPTER II
LITERATURE REVIEW

2.1 Reflex study.

The reflex studies in human body concern with sensory receptor and reflex circuitry of kinesiological mechanisms. The basic function of sensory receptors is to provide information to the system on its own state and that of its surrounding environment that sometimes is referred to as feedback for the information flow of them (1). The ability of sensory receptors is also to provide rapid responses to perturbations that based on the existence of short-latency connections between the input (afferent signal) and the output (motor response or efferent output). Such responses are termed reflexes and are defined as a stereotyped motor response of an organism to a sensory stimulus. The simplest neural circuit underlying a reflex involves a sensory receptor, its afferent innervations, and a group of motor units that receive input from afferent.

Reflexes are developed as mechanisms that can protect the system against unexpected disturbances. They can generate a rapid response to counteract the perturbation when the system is perturbed. In this sense, reflexes are considered regulators because they compensate for disturbances and maintain a prescribed state (Houk, 1988s). The neural circuits that enable input-output connections to compensate for disturbances perform a negative feedback function, in which the motor response tends to counteract the stimulus that initially activated the sensory receptor.

In the analysis of human kinesiology, reflexes are measured to address clinical and experimental issues. Clinicians test reflexes to determine the strength of the input-output connection and the ability of the patient to recompense for the disturbance. Measurements that differ from normal provide clues as to the deficits undergo by that individual and assist clinicians in formulating a diagnosis. Researchers in a laboratory setting use the reflex as a probe to determine the effect of various conditions and

manipulations on an individual. In this literature review, the H-reflex will be considered that are commonly used for both purposes.

2.2 H-reflex study.

The H-reflex is named after early work of P. Hoffmann, who first discovered it in 1918. He demonstrated that the compound muscle action potentials (CMAPs) associated with ankle and knee jerks was comparable in latency and configuration to that evoked by submaximal electrical stimulation delivered percutaneously to the tibial nerve in the popliteal fossa or femoral nerve, respectively. He concluded that the results of both CMAPs: tendon jerks and electrically induced late responses, represented activity in the same kind of stretch reflex. On the basis of his research, which included abolition of the late response with supramaximal stimulation to the mixed nerve and relatively brief latency of the late response, he summarized that the afferent part of this reflex is composed fast conducting nerve fibers (early response) and that the central delay was extremely short (late response) (3). Many years later, Magladery and Mc Dougal confirmed the conclusions of Hoffmann's remarkable experiments. They designated the electrically induced late responses the H-reflex after its discoverer. The early response or the shorter latency compound muscle action potential evoked by direct electrical stimulation of motor axons was called the M-response. In contrast to late response called H-reflex, which is reflex response of monosynaptic reflex in spinal cord.

Therefore, H-reflex is defined as an electrical analogue response of the monosynaptic stretch reflex by bypassing the muscle spindle and directly stimulating the afferent nerve. This reflex represents a monosynaptic reflex in which the afferent arc involves Group Ia fibers from muscle spindles and the efferent arc consists of alpha motor fibers. Because the H-reflex depends on the selective activation of Group Ia afferents, the classification and properties of fibers can be shown in Table 2.1 (1, 4).

The neural circuit for the H-reflex can be shown in Figure 2.1. It is elicited by applying a single electrical stimulus to a peripheral nerve. This nerve involves the selective activation of the Group Ia afferents and the subsequent generation of action potentials in the motor neurons innervating the muscle. The response of stimulus with a single shock is a twitch in the muscle innervated by the stimulated nerve. The result

of this twitch is a population response that involves many Group Ia afferents as well as a number of motor units (1). The selective activation of Group Ia afferents is achieved by beginning with a low intensity stimulation and slowly increasing it until action potentials are generated in the largest diameter axon. They are propagated centrally to spinal cord where elicit postsynaptic potentials in the motor neurons.

Table 2.1 Classification of nerve fibers.

Fiber Type			Fiber Diameter (μm)	Conduction Velocity (m/sec)
Erland & Casser's Sytem	Lloyd's System for Sensory Fibers	Function		
Myelinated fibers				
A	Ia	Proprioception; Primary muscle spindle afferents; motor to skeletal muscles	12-20	70-120
Aα	Ib	Afferents from Colgi tendon organ		
Aβ	II	Cutaneous touch and pressure	5-12	30-70
		Motor to muscle spindle	3-6	15-30
Aδ	III	Cutaneous temperature and pain	2-5	12-30
B		Sympathetic preganglionic	3	3-5
Unmyelinated fibers				
C	IV	Cutaneous pain	0.4-1.2	0.5-2
		Sympathetic postganglionic	0.3-1.3	0.7-2.3

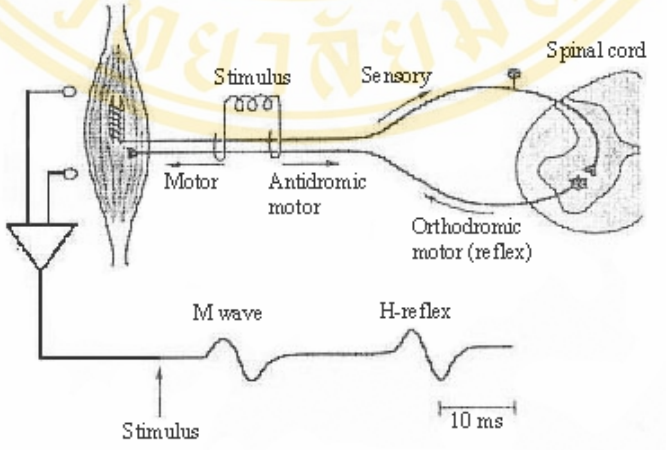

Figure 2.1 Neuron circuit diagram for H-reflex.

The possible results of these action potentials depend on the size of the synaptic potentials and the level of the membrane potential. The closer the membrane potential

is to threshold for action potential generation, the more likely the stimulus (synaptic potentials) is to elicit an action potential. Then, the stimulus will generate action potentials in more motor neurons and the response will be larger if the membrane potentials of more motor neurons are closer to threshold.

The H-reflex studies can be activated in several parts of human body. Most areas where is readily generated by stimulating electrodes are at stimulus to tibial nerve of the popliteal fossa (the hollow at the back of the knee). It is commonly captured in the gastrocnemius and soleus muscle, and it can be elicited in other muscles such as quadriceps femoris, tibialis anterior, and muscles of the hand, foot, and forearm. When the Ia fibers from the soleus and its synergist are excited by an stimulating electrode placed above the tibial nerve behind the knee, the muscle spindle discharge of tibial nerve is carried to the central nervous system via fast conducting A-alpha fibers which enter the spinal cord through the dorsal roots and synapse in the anterior horn with motor neurons of the same extensor muscle. The response recorded from the soleus muscle depends on stimulus strength. An important feature of stimulation for reflex is two distinguishable responses in recording site. A pure H-reflex is evoked early at low stimulus strengths because of the threshold for selective activation of Group Ia afferent fiber is lower than the threshold for motor axons (5). The amplitude of H-reflex will increase initially following the stimulus intensity, as changes from subthreshold to submaximal, then H-reflex amplitude is decreased. Since a further increase in stimulus strength enables motor axons supplying the soleus are activated, and two distinct responses are measured. The first results from direct activation of the motor axon. The second is the H-reflex evoked by stimulating to tibial nerve. These two components of the evoked potential are called the M-wave and H-reflex, respectively. The M-wave occur former because it results from direct stimulation of the muscle. The later is the H-reflex that results from signal travel to the spinal cord, across a synapse, and back again to the muscle. As the stimulus strength is increased further, the M-wave continues to become larger and the H-reflex progressively declines. Amongst possible causes for the decrease of the H-reflex with increasing stimulus (11), are:

- Collision of the reflex impulse with the motor nerve activity in antidromic activity, opposite direction.

- Refractioness of the axon hillock, the region of the neurons which becomes axon, although it is argued that this is a secondary activity to antidromic process.

At very high stimulus intensity only the M-wave is evoked.

On the function of these H-reflex characteristics, eliciting and measuring the H-reflex is mostly considered to be a sufficient method of studying the strength of the short latency loop in clinical application and is used as a test of the level of excitability of the motor neuron pool. Furthermore, evaluating the shape and the occurrence of the H-reflex can disclose important aspects of central nervous system. In combination with other tests, the H-reflex can support necessary diagnosis and prognosis regarding neurological disorders of the central nervous system such as Huntington, or Parkinson's disease, and other upper motor neuron (UMN) diseases.

The most commonly used tests for clinical usefulness are as follow:

a.) The onset latency and the peak-to-peak amplitude of the H-reflex and M-wave.

b.) Comparison of the maximum amplitude of an H-reflex with the maximum amplitude of the direct compound muscle action potential in the same muscle (H_{max} / M_{max} ratio).

c.) Excitability and the recovery curve of the H-reflex.

d.) Vibratory inhibition of the H-reflex.

(a) The H-reflex latency and amplitude

The latency is termed of time (ms) from the stimulus onset to the beginning of the initial deflection of the compound muscle action potential (4). The H-reflex latency enables a measure of nerve conduction along the entire length of the afferent and efferent pathways that depends on several factors consisting of the time required for activation of the Group Ia spindle afferent fibers, the conduction time along these fibers to the cord and along the alpha motor axons to the neuromuscular junctions from the cord, the central delay in the cord (involving conduction, synaptic transmission, and activation of anterior horn cells) and delay at neuromuscular junction, and the time required for conduction of action potentials along muscle fibers to the recording site (6). There may be considerable differences in latencies evoked by the H-reflex, reflecting differences in either peripheral conduction velocity, central

activation time, or both. The latency will vary with age and limb length or height in different subjects. Therefore, these factors must be considered when normal values are obtained. From the studies of Braddom and Johnson in 1984, they found that the latency recorded from the soleus muscle is usually approximately 30 ms, with a standard deviation (SD) of 2.4 in adults. Its mean value increases by about 1 ms for each decade of age. An interside difference in latency of 2 ms or more is abnormal (6).

The amplitude of the H-reflex normally exceeds 1 mV, ranging up to almost 20 mV in different subjects and may show marked interside variation, since this amplitude is influenced by a variety of technical factors consisted of the stimulus intensity and duration, the site of recording electrodes, posture, age, and degree of contraction of the muscle (and its antagonists) from which the recording is being made. A ratio of the contralateral amplitude can express in the amplitude on the side with the smaller response. This ratio had a mean value of 0.74, with a standard deviation of 0.17, in recent study.

In medical applications for these tests, the H-reflex latency is more clinically useful than the H-reflex duration and amplitude. Its latency increases in patients with alcoholic (7), uremic (21), and various other polyneuropathies (22). In patients with diabetes, this test rivals the conventional nerve conduction studies in detecting early neuropathic abnormalities (23) and a clear-cut proximal-to-distal gradient of conduction slowing (24, 25). The test also helps establish maturational changes in the proximal versus distal segment of the tibial nerve (26). The use of H-latency and distal motor latency allows the calculation of a segmental conduction velocity along the reflex pathway (24, 25). With more recent researches, H-reflex latency is used as a test for radioculopathies including lumbar (L_5) and sacral (S_1) root compression. In S_1 radiculopathy or S_1 root compression, the H-reflex is often absent or prolonged in latency like a depression of the ankle reflex in the neurologic examination (27). In patients with L-5 radiculopathy, comparison of H-reflex latency recorded from the extensor digitorum longus after stimulation of the common peroneal nerve may be demonstrated to abnormalities (28). Abnormality of H-reflex latency in flexor carpi radialis indicated lesions of the C-6 or C-7 root or both in-patients with cervical radiculopathy (29).

(b) Ratio of H_{max} to M_{max}

The H_{max} / M_{max} ratio have been used to study levels of control excitability of the motor neurons (1, 3). It reflects the percentage of motor neurons in the soleus motor neuron pool that reflexly excited by an electrical stimulus via the tibial nerve in the popliteal fossa. The maximum amplitude of an H-reflex is acquired by applying a series of single electric stimuli with stimulating electrodes. A recording response is made by placing surface electrodes over the soleus muscle. The stimulus intensity is adjusted to produce the maximum amplitude H-reflex. The maximum amplitude of M-wave is recorded in the usual manner by delivering a supramaximum stimulus to the same nerve in the popliteal fossa.

The ratio of H_{max} to M_{max} is clinically exploited for diagnosis in patients with upper motor neuron lesions and cataplexy or spinal shock. In condition in which the excitability of motor neuron pool is increased, as in upper motor neuron lesions, a great percentage of motor neurons are excited, the amplitude of the H-reflex is increased, and the H_{max} / M_{max} ratio is greater than normal. In another condition in which the excitability of motor neuron pool is decreased, as in cataplexy, the H-reflex may be impossible to record it, or, when the H-reflex is recordable, the amplitude of it is diminished. Consequently, the H_{max} / M_{max} ratio may be either zero or lower than normal, respectively.

(c) Excitability and the recovery curve of the H-reflex

The H-reflex excitability and the recovery curve have been studied in various neurologic disorders and providing information about spinal interneuronal networks. It is a technique that concerned with the facilitation and inhibition of the H-reflex. This technique is provided by delivering double stimulation composed conditioning and test stimuli. These stimuli are delivered to tibial nerve in the popliteal fossa. In studies of these curves, the intensity of the conditioning stimuli is adjusted to produce an H-reflex of standard amplitude and area. The amplitude of the H-reflex elicited by the second test stimuli is then plotted as a function of the interval between conditioning and test stimuli. The curve normally has two phases of inhibition, the first at interstimulus intervals of between 30 and 70 ms, and the second between 300 and 900 ms (6). They are separated by a phase of partial recovery curve or facilitation at an interstimulus interval of 200 ms. Changes of curve show characteristic hypoexcitable

and hyperexcitable phases in normal subjects (51). These curves are often altered in patients with central nervous system (CNS) lesions. Plotting of H-reflex excitability curve is emphatically considered to affect independent variables such as the amount of ballistic voluntary reflex activity and the position of the patient. To obtain reproducible results, the subject must be still, relaxed, and in a comfortable position, and the limb must be rigidly fixed at various joints at suitable angles to avoid tinges of proprioceptive input. Eliciting a small preceding M response of constant amplitude and shape from one stimulus to the next are also important studies of H-reflex excitability curve, as a poof of the stability of the relationship between the nerve and the stimulating electrodes.

Mostly studies have demonstrated that reciprocal inhibition of the H-reflex can provides further information about certain spinal interneural networks. There are three phases of inhibition in normal subjects: when the test and conditioning stimuli are applied simultaneously, when the conditioning stimulus precedes the test stimulus by 10 to 20 ms, and when the interstimulus interval is approximately 70 ms. In the normal subjects, the level of inhibition is such that the mean amplitude of the H-reflex is 47% of the unconditioned amplitude with simultaneous stimuli, 61% with an interstimulus interval of 10 ms, and 69% with an interstimulus interval of 75 ms. Reduced inhibition at some or all of these periods has been related with several groups in writer's cramp or other forms of dystonia (6).

(d) Vibratory inhibition of the H-reflex

In clinical conditions, the vibratory inhibition of H-reflex has been reported in patients with chronic spasticity. The reflexes are significantly inhibited when the muscle of a normal individual is vibrated during elicitation of phasic proprioceptive reflexes. Such vibratory inhibition of the H-reflex is diminished. Reducing inhibition may be caused by presynaptic suppression. However, effects of vibration as studied in human subjects are probably more complex. It is possible to calculate an index of vibratory inhibition under standardized conditions as follows: $[H_{max(vibrated)} / H_{max}] * 100$ (3).

From studies of H-reflex, the characteristics of H-reflex bring to exploit in many clinical applications. The design and construction for stimulation, capture and display device of H-reflex provide insight into conditions for clinical usefulness. The

basic theories of investigating the H-reflex device are reviewed to understand in mechanisms of acquired H-reflex response.

2.3 The principle of electrical neurostimulator

The electrical neurostimulator represent a class of biomedical instruments that are useful on many clinical applications. They have been powerful tools restoring partial functionality to neurologically damaged individuals while providing a medical diagnostic of the nervous system. Stimulation to innervated muscles can be used in physical therapy to regain some degree of muscular control. Lesions in the nervous system that provoke disruption in the flow of the sensory and motor signals to the brain and spinal cord may cause neurological handicaps. Functional neuromuscular stimulation (FNS) systems are mainly useful in cases dealing with the electrical activation of paralyzed muscles and can be applied to restore partial functionality including providing a clinical diagnosis or prognosis of the nervous system. FNS is embedded in many prosthetic devices aiming different applications such as control activity of motor nerves and urinary bladder, pain relief, stroke victims, etc. (52).

Stimulation parameters vary widely according to the type of muscle stimulation, the number of channels, the type of electrodes and the specified safety-factor. Many commercially available stimulators deliver voltage pulses and require additional features to monitor and set up the current level as it depends on the electrode/skin load-characteristic. Hence, constant-current stimulators are mostly indicated since the charge transferred per stimulus is constant regardless the load impedance.

2.3.1 Electrical neurostimulation requirements

Electrical neurostimulation provides a clearly defined, reproducible response for nerve reflex studies. A current of short duration, 50 μs to 1 ms, is induced in the fluid surrounding a nerve bundle by applying a potential to electrodes. The stimulating current is directed primarily along the nerve, depolarizing one point and hyperpolarizing another. Increasing the current to obtain a repeatable and maximal recorded response ensures that essentially every nerve in the bundle fired. Surface electrode stimulation requires 100 to 500 V to drive currents of 5 to 75 mA. The higher values are necessary when neuropathy decreases excitability or the stimulating

electrodes are distant from the nerve. Subcutaneous needle electrodes require much less voltage and current for adequate stimulation.

Effective depolarization displays an inverse relationship between stimulus intensity and duration. Thus, a lower intensity suffices if applied for a longer duration, within limits. Generally, stimulus durations exceeding 1 ms are not well tolerated. Durations less than 50 μs become ineffective, because tissue capacitances limit the rate of rise, and the stimulus dose not reach full amplitude (14). The equipment must also provide control and timing of stimuli for different types of measurements. Some collision techniques require two or three precisely timed stimuli, with adjustable intensities, durations, and latencies, delivered to the same or to the different sets of electrodes. In the paired-shock facilitation technique, the first shock has reduced intensity to give only a subliminal excitation of the motor neuron pool, and a second shock follows within a few milliseconds on the same electrodes at full intensity. Such complex stimulus generators must have adequate programmability and fail-safe protection features.

2.3.2 Stimulus isolation

Electrical neurostimulators are isolated from the recording amplifiers and other equipment circuits for artifact reduction and safety. This means that the stimulation circuits have no conductive path except through the patient's body when stimulating and recording electrodes have been applied. Isolation ensures that stimulus current flows only in the loop provided by the two stimulating electrodes. If the stimulator circuit has any connection to the recording circuit, then the stimulus current that is distributed in the body can divide into additional paths, causing a large stimulus artifact, amplifier overload, or even spurious stimulation at unintended sites. Furthermore, under conditions of component failure, these additional paths can conduct hazardous levels of current. Stimulus isolation is usually accomplished by magnetic coupling of energy to the stimulating circuits, although battery-powered stimulators with optical coupling of the control signal have also been used.

2.3.3 Constant-voltage versus constant-current

Constant-voltage neurostimulators deliver an adjustable voltage across the stimulating electrodes, essentially independent of stimulus current. One can adjust the voltage to vary the current through the stimulating electrodes to achieve the desired

level of stimulation. At a fixed output voltage, changes in stimulating electrode impedance alter the stimulus current level. Constant-current neurostimulators deliver an adjustable current through the stimulating electrodes, essentially independent of their impedance. The voltage across the stimulating electrodes adjusts dynamically to maintain a constant stimulus current. Constant-current neurostimulators provide more consistent stimulus control, especially for techniques that require a train of stimuli or response averaging.

2.4 The principle of data acquisition

The data acquisition systems are defined as a way in which information about user is conveyed to the computer. The purpose of them is to acquire, store, and analyze data. Figure 2.2 shows how information from the human is passed to the computer. It separates the process into three parts: sensors, signal conditioning, and data acquisition. The choices made in the design of these systems ultimately determine how intuitive, appropriate, and reliable the interaction is between human and computer.

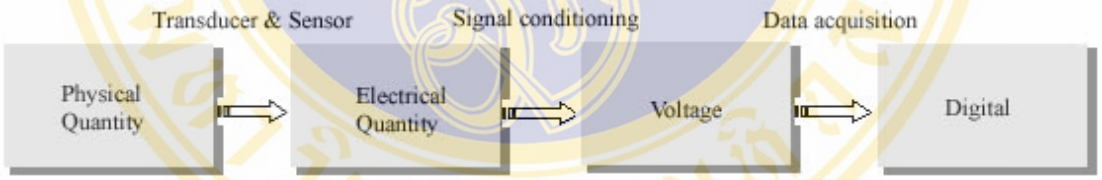

Figure 2.2 The path from human to computer.

2.4.1 The transduction and sensor

The measurand is defined as the measurement of system including the physical quantity, property, or condition. The accessibility of the measurand is important because it may be internal (blood pressure), it may be on the body surface (electrocardiogram potential), it may emanate from the body (infrared radiation), or it may be derived from a tissue sample (such as blood or a biopsy) that is removed from the body. Most medically important measurands can be grouped in the following categories: biopotential, pressure, flow, dimensions (imaging), displacement (velocity, acceleration, and force), impedance, temperature, and chemical concentrations. The measurand may be localized to a specific organ or anatomical structure.

Generally, the term transduction is described as a process that converts one form of energy to another. A sensor converts a physical measurand to an electric output. One approach to choosing an appropriate sensor would be to model computer sensing after the five human senses: gustatory (taste), olfactory (smell), tactile, auditory, and visual. The better approach, however, is to decide what volitional (or even non-volitional) actions of the user will be important for the particular computer application. In other words, it is important to decide what gestures by the human are appropriate for the application and determine what sensor is optimal in measuring that gesture. Before determining what computer inputs to use we must determine what human outputs are appropriate.

Sensors can be categorized in many ways. They can be categorized by the underlying physics of their operation. However, one physical principle can be used to measure many different phenomena. For example, the piezoelectric effect can measure force, flexure, acceleration, heat, and acoustic vibrations. Sensors can be categorized by the particular phenomenon they measure. However, one phenomenon can be measured by many physical principles. For example, sound waves can be measured by the piezoelectric effect, capacitance, electromagnetic field effects, and changes in resistance. Sensors can also be grouped by a particular application. For example, one could group all sensors together that can be used to measure distance. However, since there is a clever way to use almost any sensor to measure distance, this is not necessarily a good way to analyze sensors either.

2.4.2 Signal conditioning

After the information about the user is measures by a sensor, it must be changed to a form appropriate for input into the data acquisition system. In most applications this means changing the sensors output to a voltage, modifying the sensors dynamic range to maximize the accuracy of the data acquisition system, removing unwanted signals, and limiting the sensor's spectrum. Additionally, analog signal processing (both linear and nonlinear) may be desired to alleviate processing load from the data acquisition system and the computer. The correct design of the signal conditioning system is critical in mapping the sensor output to the data acquisition input. Incorrect choices can affect the way the computer reacts to the

human input. Thus, it is important to note the changes in the properties of the sensor signal caused by the conditioning circuitry.

Additional requirements for signal conditioning

- Signal isolation

In many applications it is necessary to isolate the sensor from the power supply of the computer. This is done in one of two ways: magnetic isolation or optical isolation. Magnetic isolation is primarily used for coupling power from the computer or the wall outlet to the sensor. This is done through the use of a transformer. Optical isolation is used for coupling the sensor signal to the data acquisition input. This is usually done through the use of a light emitting diode and a photodetector.

- Signal preprocessing

Many times it is desirable to perform preprocessing on the sensor signal before data acquisition. Depending on the application, this can help lower the required computer processing time, lower the necessary system sampling rate, or even perform functions that will enable the use of a much simpler data acquisition system entirely. For example, while an accelerometer system can output a voltage proportional to acceleration, it may be desired to only tell the computer when the acceleration is greater than a certain amount. This can be accomplished in the analog signal conditioning circuitry. Thus, the data acquisition system is reduced to only having a single binary input.

- Removal of undesired signals

Many sensors output signals that have many different components to them. It may be desirable or even necessary to remove such components before the signal is digitized. Additional other signals may corrupt the sensor output. This noise can also be removed using analog circuitry. For example, 50Hz interference can distort the output of low output sensors. The signal conditioning circuitry can remove this before it is amplified and digitized.

2.4.3 Data acquisition (DAQ)

The analog and continuous time signals measured by the sensor and modified by the signal conditioning circuitry must be converted into the form a computer can understand. This is referred as data acquisition. It should be clearly understood that this step is only necessary when interfacing human gestures to a

digital computer. If, for example, one wanted to use the direction of eye gaze to control a wheelchair, no data acquisition would be needed. The continuous analog voltages could be directly used to control the analog steering mechanism. The procedures of data acquisition can be divided into the steps shown in Figure 2.3.

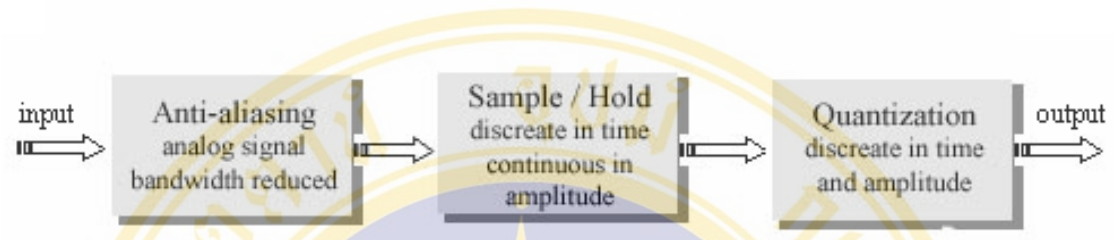

Figure 2.3 The procedures of DAQ.

2.4.3.1 Anti-aliasing

The Nyquist criterion dictates that all signals must be bandlimited to less than half the sampling rate of the sampling system. Many signals already have a limited spectrum, so this is not a problem. However, for broad spectrum signals, an analog lowpass filter must be placed before the data acquisition system. The minimum attenuation of this filter at the aliasing frequency should be at least:

$$A_m in = 20 \log (\sqrt{3} \times 2^B) \quad \text{.....(2.1)}$$

where B is the number of bits of the analog-to-digital converter (ADC). This formula is derived from the fact that there is a minimum noise level inherent in the sampling process and there is no need to attenuate the sensor signal more than to below this noise level.

2.4.3.2 Sample and hold

The purpose of the sample and hold circuitry is to take a snapshot of the sensor signal and hold the value. The ADC must have a stable signal in order to accurately perform a conversion. An equivalent circuit for the sample and hold is shown in Figure 2.4. The switch connects the capacitor to the signal conditioning circuit once every sample period. The capacitor then holds the voltage value measured until a new sample is acquired. Many times, the sample and hold circuitry is incorporated into the same integrated circuit package.

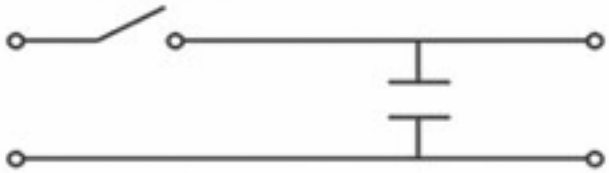

Figure 2.4 Equivalent circuits for a sample and hold.

2.4.3.3 Analog to digital conversion

The purpose of the analog to digital is to quantize the input signal from the sample and hold circuit to 2B discrete levels - where B is the number of bits of the ADC. The input voltage can range from 0 to V_{ref} (or $-V_{ref}$ to $+V_{ref}$ for a bipolar ADC). What this means is that the voltage reference of the ADC is used to set the range of conversion of the ADC. For a monopolar ADC, a 0V input will cause the converter to output all zeros. If the input to the ADC is equal to or larger than V_{ref} then the converter will output all ones. For inputs between these two voltage levels, the ADC will output binary numbers corresponding to the signal level. For a bipolar ADC, the minimum input is $-V_{ref}$ not 0V.

2.4.4 LabVIEW

LabVIEW (Laboratory Virtual Instrument Engineering Workbench) is a graphical programming language that sometimes is called as G program. This program has been developed by National Instruments (NI) Corporation in the mid-1980s. LabVIEW uses icons instead of lines of text to create applications. In contrast to text-based programming languages such as Visual Basic, Visual C++, where instructions determine program execution, LabVIEW uses dataflow programming, where the flow of data determines execution. A program written in LabVIEW is defined as virtual instruments (VIs). These VIs simulate hardware devices that acquire and analyze electrical signal. Analog electrical signals output from measuring devices, and sensors are interfaced with a computer via various input device (such as analog-to-digital convert board) and fed to LabVIEW program. Signals from virtually any device that emits a direct-current analog signal (±10 volts) may be acquired and analyzed by LabVIEW VIs. LabVIEW is used in industry to run and monitor assembly lines; for process control; by engineers to develop and test sophisticated electromechanical devices; and by computer programmers, educators, and scientists of every persuasion.

The strength of LabVIEW is its generalizability to many uses over a broad range of commercial and scientific applications (19). The ease with which even complicated and sophisticated programs can be written is due to LabVIEW's graphical interface. Compare with traditional text-based programming code, VIs written in LabVIEW can be up and running very quickly. It is amazed that simple VIs can be structured and run, without errors, literally in a matter of a few minutes, whereas a program written in conventional text-based code could take hours and sometimes days, to write, debug, and run. Besides the ease of operation issues, also there are many advantages with using LabVIEW. The received obviously benefit of using LabVIEW is flexibility and adaptability of software that can be used as a front-end replacement for expensive, dedicated hardware device. When conditions require changing, objectives are reoriented, and the need for more processing power become apparent, LabVIEW VIs are simply modified to meet those needs.

The focus of this literature is the use of LabVIEW to acquire and analyze physiological and mechanical signals that measure various aspects of normal and pathological human performance. Examples of usually exploited measurement devices in the clinical sciences include electromyographs to measure electrical output of contracting muscle, transducers and other strain gauges to measure the amplitude of forces applied to human tissue, and dynamometers to analyze torque and angular velocity of joints. Traditionally, electrophysiological testing device are expensive, become obsolete quickly, and are subject to wear-and-tear, eventually breaking down and requiring frequent replacement or upgrades. Today, many of these devices are operated by proprietary software that requires a steep learning curve and often upgrades and that sometimes has or develops bugs causing programs to crash or operate unpredictably. It is an expensive and time-consuming proposition to ask the manufacturer to repair or modify proprietary software when the intervention is required. Because of LabVIEW VIs are specially written by a user him- and herself, troubleshooting problems and changes can be manipulated locally, inexpensively, and with substantially less downtime.

The areas of human performance analysis and physiological parameters that LabVIEW VIs can measure and handle include:

- Electromyographic (EMG) measurement.

- Spectral and power analysis.
- Dynamometry and Electrogoniometry.
- Biofeedback.
- Event markers and Timers.
- Simple oscilloscopes.
- Data calculations and Statistical analysis.

One of LabVIEW's principle features is the ability to configure software as hardware devices ("the Software is the instrument"). This is achieved via LabVIEW's graphical user interface with which software programs are written. The software programs written in LabVIEW are called as a virtual instrument, or VI. These programs use icons representing the equivalent of text-based code (e.g., BASIC or C++). Each icon with predetermined connection points is wired to establish the orderly flow of information in the VI. Repetitive function in text-based programming known as subroutines is configured in LabVIEW as subVIs. This subVIs can be chosen in LabVIEW's menu structure or may be written and saved and latter inserted into subsequent VIs when needed. In the case that a subVI must be created, the user can build a subVI icon face that helps the programmer or user more easily identify a particular subroutine's function in the context of a large VI.

The fundamental structure of a VI is included three main parts: front panel, icon and connector pane, and block diagram. The front panel and block diagram represent to two blank overlapping panels. The front panel is the user interface from which the VI is operated. This is areas for various controls and indicator of the VI. It consists of various types of controls (e.g., knobs, dials, slides, etc.) gauges, graphs, and tables lay out and positioned by the user. The front panel is created and controlled by selecting menu items from the task bar across the screen. Each time an element is accessed and placed on the front panel, an icon (or a subVI) will appear on the block diagram. For the block diagram, it is the area where the actual programming occurs. The block diagram includes the actual "program" being written and migh be linked to a writing diagram on a plan to build an electronics device. Icons represent a wide variety of data collection and processing and analysis functions of VIs. Each VI has a series of terminals to which links (wires) are attached, establishing the flow of information between various functions. Similar to the front panel, the block diagram is controlled

and functions are accessed using the task bar across the top of the screen. The principles tools with which VIs are built and controlled are referred as the Tools, Control, and Functions palettes. The Tools and Control palettes are exploited for the front panel and block diagram, while the Functions palette appears only in the block diagram. The VI's structure can be shown in Figure 2.5. LabVIEW has extensive libraries of functions and subroutines for most programming tasks. For Window, Macintosh, and Sun, LabVIEW contains application specific libraries for data acquisition. Also, LabVIEW includes conventional program development tools so you can set breakpoints, animate program execution to see how data passes through the program and single-step through the program to make debugging and program development easier.

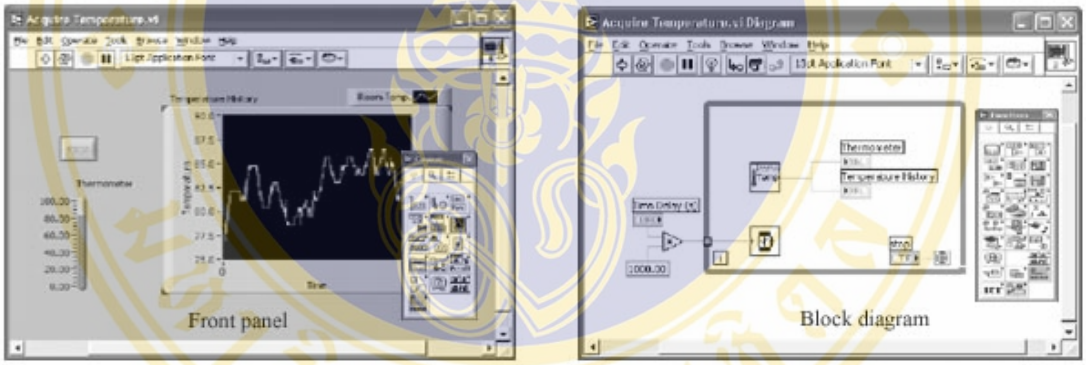

Figure 2.5 An example of components in a VI.

The following are descriptions of these VI features.

- VIs contains an interactive user interface, front panel. The front panel is similar to the panel of a physical instrument that can contain knobs, push buttons, graphs, and other controls and indicators.
- VIs receives instructions from a block diagram that is provided as the source code of the VI.
- VIs uses a hierarchical and modular structure that can use them as top-level programs, or as subprograms within other programs or subprograms.
- The icon and connector pane of a VI work like a graphical parameter list so that other VIs can pass data to it as a subVI.

With these features, LabVIEW adheres and promotes to concept of modular programming. The user divides an application into a series for tasks, which they can divide again until a complicated application becomes a series of simple subtasks. The user builds a VI to accomplish each subtask and then combine those VIs on another block diagram to accomplish the larger task. Finally, the top-level VI contains a collection of subVIs that represents application functions.

CHAPTER III
METHODOLOGY

This chapter shows the methodology for the optimum elicitation and measurement of H-reflex in human. These methods will be divided into three main processes. These processes consist of the muscle electrically stimulating process, the data acquisition process and the signal analysis process. The first process is the muscle stimulus with an electrical intensity. This process purposes to evoke H-reflex out of the body. Hence, in the construction and design the stimulator or neurostimulator for this process has to get a specific feature to relate with the characteristics of elicited response. When the H-reflex gets to activate suitably, the process of data acquisition is secondly follow work. The purpose of this second process is to amplifier the input signal that takes place from the reflex of electrical stimulating, and to filter the noise signal that affected the original signal, then, to convert from analog signal to digital signal and display the H-reflex on the computer. The final process will analyze and indicate the parameters of H-reflex signal with software to use in diagnosis and prognosis clinical conditions.

The additional details of these processes are described in the following section: section 3.1, 3.2 and section 3.3, respectively. In section 3.1 and 3.2 will describe to construct and design the stimulator and data acquisition system, respectively, including the required reasons of them for both construction and design. In the section 3.3 will describe to method of set systems and measurable procedure with subject that get to solicit in test. In addition, the LabVIEW software is described in useful for signal analysis.

3.1 The method of design and construction neurostimulator

The main concept of design and construction of neurostimulator is to deliver available parameters, including electrical intensity, frequency, and duration, into required target following the characteristics of such signal. For this thesis will be

emphatically focused on designing and constructing the available stimulator for eliciting H-reflex in the human body, particularly on gactrocnemius-soleus muscle. The stimulator is used for stimulating mixed nerve fiber (sensory and motor nerve) of Group Ia afferents by passing the bipolar stimulating surface electrodes in the suitable area, typically tibial nerve of popliteal fossa, that will be described in section 3.3. This stimulator used in activation nervous system is called neurostimulator.

The important parameters of stimulating to evoke H-reflex are consisted of current or voltage intensity, duration, and frequency of stimuli. For the case of intensity of stimuli, the neurostimulator is designed as constant current intensity because the charged transfer per stimulus is constant regardless load impedance and is more appropriate than constant voltage. The constant current intensity is delivered through the bipolar stimulating surface electrodes via to nerve fiber. Stimulated nerve fiber is mixed nerve fibers that consist of sensory and motor nerve. With electrical stimulating on these nerve fibers, the intensity of stimulus will relate to threshold of each nerve fiber. From precedent literature review, the threshold of sensory nerve fiber is lower than motor nerve fiber. Therefore, the sensory nerve fiber is firstly activated or depolarized before motor nerve fiber. The reflex signal of sensory nerve fiber is measured as H-reflex. On the other hand, the signal of motor nerve is measured as M-wave. The level of current intensity is provided from 0 mA to 20 mA (0-200 V) to investigate changes of H-reflex waveform. The output shape of constant current intensity is determined as a monophasic pulse like a rectangular pulse as follow the characteristic of evoked H-reflex that is similar to a twitch with a single electrical shock. The duration of stimulus serves as a short duration of 100 μs – 1000 μs with resolution in order of 100 μs as follow electrical stimulation requirement and clinical safety. Pulse-repetition is chosen from 0.1 Hz to 1 Hz because of H-reflex response will usually display the latency of 30 ms if the frequency exceeds 1 Hz, the detection of H-reflex is not obvious or not be found (8).

The structure of neurostimulator can be designed and demonstrated to components as follow the block diagram in Figure 3.1 below. This proposed neurostimulator consists of the part of power supply, voltage regulator, an adjustable amplitude oscillator, a transformer followed by full-bridge rectifiers, multivibrators, an optocoupler, a switching circuit, and a V/I converter. The load represents both

resistive and reactive components of the electrode/skin interface as well as the bulk tissue resistance. The approach of circuit operation is based on a research of Lima and Corderio (13). They gave an alternatively idea of design of a constant-current neural stimulator that can be applied to work about the electrical stimulation of nerve fiber. The circuit operation is now briefly depicted as follow. The two rechargeable batteries 12V are used as power supply that its voltage output is input to feed a regulator circuit, whose output is adjustable within the interval 0-20V and sets the supply voltage to controlled-amplitude oscillator circuit. The oscillator operates as an astable whose is loaded by the primary of step-up transformer. A self-exited oscillation across the secondary obtains high-voltage amplitudes and provides the necessary compliance voltage to generate the desired stimulation currents. As function of the regulated voltage, the peak-amplitude at the secondary of transformer is proportional to regulated output voltage, which varies from 0 to 210V. After rectification and filtering, a high dc voltage is supplied available to a switched voltage-to-current (V/I) converter built upon a cascade current-mirror that delivers to the load a pulsed current with constant amplitude. The pulse-repetition and pulse-duration are externally determined by a program which is software controlled by LabVIEW program. The resulting one-shot pulse is delivered to a photocoupler that drives a switching circuit made up of discrete transistor. The more descriptions of circuit operation and design are split into four main elements: the power supply, the amplitude control, the switching and timing circuit, and the output V/I converter. These parts are explained below in more details.

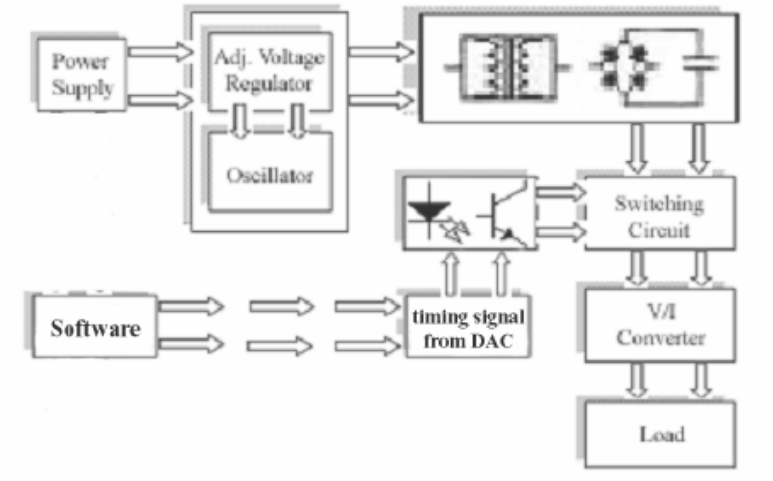

Figure 3.1 Block diagram of stimulator.

3.1.1 Power supply

The single requirement common to all phases of electronics is the need for a supply of DC power. The objective of power supply is to provide a dc power to feed all circuit enough. On this thesis, the power supply is significantly considered to electrical requirement and electrical safety concerns. To meet the demand for the electrical requirement and electrical safety, battery power is chosen to exploit in this thesis. The battery power offers a reasonably constant voltage with large current flow for a short period of time adequate to load current demand, and is available to portability for uses. Additional to, the battery power supply with low power is safer than the power supply built from AC power line source. Because failure of any electrical device making direct or indirect galvanic contact with the skin can cause a potentially harmful fault current to pass into the subject. This concern is less relevant in devices supplied by low voltage battery (30, 31, 32). To ensure safety, the subject is electrically isolated from any electrical connection associated with the power source by through the use of isolation transformer and optical isolator again. Using the battery power supply and isolation transformer also offers an additional benefit of reducing the amount of radiated power line noise at the electrode detection surfaces (33, 34). A disadvantage of batteries is the voltage decays and maintenance; they must be replaced or periodically recharged. In this section, the used battery power supply can be rechargeable. Charger system is achieved when the check circuit detects the decay of battery lower level at setting.

For relatively large power requirements, a lead-acid (La) rechargeable battery is used (31, 35). The type of this battery is available in many different sizes and with voltage 12V. The discharge rate is quite high from 2.2 to 4.4 A/hr (ampere per hour) and capacity in A/hr is a function of size. With choosing rechargeable battery power at 12V, the battery exhibits a capacity in order of 12 VAh/lb. Storage life is temperature dependent and will exceed 6 to 8 months space at normal room temperature (38-42 °C) (36). Its can be recharged about 1000 times if the extent of discharge is limited to 50 percent of the capacity. Because this class of battery is completely sealed, it can be used in any position and treated as a dry cell.

3.1.2 Amplitude control

The operation of this section consists of the part of voltage regulator, which is tunable its output voltage, a controlled-amplitude oscillator, step-up transformer, full-bridge rectifier, and filter-capacitor that can be shown the schematic of circuits in Figure 3.2 as follow below.

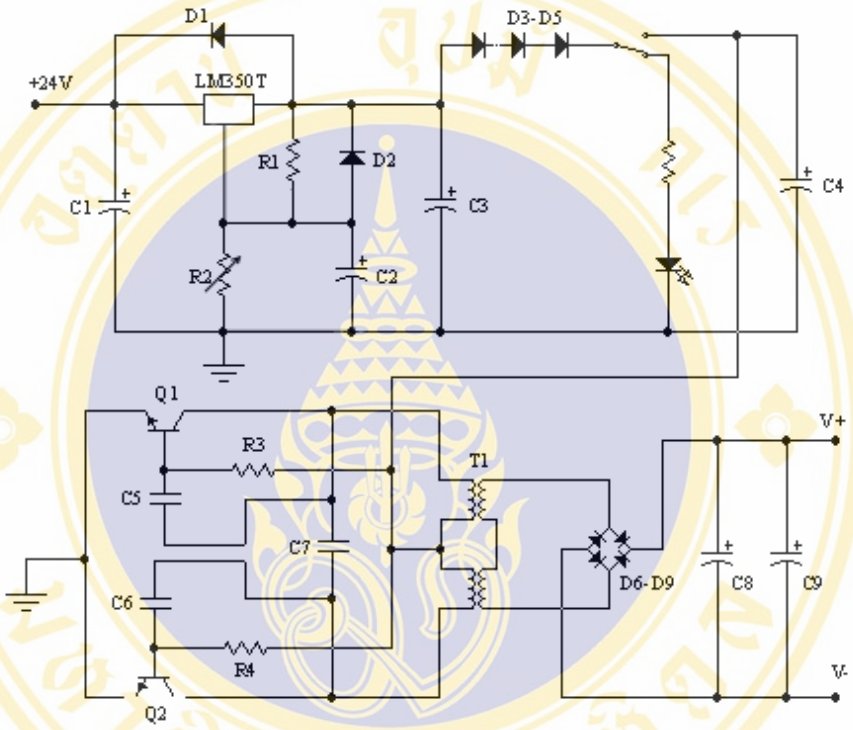

Figure 3.2 Schematic of amplitude control part.

This circuit functions to generate and control the output voltage sufficient to load demand. Here, the resulting dc voltage from battery is input to a voltage-regulator. The LM350T of adjustable 3-terminal positive voltage regulator is selected for this thesis because it is capable of supplying in excess of 3A over a 1.2V – 33V output range. It is exceptionally easy to use and require only 2 external resistors to set the output voltage. Its package is in the standard transistor packages which are easily mounted and handled. In addition to higher performance than fixed regulators, the LM350T offers full overload protection available only in IC's. Included on the chip are current limit, thermal overload protection and safe area protection. All overload protection circuitry remains fully functional even if the adjustment terminal is accidentally disconnected. In operation, the LM350 develops a nominal 1.25V

reference voltage, V_{REF}, between the output and adjustment terminal. The V_{REF} is impressed across program resistor R1 and then a constant current flows through the output set resistor R2, giving an output voltage of

$$VR = V_{REF}\left(1 + \frac{R2}{R1}\right) + I_{ADJ}R2. \qquad \text{.....(3.1)}$$

Since the current from the adjustment terminal exhibits an error term, the LM350 was designed to minimize I_{ADJ}, not excess 100 μA, and make it very constant with line and load changes. To do this, all quiescent operating current is returned to the output establishing a minimum load current requirement. An input bypass capacitor C1 is achieved for eliminating possible problems of the device, whose is more sensitive to the absence of input bypassing when adjustment or capacitors are used. In here, a 1 μF solid tantalum is recommended. The adjustment terminal is bypassed to ground by C2 for improving ripple rejection. The C2 prevents ripple from being amplified as the output voltage is increased. With a 10 μF bypass capacitor 86 dB ripple rejection is obtainable at any output level. If the bypass capacitor is used, it is sometimes necessary to include protection diodes (D1, D2) to prevent the capacitor from discharging through internal low current paths and damaging the device. In general, the best type of capacitors to use is solid tantalum. Solid tantalum capacitors have low impedance even at high frequencies. Depending upon capacitor construction, it takes about 25 μF in aluminum electrolytic to equal 1 μF solid tantalum at high frequencies. Although the LM350 is stable with no output capacitors, like any feedback circuit, certain values of external capacitance can cause excessive ringing. C3 and C4 bypassed on the output can help to swamp this effect and to insure stability.

The set resistor R2 is a potentiometer that is used to adjust the regulated voltage VR. The VR passes a group of diodes (D3-D5). These diodes produce the voltage drop that ensures 0V as the minimum dc-voltage VR, resulting VR can be tunable from 0V to 20V when R1 and R2 are of 10 kΩB and 469 Ω, respectively. The VR supplies to a multivibrator astable which includes a pair of power MOSFET Q1-Q2 (IRFP150), gate resistors R3-R4, and drain-coupling capacitors C5-C6. The IRFP150 is N-channel enhancement mode silicon gate power field effect transistor which is an advanced power MOSFET designed, tested, and guaranteed to withstand a specified level of energy in the breakdown avalanche mode of operation. This power MOSFET is

designed for applications such as switching regulators, switching converters, motor drivers, and drivers for high power bipolar switching transistors requiring high speed and low gate drive power. On this work, the IRFP150 is used as a switching converter. For the consideration to power supply from battery, MOSFET is more suitable than bipolar transistor in used power consumption.

In the astable multivibrator circuit above, the transistors Q1 and Q2 functioned as switching element is used in conjunction with a transformer. The following the pattern of circuit may be called as a relaxation oscillator. This oscillator has a nonsinusoidal output waveform. In operation, it uses a regenerative circuit in conjunction with resistance-capacitance (RC) components to provide a switching action. The charge and discharge of the capacitors are used to produce square output waveform. Basically, this operation depends on the switching action of transistors Q1 and Q2. When Q1 conducts heavily, Q2 will be cutoff. The transition from cutoff to heavy conduction and charge-discharge of the capacitors give a square wave output. Staring oscillations in the circuit relies on the unbalance existing between the apparently identical circuits of Q1 and Q2. This is due to a small unbalance in both external circuits and the transistor themselves. Because of this small unbalance, more current will flow in one of the primary windings of transformer T1 than in the other. Ultimately, the oscillation takes place across the center-taped primary of transformer T1 which has ratio of windings N1:N2=1:14. Assuming that the astable produces a square waveform and approximating the analysis to the case of a purely resistive load at the drain of Q1-Q2, the oscillation period is

$$T_a \cong 2R_3C_X \ln\left[\frac{(VR - V_{GS})}{(2VR + V_{GS} - V_{DSsat})}\right] \qquad \text{.....(3.2)}$$

where C_X exhibits the series association of C_5 and $0.5C_7$ (12, 37, 38). By selecting R_3 = R_4 = 10 kΩ, C_5 = C_6 = 0.47 μF, C_7 = 2.2 μF, preliminary measurements denoted an oscillation-frequency interval of 200 Hz ≤ f_a ≤ 310 Hz, for 1 V≤ VR ≤ 20 V. A high-voltage oscillation is developed at its secondary. Supply voltages V^+ and V^- are available after ac/dc conversion by the bridge diodes D6-D9 and capacitors C8-C9.

3.1.3 Switching and timing circuit

The timing and switching circuit are designed and constructed to control driving stimulation current to load appropriately. The timing circuit is used to generate

a rectangular pulse which can be variable frequency and duration. In operation of timing circuit, it is derived by software controlling via counters in DAQ board. Counters add counting or high-precision timing to drive the switching circuit for controlling the pulse stimulation of stimulator. Counters respond to and output TTL signals—square-pulse signals that are 0 V (low) or 5 V (high) in value. Although counters count only the signal transitions (edges) of a TTL source signal, it can use this counting capability in generating square TTL pulses for imposing pulse stimulation and triggers for data acquisition application. There are two basic types of counter signal generation; toggled and pulsed. When a counter reaches a certain value, a counter configured for toggled output changes the state of the output signal, while a counter configured for pulsed output outputs a single pulse. The width of the pulse is equal to one cycle of the counter's SOURCE signal. The following is a list of terms which should know before outputting a pulse or pulse train using LabVIEW:

• Phase 1 refers to the first phase or delay to the pulse.

• Phase 2 refers to the second phase or the pulse itself.

• Period is the sum of phase 1 and phase 2.

• Frequency is the reciprocal of the period (1/period).

• In LabVIEW, it can adjust and control the times of phase 1 and phase 2 in counting operation. It does this by specifying a duty cycle. The duty cycle equals

$$\frac{phase2}{period} \quad \text{where } period = phase\ 1 + phase\ 2 \qquad \ldots\ldots(3.3)$$

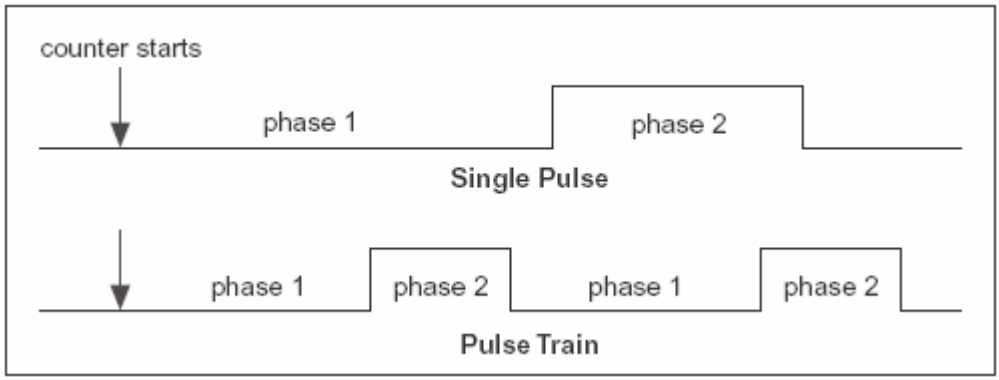

Figure 3.3 Pulses Created with Positive Polarity and Toggled Output.

Each counter-generated pulse consists of two parts, phase 1 and phase 2. If the counter is configured to output a signal with positive polarity and toggled output, as shown in the following above diagram, the period of time from when the counter starts counting to the first rising edge is called phase 1. The time between the rising and the following falling edge is called phase 2. If users configure the counter to generate a continuous pulse train, the counter repeats this process many times as shown on the bottom line of Figure 3.3. The counter chip used for generating a continuous pulse train is DAQ-STC chip that can configure the DAQ-STC to count either low-to-high or high-to-low transitions of the SOURCE input. The counter has a 24-bit count register with a counting range of 0 to 224–1. It can be configured to increment or decrement for each counted edge. Furthermore, whether the count register increments or decrements can be controlled with an external digital line, which is useful for encoder applications.

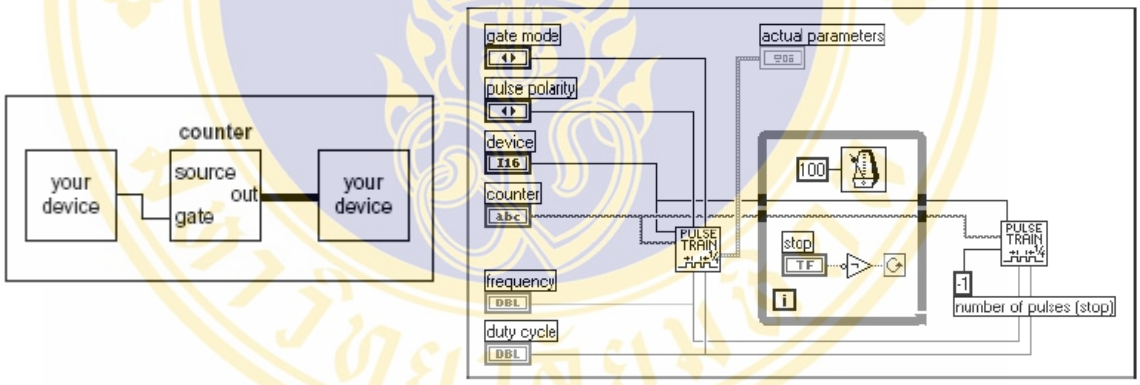

(a) (b)

Figure 3.4 a) Physical Connections for Generating a Continuous Pulse Train.
b) Diagram of Continuous Pulse Train (DAQ-STC) VI.

Figure 3.4a illustrates to connect the counter and device to generate a continuous pulse train. The edges of the internal source signal are counted to generate the output signal. The continuous pulse train is obtained for external device from the OUT pin of counter. It can optionally gate the operation with a signal connected to the GATE input pin. Instead of having an internal timebase as SOURCE, it can connect an external signal. Figure 3.4b shows the diagram of the continuous pulse train VI written by LabVIEW. This shows to use the Easy Counter VI, Generate Pulse Train, to

specify the frequency, duty cycle, and pulse polarity of pulse train output. The number of pulses parameter defaults to 0 for continuous generation. When you click the STOP button, the While Loop stops, and a second call to Generate Pulse Train with the number of pulses set to –1 stop the counter. With this VI it can specify the frequency, duty cycle, and pulse polarity of pulse train output.

The device number is assigned to the plug-in DAQ board during configuration. This parameter defaults to 1. The counter parameter is the number of the counter that wants to use. The default input is 0 which may select to use counter 0 or 1 on DAQ-STC based MIO boards. The frequency parameter is the desired repetition rate of the continuous pulse train that is set in range from 0.1 Hz to 1.0 Hz. The default input is 0.5 Hz. The duty cycle parameter is the desired ratio as follow the equation 3.3. If duty cycle is equal to 0 or 1, the VI computes the closest achievable duty cycle using a minimum period of three timebase cycles. A duty cycle very close to 0 or 1 may not be achievable. Both frequency and duty cycle are used to calculate pulse durations (phase 2) of continuous pulse train. Referring to the equation 3.3 the duration is obtained in range of 0.1–1.0 ms. The Continuous Pulse Generator Config VI configures the counter for the operation, and the Counter Start VI controls the initiation of the pulse train. In here, it wants to generate a continuous pulse train as the result of meeting certain conditions. If the Easy VI is used, the pulse train will start immediately. With the Intermediate VIs, it can configure the counter at the beginning of the application, and then wait to call Counter Start after the conditions are met. This approach will improve performance. When the STOP button is clicked, the While Loop stops, and Counter Stop is called to stop the pulse train.

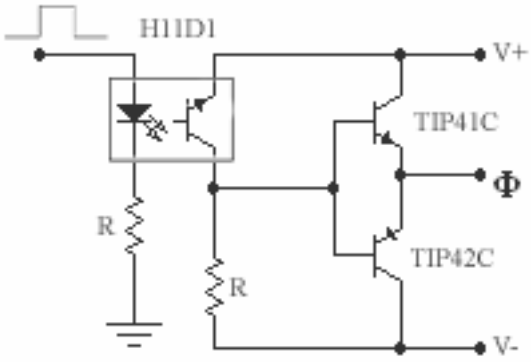

Figure 3.5 The switching circuit.

On the present thesis, the pulse duration of load current is imposed by the pulse output of the counter's OUT pin on DAQ board. This pulse is input to the optocoupler (H11D1) before the switching circuit is achieved. This optocoupler functions to isolate electrically between the circuit used for stimulating and the circuit used for imposing the pulse duration. The H11D1 is an optocoupler with very high collector-emitter breakdown voltage (BV_{CER} = 300V). It is intended for any DC application requiring a high blocking voltage that is suitable for using in here. High-voltage control phase Φ is available at the push-pull (TIP41C, TIP42C) output. The schematic of switching circuit can be shown as follow in Figure 3.5 above.

3.1.4 Voltage-to-Current Converter

In this part, the V/I converter is a driving stage that based on a self-biased current mirror formed by MOS transistors M1-M5 (MTP2N60). The standard cascade configuration was chosen by its simplicity while providing a high dynamic output-impedance (12, 41). All transistors are high-voltage N-channel MOSFET which use an advanced termination scheme to provide enhanced voltage-blocking capability without degrading performance over time. In addition, this advanced TMOS E-FET is designed to withstand high energy in the avalanche and commutation modes. The new energy efficient design also offers a drain-to-source diode with a fast recovery time. They are designed for high voltage, high speed switching applications in power supplies, converter and PWM motor control. These devices are particularly well suited for bridge circuits where diode speed and commutating safe operating areas are critical and offer additional safety margin against unexpected voltage transients. The schematic of the driving stage can be shown in Figure 3.6 as follow below.

The following the schematic circuit below Re and Ce are the reactive components of the electrode/skin interface and Rs is the tissue resistance. Fixing R_{ref} and denoting $V_{hv} = V^{+} - V^{-}$, it comes out

$$I_{skin} = (V_{hv} - V_{GS1} - V_{GS3})/ R_{ref} \qquad \text{……..(3.4)}$$

Thus, V_{hv} determines the current through the skin, which is independent of load characteristic, at good approximation. Adjusting I_{skin} by means of R2 in the voltage-regulator compensates for the poor matching between discrete transistors in the current

mirror (13, 41). Upon assertion of phase Φ, M5 switches on the current mirror, so that a pulsed current is delivered by the stage.

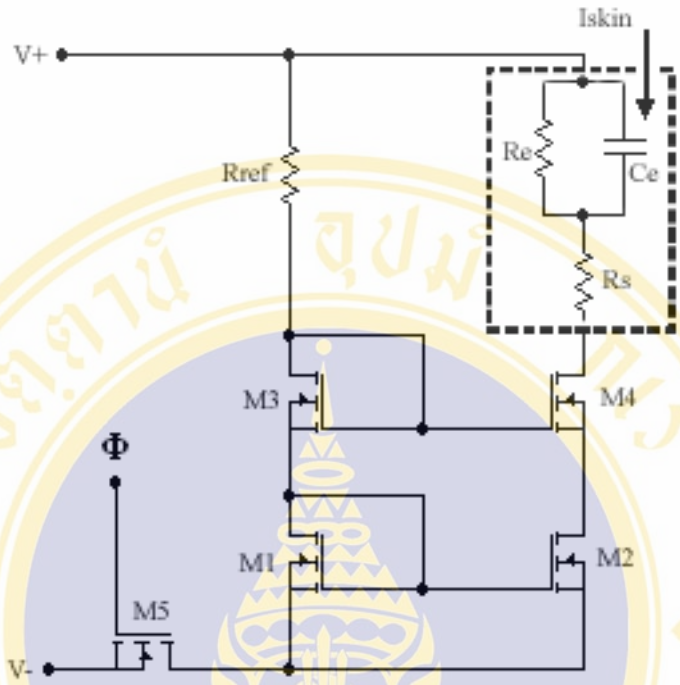

Figure 3.6 The schematic circuit of Voltage-to-Current Converter.

3.2 The methods and materials of data acquisition

In this section, the procedures of design and construction for the data acquisition system are described. The processes of data acquisition cover both in part of analog and digital system. In the part of analog system, the sensor and signal conditioning circuitry are achieved to prepare the signal appropriately for the digital process. The measured response known as H-reflex and M-wave must be acquired and adjusted to a form appropriate for input into the data acquisition system. Because of the measured physical quantity, or reflex, is in a form of electrical quantity (voltage) that is provided as a biopotential and has only a few millivolts, the surface recording electrodes are sufficiently used as a sensor for the detection of reflex and the signal condition consisted of the preamplifier and the filter are essentially used for modifying the dynamic range to maximize the accuracy of the data acquisition system, removing unwanted signals, respectively. The output voltage of the surface recording electrode are first collected, then amplified and conditioned, and then passed on to a computer for digital conversion and ultimate used by LabVIEW program. The total process is

also reffered to as analog-to-digital conversion. The Figure 3.7 illustrates the block diagram of the entire process in data acquisition system.

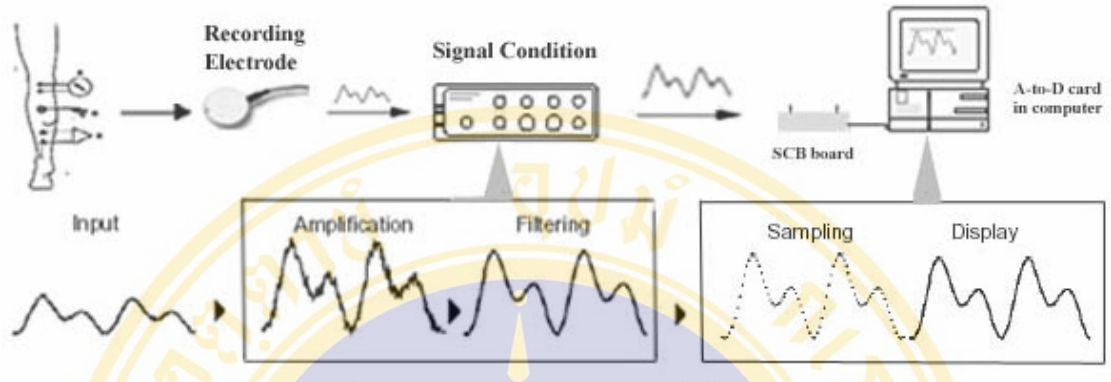

Figure 3.7 The process of data acquisition system.

From the previous paragraph, the feature of H-reflex measurement is provided as a biopotential that is in a pattern of voltage. The output voltage of H-reflex is often very small that may be either microvolts or millivolts. Because of the latency of H-reflex is initially released in order of 28-35 milliseconds and has the pulse width about 5-10 milliseconds, its frequency response is thus from 5 Hz to 10 kHz. In the block diagram of Figure 3.7, the recording electrodes measure voltage output from a muscle. As such, this small reflex potential need to be amplified and conditioned (e.g., filtered) before digital conversion. For this case, the H-reflex is usually amplified by a preamplifier and again by a selecting amplifier to provide sufficient signal gain. The signal conditioning is achieved using a combination of both hardware and software. The analog filtering using a Butterworth filter is designed and constructed in the part of hardware to offer low-pass filtering option. Then, LabVIEW is used for the software conditioning again. The digital filtering using a Butterworth filter was discussed, and a software filter was constructed as a subvirtual instrument (subVI) to offer bandpass option. After, the reflex is completely amplified and conditioned, hardware interface devices are used to acquire this reflex and pass it on to a computer for digital conversion by an A-to-D board. The options for this process will be described in the next section. After, the reflex have been digitized, it is ready to be accessed by LabVIEW functions. The program to be constructed by LabVIEW is

defined as a virtual instrument, VI. This VI communicates with the computer's A-to-D board and acquires data from a measurement tool.

For more procedures and details of this section are reasonably discussed out to be four parts. These parts are composed the recording electrode used for detection of reflex, the signal conditioning circuitry, hardware interface devices and A-to-D conversion, and LabVIEW functions.

3.2.1 Electrode for reflex measurement

The electrodes used for the reflex measurement consist of a pair of recording electrodes and a ground electrode. The type of used recording electrodes is a surface silver/silver chloride disc recording electrodes. This recording electrode is beneficial and appropriate for the study of reflex measurement because its characteristic shows several advantages. These advantages include low input impedance, small size that can pick up any place on the body, safer and easier to use than needle electrode, and high efficiency in detecting signal. The silver/silver chloride disc electrodes can be shown in Figure 3.8a below.

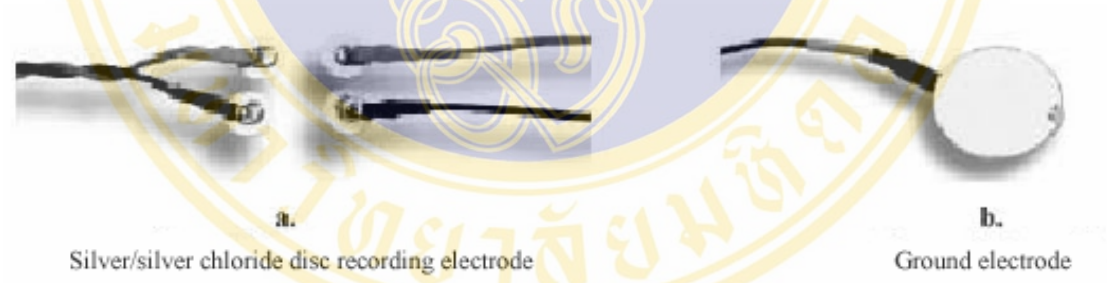

Figure 3.8 Electrodes for reflex measurement.

The recording electrodes use to record a reflex of electric potential difference. The recording of this reflex require commonly two electrodes. One electrode closed to the source of the activity to be recorded is called the active or exploring electrode. The other electrode is called the reference electrode. The use of both electrode associates with the efficiency of signal detection. Because of the unwanted signal may disturb to detect reflex, the ground electrode should be exploited to guard these noises. The Figure 3.8b shows the ground electrode used in measurement system. The specification of ground electrode requires sufficiently a large cross-section diameter because this electrode is connected to subject and a large conducting body that used as

common returns for an electric circuit and as an arbitrary zero potential reference point. After the reflex is measured by the recording electrodes, the small reflex is passed to the part of signal conditioning for amplifying and filtering next.

3.2.2 Signal conditioning

The signal conditioning is an important part for the preparation of signal before to be passed to A-to-D conversion. The signal conditioning circuitry is consisted of the preamplifier unit, the filter unit, and driver amplifier unit. The entire procedures of these units are shown the block diagram in Figure 3.9.

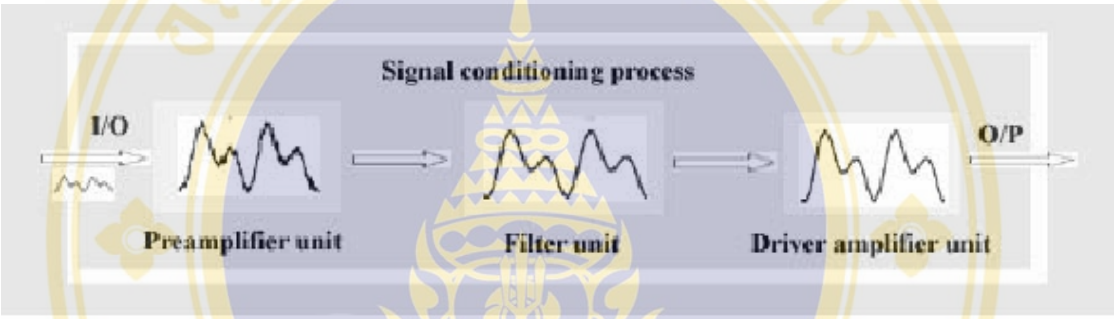

Figure 3.9 Block diagram of signal conditioning.

From the block diagram in Figure 3.9, the first stage of signal conditioning process is preamplifier. The preamplifier unit is designed to use an instrumentation amplifier since this amplifier is a differential amplifier with high input impedance, low output impedance, high common mode rejection ratio (CMRR), and easy to adjust amplify gain. Consequently, the precision instrumentation amplifier AD524 is chosen to use as a preamplifier in the first stage of signal conditioning process (31, 42, 43). The preamplifier circuit with AD524 can be shown in Figure 3.10.

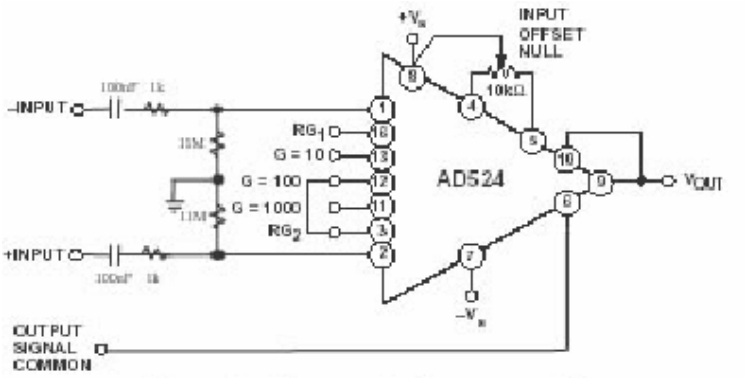

Figure 3.10 Preamplifier circuit (AD524).

The AD524 is a precision monolithic instrumentation amplifier designed for data acquisition applications requiring high accuracy under worst-case operating conditions. An outstanding combination of high common mode rejection, high linearity, low noise, and low offset voltage drift makes the AD524 suitable for use in many data acquisition system. Its specification has input and output offset voltage drift of less than 25 μV/°C, common mode rejection (CMR) above 90 dB at unity gain and 120 dB at gain of 1000, and maximum nonlinearity of 0.003% at unity gain. Furthermore, the outstanding DC specification the AD524 also has a 25 MHz gain bandwidth product (gain = 100). To make it suitable for high speed data acquisition systems the AD524 has an output slew rate of 5V/μs and settles in 15 μs to 0.01% for gains of 1 to 100. As a complete preamplifier (AD524 IC) does not require any external components for fixed gain of 10, 100, and 1000. For other gains setting, the only a single resistor is required. The AD524 input is fully protected for both powers on and power off fault conditions (32, 33, 44, 45, 46).

The signal measured by the AD524 preamplifier will be amplified together to noise signal. This noise signal disturbs to the real required signal in system that usually include as either high noise frequency or low noise frequency, or both. The elimination of noise or unwanted frequency response can be achieved by using an analog filter technique. The method of filtering is the next step of the signal conditioning process. There are two kinds of filter that are used in this filter unit: low-pass and notch filter. For low-pass filter unit, the active filter in type of butterworth filter is chosen and achieved for design and construction. This filter is implemented by using three fundamental components: resistors, capacitors, and operational amplifier (Op-amp). The benefits and outstanding reasons of choosing this filter are:

- It has bandwidth covering required frequency response to be lower 1 MHz.
- It allows the more constant gain and smoother signal in interval transmission pass band than when compare with other filter type, i.e., Chebyshey and Bessel filter.
- It is best suited for application requiring preservation of amplitude linearity in the passband region.
- The maximum overshoot in the passband allows the determination of the minimum necessary order to achieve the desired response.

- The filter's transition band attenuates the input signal -60 dB for every 10-fold change in frequency value. This assists to perform the precise cutoff frequency.

The Butterworth filter is designed in the mode of low-pass filter by using the frequency cut-off approximately 10 kHz. The low-pass Butterworth filter is planed by using the cascade technique of the second order filter connecting with the first order filter. The low-pass filter's transition band is become to attenuate the input signal -60 dB/decade. This takes from the attenuation in the second order (-40 dB/decade) combining with the first order (-20 dB/decade). This helps to increase the slope of cut-off frequency. Next, the notch filter is achieved. This filter is used for eliminating the electrical noise, generated from power line radiation (50 Hz), by using twin-T notch filter. The twin-T notch filter is designed and constructed to attenuate at least 40dB at 50 Hz, and its pass-band attenuation does not exceed 0.5 dB (42, 49, 50). To do these, TL084 is used to construct low-pass filter and notch filter. The TL084 is an operational amplifier combined two state-of-art linear technologies on a single monolithic integrated circuit (47, 48, 49). Each internally compensated operational amplifier has well matched high voltage JFET input devices for low input offset voltage. The BIFET technology provides wide bandwidth and fast slew rates with low input bias currents, input offset current, and supply current (31, 49, 50). The low-pass filter circuit and notch filter can be shown in Figure 3.11.

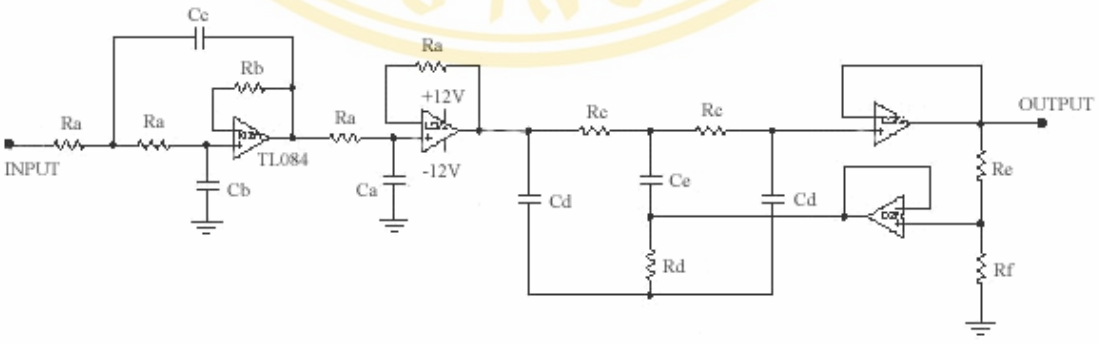

Figure 3.11 Schematic of Low-pass and Notch Filter.

As follow in Figure 3.11, the cutoff frequency of low-pass filter can be calculated by $\omega_C = 2\pi f_C$, where f_c is cutoff frequency in hertz that will be determined about 10 kHz. The resistance of R_a is given by $1/\omega_C C_a$. C_a is determined in range from

1 nF to 0.1 μF. Here, C_a is chosen in order of 0.022 μF. After R_a and C_a are obtained, R_b, C_b, and C_c are given by

$$R_b = 2R_a \quad , \quad C_b = 0.5C_a \quad . \quad C_c = 2C_a$$

At f_c = 10 kHz, R_a is equal to 722 Ω, R_b = 1.44 kΩ, C_b = 0.012 μF, and C_c = 0.047 μF, respectively.

For notch filter, 50 Hz generated from power line radiation is rejected. The frequency reject (f_r) is given by

$$f_r = \frac{\sqrt{C_1 + C_3}}{2\pi\sqrt{C_1 C_2 C_3 R_1 R_3}} \qquad \ldots\ldots(3.5)$$

Commonly, $C_1 = C_3 = 2C_2$ and $R_1 = R_3 = 0.5R_2$. By choosing $C_1 = C_d$ = 47 nF, the value of components is equal to $C_2 = C_e$ = 94 nF, $R_1 = R_c$ = 680 kΩ, $R_2 = R_d$ = 340 kΩ, respectively.

The filter circuit does not only eliminate noise but also reduce the required signal. Therefore, the output signal level may be insufficient for displaying and processing in next part. The driver amplifier is then used for adjusting gains of system again. LM741 is used for this purpose by applying as a non-inverting amplifier, whose can adjust gain from 1 to 50 times. The LM741 amplifier offers many features which make their application nearly foolproof: overload protection on the input and output, no latch-up when the common mode range is exceeded, as well as freedom from oscillations (47, 48, 51, 52). The schematic of selecting gain can be shown in Figure 3.12 below.

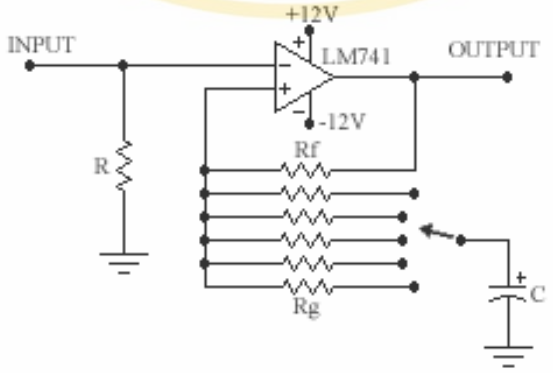

Figure 3.12 Schematic of selecting gain circuit.

After the reflex signal is passed through the selecting gain circuit, the signal level will be high sufficient for displaying and signal processing (36, 47, 49, 52).

3.2.3 Analog to digital conversion (A-to-D conversion)

After the signals obtained the suit preparation from the previous parts, these signals are ready to convert them to digital format. The methods and materials of this conversion are commonly referred as analog to digital conversion, A-to-D conversion. For this thesis, the A-to-D converter is a plug-in data acquisition (DAQ) device of National Instruments Corporation that is a board to be sat in a slot in a computer's motherboard and is connected to signal source with cables. This device is chosen and often considered to be the entire DAQ system, although it is actually only one system component. The DAQ system selected in this thesis cannot always directly connect the signal to a plug-in DAQ device. It must use accessories to condition the signal before the plug-in DAQ device converts analog information to digital information. Then, the software controls the DAQ system by acquiring the raw data, analyzing the data, and presenting the results.

The plug-in DAQ device of National Instruments Corporation offers a wide variety of A-to-D boards for a number of platforms including Windows, Macintosh, and Sun workstations. For this thesis, the AT-MIO-64E-3 multifunction DAQ board for Windows NT/95/3.1 was used. This board uses E-series technology to deliver high performance and reliable data acquisition capabilities for a wide range of applications. Furthermore, this board offers 64 channels using 12-bti resolution with trigger capability and a total sampling rate of 500,000 Hz. All instruments and sensors used to make measurements output their amplified/conditioned signals via standard SCB connectors and coaxial cables. Data input to the DAQ board was via a SCB-100 adapter interface board and was connect with a 100-pin cable. The SCB-100 is shielded I/O connector blocks for rugged, very low noise signal termination for connecting to 100-pin E series DAQ devices. The hardware connections between the computer's A-to-D board, a SCB interface board, and an analog input can be shown in Figure 3.13a.

NI-DAQ™ software was used to configure the DAQ board. This board has Windows "plug and play" capability, making board configuration relatively easy. The DAQ board is automatically detected by the computer, and a Windows setup Wizard guides the user through several setup procedures assigning device numbers and channel interrupts (19). Typically, DAQ software includes drivers and application

software. Drivers are unique to the device or type of device and include the set of commands the device accepts. Application software, LabVIEW, sends the commands to the drivers for configuring, acquiring data from and sending data to DAQ device. All National instruments DAQ devices are packaged with NI-DAQ driver. This prompts to have the NI-DAQ driver software installed. The LabVIEW and NI-DAQ driver are installed to set up hardware installation and configuration and software configuration instructions. LabVIEW uses the software configuration information to recognize hardware and to set default DAQ parameters. The NI-DAQ driver provides LabVIEW with a high-level interface to DAQ device and signal conditioning hardware. The relationship between LabVIEW, NI-DAQ, and DAQ hardware can be shown in the Figure 3.13b.

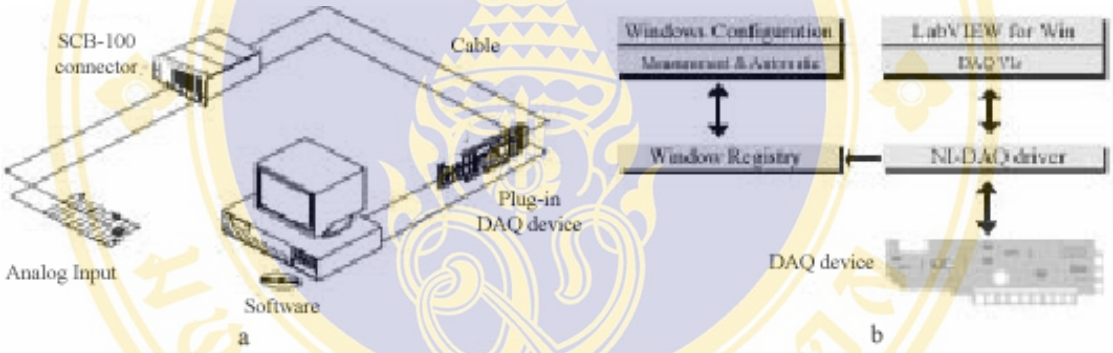

Figure 3.13 a) Hardware connection of DAQ system.
b) How NI-DAQ relates to Hardware and DAQ device.

From the block diagram in Figure 3.13b, the LabVIEW installer copies the required files for DAQ to computer. The DAQ VIs access the standard NI-DAQ for Windows 32-bit DLL. The NI-DAQ DLL then interfaces with the Windows registry to obtain the configuration parameters defined by Measurement & Automation Explorer. Because of the DAQ board have a Plug & Play device, the Windows Configuration Manager automatically detects and configures the device. LabVIEW installs a configuration utility, Measurement & Automation Explorer, for establishing all device and channel configuration parameters. This reads the information the Device Manager records in the Windows registry and assigns a logical device number to each DAQ device. Use the device number to refer to the device in LabVIEW. With DAQ device, the hardware only converts the incoming signal into a digital signal that is sent to the

computer. The DAQ device does not compute or calculate the final measurement. That task is left to the software that resides in the computer. LabVIEW comes with many acquisition and analysis functions to make that task easy. When installing and configuring DAQ hardware are achieved completely, LabVIEW is ready to take the data and present it in a form the user can understand.

Because of VIs written by that LabVIEW depend on form of individual input signal, therefore, a definition and understanding of H-reflex's form relative in data acquisition with LabVIEW has firstly to be achieved before LabVIEW program will be written to control these conditions or applications. The characteristics of H-reflex signal can be defined as follow:

- H-reflex is an analog input that is in group of time domain. It varies to follow time that acquires several points of data at a fast scan rate. This cause the measured signal will display a waveform.
- H-reflex comes in a form of non-referenced signal source, or floating signal, because of the output signal is not connected to an absolute reference such as earth or a building ground, and the system use battery-supply and transformer that explicitly floats its output signal.

3.2.4 LabVIEW function

For this thesis, LabVIEW is written as a VIs to program data acquisition for acquiring, displaying, analyzing, and storing the data of H-reflex. Because of the purpose of measured H-reflex would like its waveform, displaying continuously, analyzing some parameter, and option for either saving or opening data, therefore, the data acquisition worked with LabVIEW function can be serially explained out to be four main parts: the acquiring data, the monitoring data, the analyzing data, and the saving/opening data.

A. The acquiring data part

In this part, LabVIEW is written to obtain the data continuously with using a technique of circular buffering method. This method is appropriate for viewing, processing, or logging portions of data as it is being acquired similar to continuous data acquisition. The VIs is set up a circular buffer to store acquired data in memory. Portions of data are read from the buffer while the buffer is being filled. Using this technique, the system can set up device to continuously acquire data in the background

while LabVIEW retrieves the acquired data. The procedures of a circular buffer can be shown in Figure 3.14a below.

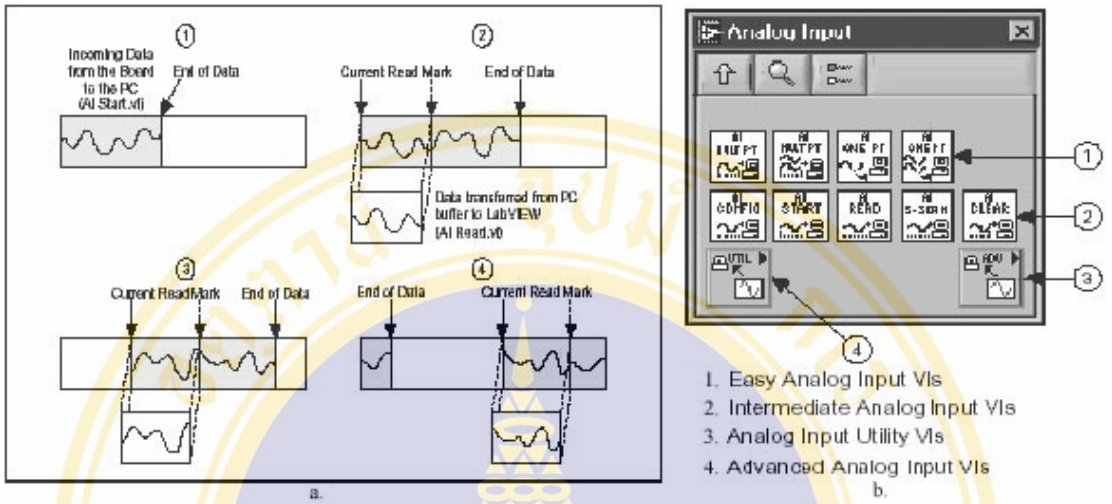

Figure 3.14 a) How a circular buffer works.
b) Analog Input VI palette organization.

When the circular buffer gets data to the end of it, it returns to beginning and filling up the same buffer again. This means that data can read continuously into computer memory, but only a defined amount of memory can be used. The VI must recover data in the blocks, from one location in the buffer, while the data enters the circular buffer at a different location, so that unread data is not overwritten by newer data. Continuous data acquisition is useful for this application with streaming data to disk and displaying data in the real time. There are two possible problems that can occur with this technique of acquisition: (1) VI could try to retrieve data from the buffer faster than data is placed into it, or (2) VI might not retrieve data from the buffer fast enough before LabVIEW overwrites the data into the buffer. When VI tries to read data from the buffer that has not yet been collected, LabVIEW waits for the data VI requested to be acquired and then returns the data. If VI does not read the data from the circular buffer fast enough, the VI sends back an error, advising that some data has been overwritten and lost.

The LabVIEW function used in this part is DAQ VIs located in Function palette in the block diagram of LabVIEW program. The Function>>DAQ palette consist of six sub-palettes that contain the different classes of DAQ VIs, including

Analog Input VIs, Analog Output VIs, Digital I/O VIs, Calibration and Configuration VIs, and Signal Conditioning VIs. These sub-palettes arrange the VIs in different levels according to their functionality. The Analog Input VIs in Intermediate level located on the second row as shown in Figure 3.14b is chosen to use for this case because they have several advantages over other VIs levels. These advantages are as follow:

- Maintain to circular buffer.
- More hardware functionality and efficiency in developing applications than the Easy VIs.
- More control over error-handing than the Easy VIs.
- More convenient to use applications than the Advanced VIs.
- More level interface to the DAQ driver than the Advanced VIs.

The following Figure 3.14b previously the Intermediate Analog Input VI used for acquiring data includes AI Config, AI Start, AI Read, and AI Clear that all is called on the block diagram. This subVIs is presented to demonstrate the order of execution of the VIs and the use of the taskID to control data flow. AI Config configures the channels of installed DAQ device, allocates a buffer in computer memory, and generates a taskID. AI Start programs the counters on the DAQ device and starts the acquisition. AI Read reads data from the buffer in computer memory. AI Clear frees computer and DAQ device resources. The LabVIEW function supports to manipulate errors when they occur. By using Simple Error Handler VI to display the error cluster propagated through from that VIs. This means when an error occurs, a dialog boxes of Simple Error Handler VI shows promptly that error. Using these functions, the flowchart of data acquisition can be shown in Figure 3.15.

In acquiring H-reflex signal, an important parameter is latency itself. The latency must be relative to time because of it is the interval between the onset of a stimulus and the onset of a response. This latency is used for analyzing the behavior of reflex. To acquire the latency of reflex appropriately and correctly, controlling data acquisition with a trigger is achieved. Following the flowchart in Figure 3.15 trigger conditions are specified in the configuration section by calling appropriate DAQ VIs in LabVIEW. Generally, a trigger is any event that start data capture. A triggered acquisition provides two key advantages to the user. First, it time-references the input

signal relative to the trigger event. Second, the user can capture the signal only in the region of interest and thus conserve hardware bandwidth and memory (20).

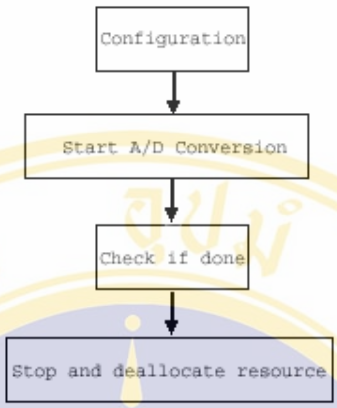

Figure 3.15 Flowchart for data acquisition.

Using a triggering technique, the system start an acquisition based on the condition or state of either an analog or digital signal. There are two basic types of triggering with LabVIEW, hardware and software triggering. Here, use it with an external device to perform hardware triggering; because of a data acquisition depends on an external stimulator for transmitting data. Hardware triggering is used to set the start time of an acquisition and gather data at a known position in time relative to a trigger signal. In neurostimulator has trigger output for producing hardware trigger signal. In LabVIEW, the user specifies the triggering conditions that must be reached before acquisition begins. When the conditions are met, the acquisition starts. The trigger signals in hardware triggering can be classified into two types: digital and analog trigger. The digital trigger is selected as it was in line with trigger output of neurostimulator. Usually, the digital trigger is a transistor-transistor logic (TTL) signal having two discrete levels: a high and a low level. When moving from high to low or low to high, a digital edge is created that may be rising or falling edge. The result of the rising or falling edge of digital trigger signal is set to begin data acquisition.

In Figure 3.16a, the acquisition begins after the falling edge of the digital trigger signal. The digital trigger signals are connect to EXTTRIG*, DTRIG*, or PFI pins on DAQ device. Figure 3.16b shows a timeline of how digital triggering works for post-triggered data acquisition. Here, neurostimulator sends a trigger, or TTL

signal, to DAQ device. As soon as DAQ device receive the signal, and trigger conditions are met, DAQ device starts acquiring data.

(a) (b)

Figure 3.16 (a) Diagram of digital trigger.
(b) Digital triggering with DAQ device.

The block diagram of VI written by LabVIEW can be shown in Figure 3.17 below. This VI continuously acquires data from one analog input channel when a digital start trigger occurs. This is a timed acquisition, meaning that a hardware clock is used to control the acquisition rate for fast and accurate timing. The VI uses the Intermediate VIs to perform a buffered acquisition, where LabVIEW stores data in an intermidiate memory buffer during acquisition. Data are retrieved from that buffer and displayed on the graph. For E-series DAQ boards, the trigger signal is connected to PFI/TRIG1 pins.

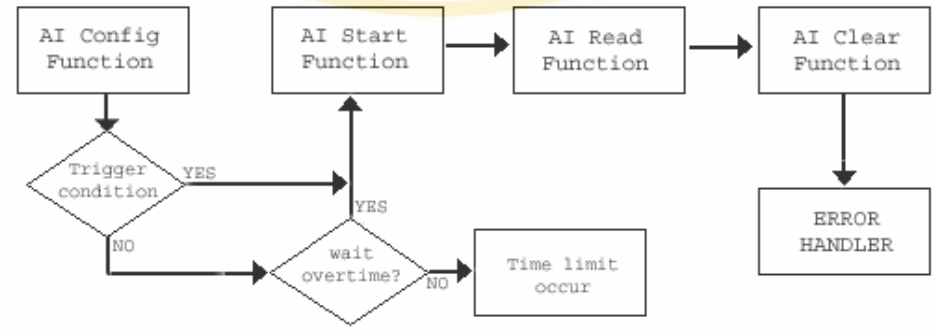

Figure 3.17 Block diagram of controlling acquisition with digital triggering.

The figures in Figure 3.17 are represented to demonstrate the order of execution of the VIs and use of taskID to control data flow. The block diagram calls

AI Config, AI Start, AI Read, AI Clear, and General Error Handler. The LabVIEW is configured for continuous DAQ by instructing AI Start to acquire data indefinitely. To initiate the acquisition, set number of scans to acquire in AI Start to 0. AI Read is called in a looping structure to retrieve data from the buffer and then the data is sent to a graph and so on. AI Clear halts the acquisition, deallocates the buffers, and frees any device resources. The user can acquire data both before and after a digital trigger signal. If pretrigger scans in AI Start is greater than 0, the DAQ device acquires data before the triggering conditions are met and subtracts the pretrigger scans value from the number of scans to acquire value to determine the number of scans to collect after the triggering conditions are met. If pretrigger scans are 0, the device acquires the number of scans to acquire after the triggering conditions are met. The default for this parameter is 0, which means LabVIEW does not save any data before the trigger. Before the user begins acquiring data, the user must specify in the trigger edge input whether the acquisition is triggered on the rising or falling edge of the digital trigger signal. The user also can specify a value for the time limit, the maximum amount of time the VI waits for trigger and requested data. For more information on parameters in Figure 3.17, refer to Advanced Analog Input VIs, of the LabVIEW Function and VI Reference Manual (21), or to the LabVIEW online Reference, available by selecting Help>>Online Reference.

B. The displaying data part

When AI Read VI called in While loop structure reads data from the buffer allocated by AI Config VI, it controls the number of points to read from the buffer, returns scaled voltage data, and sets the buffer location from which to read data. Data read by AI Read can be in form of a single value, a 1D array or a 2D array. The following the Figure 3.18 below the read data by AI Read VI is 2D array that contains analog input data in scaled data units. The data appears in columns, where each column contains the data for a single channel. The interest data are selected using a Transpose 2D Array and an Index Array function to rearrange the data channel from 2D to 1D array. The interest data become 1D array that is simple and appropriate for arrangement. The data is delivered to a digital filter before it is bring to display on the graph. This VIs provides a digital filter for smoothing a data curve of signal artifact or noises. A butterworth digital (software) filter is used to process the interested data.

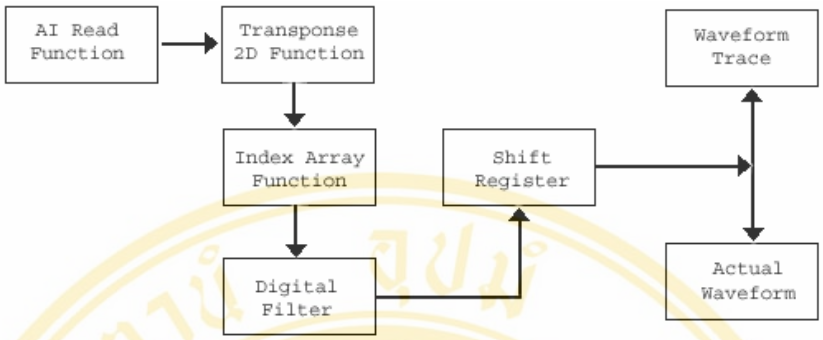

Figure 3.18 Block diagram of displaying data acquisition.

In LabVIEW, the butterworth.vi is accessed from the block diagram in the Functions/Signal Processing/Filters palette. The operative condition of this filter is bandpass. Note that along the top border of the icon is an Enum Constant labeled "Bandpass", where the string associated with an integer value are part of the data type. The filtered data are ported to an Output Array. Three Digital Controls are used to define the "Order" and "High and Low Frequency Cuttoff", respectively. The sampling frequency is fixed at 50 kHz. The default values for "Order", and "Low and High Frequency Cuttoff" have been set at "4", "5 Hz", and "10 kHz", respectively. Note in this VI that two Butterworth filters are separated by a Reverse 1D Array function. Digital filtering causes a phase shift (a constant error) and may be corrected by reversing polarity of the signal using the Reverse 1D Array function and passing it through the filter again. The on/off digital filter is controlled by a Boolean Case Structure toggled by a Boolean Labeled Button. The default case is "Off" (i.e., false condition).

After the digital filtering, the filtered data are ready for displaying them on the graph. Usually, the VIs with graphs collects the data in an array and then plots the data to the graph. The waveform graph plots only single-valued functions, as in y = f(x), with points evenly distributed along the x-axis, such as acquired time-varying waveforms. The following illustration shows the elements of displaying this VI.

The Waveform Graph to the right (G1) displays the data trace file: both present and previous data. This uses a Build Array function for building the data structure to plot nine arrays on a waveform graph, and uses Shift Registers on a While Loop

Structure to transfer values, one loop iteration to the next. The transpose option is enabled for this graph so that the data is plotted correctly. The Waveform Graph to the left (G2) only exhibits the present data. This graph provides the data available before they are analyzed. The user can use "Select" button on the front panel to select the subset of data to analyze. A Cursor Display for this graph is linked to an Attribute Node that automatically reads the start and end coordinates on the x-axis. These points are used to display the average, peak, and location of interest signal in the Waveform Graph in Figure 3.19, visible when the "Analyze" button is pushed.

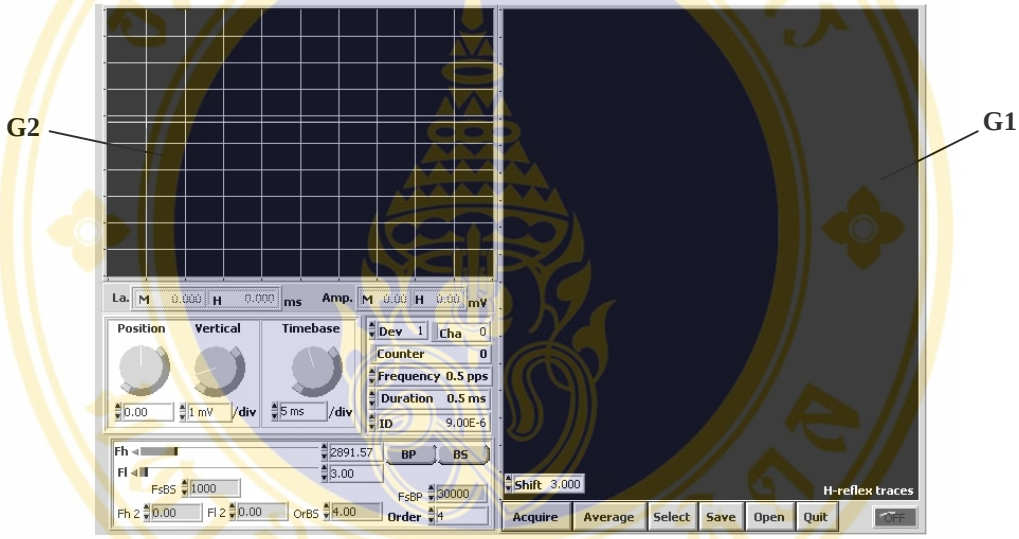

Figure 3.19 Front panel of controlling data acquisition.

C. The analyzing data part

In this part, the VI provides a generic data analysis VI that permits partitioning of a segment of data on-the-fly without having to run and rerun the program numerous times. After data is reformed by the digital filter, they are available to access analysis as desired. The function used in analyzing data consists of signal averaging for improving the accuracy of measurement and peak detection for finding the locations and amplitudes of local maxima and minima in a signal that satisfies certain properties. Averaging multiple samples to arrive at single measurement (and error) is a good way to improve the accuracy of measurement. The premise of averaging is that noise and measurement errors are random, and therefore, by the Central Limit Theorem, the error will have a normal (Gaussian) distribution. By averaging multiple

points, it arrives at a Gaussian distribution. It can then calculate a mean that is statistically close to the actual value. Furthermore, the standard deviation that is derived from the measurements gives the width of the normal distribution around the mean, which describes the probability density for the location of the actual value. The standard deviation is proportional to $1/\sqrt{N}$, where N is the number of samples in the average. Therefore, the more points are taken in the average, the smaller the standard deviation from the average. In other words, the more points averaged, the more accurately the actual value achieved.

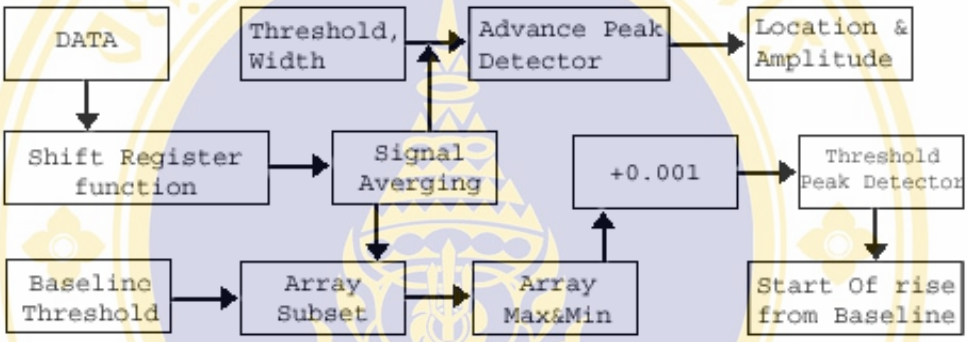

Figure 3.20 Block diagram for analyzing data.

The peak detection is one of the most important time-domain functions performed in signal monitoring. During analysis, it is necessary to establish a point in time when the signal rises from baseline and to found a location/amplitude when the signal occurs. The Threshold Peak Detector VI is achieved for establish the point that the actual signal rise from baseline (noise). This point has been determined by using the segment of code shown in the block diagram of Figure 3.20. Key elements of this routine include the Array Subset and Threshold Peak Detector.vi functions. The maximal amplitude of a predetermined, filtered, and averaged segment of baseline noise is identified. This segment is referenced using an Array Subset function. A small voltage, default = 0.001 volts, is added to the maximal amplitude determined using an Array Max&Min function. This represents the differentiation point between baseline noise and the true signal arising from baseline. For the Advance Peak Detector, it is obtained for finding locations and amplitudes on a waveform graph. The locations display the output array of the peaks, which is still in terms of the indices of the input waveform. For example, if one element of Locations is 100, that means that there is a

peak located at index 100 in the data array of the input waveform. The following equation locates the peaks and valleys:

$$TimeLocation = t0 + (\Delta t \times Location) \quad \text{.....(3.6)}$$

Once the segment of interest is selected using cursors, that segment can be saved to disk in binary format. This VI also calculates and display descriptive statistics from a segment of a presaved data file in Indicators on the front panel.

D. The saving and opening data part

For this part, the data acquisition and processing are managed by writing subVIs that (1) acquire and save (i.e. write) the data and (2) read the previously stored data file. There are basically two file format options for data acquisition and processing: spreadsheet and binary format. Here, the binary format is achieved for saving and opening the data. A major reason for saving and opening the data in binary format is that they more efficiently use hard drive storage space. They should be considered when long data collection sessions are planned, especially if hard drive space is at a premium. The writing (saving) data in binary format can be shown in Figure 3.21 that saves the analyzed data from waveform graph trace to a computer hard drive for analysis in the future analysis again. In the block diagram, the heart of this is functions of File I/O VIs found in the Functions>>File I/O palette. The functions include File Dialog, New File, Write File, and Close File function. These functions handle to write data to files.

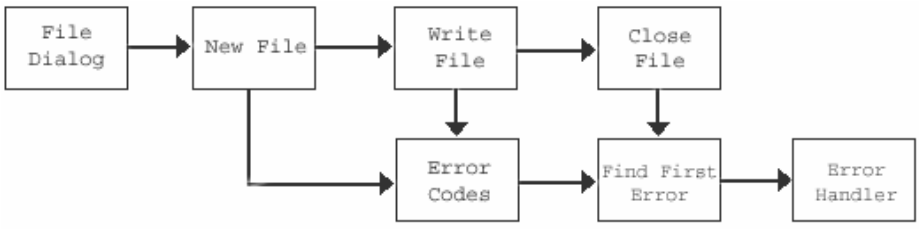

Figure 3.21 Block diagram of saving file.

When “Save” button toggled on the front panel, the File Dialog displays a dialog box with which the user can specify the path to a file or directory. This dialog box is used to select a location and name for a new file or directory. A message-

“Enter Filename:” - appears below the list of files and directories in the dialog box. The Select Mode is selected to 1 in order to indicate the name of a file to create. Then, the program creates the file using the New File function. The New File function creates the file specified by file path and opens it for writing next. The Write File function writes data to file specified by refnum. Writing begins at a location specified by pos mode and pos offset for byte stream file and at the end of file for dialog files. The current value default is set to 2, which the write operation stars at the current file mark. The saved file is closed using the Close File function. The Simple Error Handler VI checks the error cluster and displays a dialog box if an error occurred.

The data that were saved to disk may be requested again for displaying and analyzing in the future. In this VI, the program provides an option for opening and reading binary file of saved data. The read data are displayed on the Waveform Graph. The structures of reading binary file will be similar to write binary file. The Open File and Read File functions are selected instead of New File and Write File function, respectively. The block diagram of reading data in binary format can be shown in Figure 3.22 below. In block diagram, a dialog window prompts the user for selecting an opened file when the “Open” button is pressed on the front panel. Before the program will open the selected file using the Open File function, the select mode of File Dialog function is fixed to 0 for selecting the name of a file to open. The Open File function opens the file specified by file path for reading that its open mode defaults to 1 (read only).

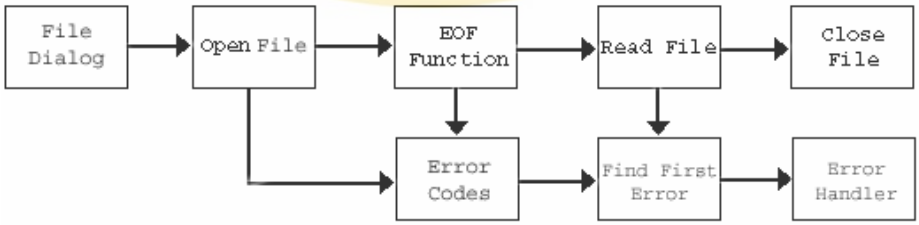

Figure 3.22 Block diagram of opening binary data.

The EOF function is handled to set the logical end-of-file (EOF) of the file identified by refnum. The offset of EOF function is used for calculating the number of instances of byte stream type to read, which it has units in bytes for byte stream files. This is wired to count in Read File function, where it reads data from the file specified

by refnum and returns it in data. Reading begins at a location and depends on the format of the specified file. The Close File function closes the specified refnum and returns the path to the file associated with the refnum. The Simple Error Handler VI determines whether an error occurred. It contains a database of error codes and descriptions, from which it creates a description of the error and optionally displays a dialog box.

3.3 Experimental setup of H-reflex measurement

The H-reflex study on gastrocnemius-soleus muscle measures the latency and the amplitude over the monosynaptic reflex arc through the afferent Ia fibers and efferent alpha motor fibers of the S_1 root. The materials consist of constructed stimulator, computer (LabVIEW installed), DAQ card, recording surface electrodes, set of connectors and cables (shielded, coaxial), and bipolar stimulating electrodes. These can be connected as shown in Figure 3.23 below.

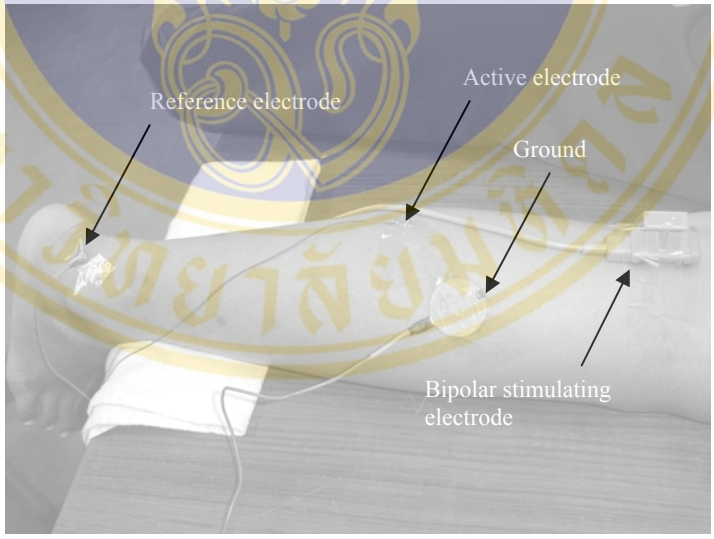

Figure 3.23 The experimental set up.

The procedure of H-reflex experimentation can be described as follow. First, the subject was positioned comfortably in the prone position, with feet suspended over the edge of the table, and was solicited to place electrodes on the muscle. Before the electrodes are placed, the subject's skin was abraded and an electrolyte gel applied to improve contact with the electrode leads. Also, a pillow placed beneath the legs was

exploited to help the effect caused slight knee flexion. Both left and right H-reflexes can be achieved in this position with little difficulty. The active recording electrode is disposed by first flexing the leg and drawing a line across the poppilteal fossa (67). A line connecting the mid-popliteal fossa with the proximal flare of the median malleolus is bisected for the active electrode location. This site commonly approximates the musculotendinous junction of the gastrocnemius muscle. The reference electrode is secured to the distal portion of the Achilles tendon just proximal to its insertion on the calcaneus. A ground electrode is positioned just proximal to active electrode.

For the stimulation setting, the cathode is placed in the mid-popliteal fossa with the anode distal. The pulse duration of between 0.5 ms and 1.0 ms is recommended. The current intensity is slowly increased until the stimulus just activates the large Ia afferent fibers without concomitant activation of the motor fibers or is just threshold for only a few motor fibers. The stimulation should be delivered at a rate of once every 2-3 seconds to avoid suppressing the H-reflex through central mechanisms. It is often necessary to move the stimulating electrodes either slightly medially or laterally to optimize the cathode directly over the tibial nerve. Care should be taken to avoid proceeding too far laterally, as the peroneal nerve may be excited. This is relatively easy to define, as foot no longer plantar flexes but dorsiflexes with each stimulus.

CHAPTER IV
EXPERIMENTAL RESULT

This chapter demonstrates testing and results of the constructed device as well as developed program for processing H-reflex response. The technical and functional testing of the constructed device is used for evaluating an efficiency of this working system before using with patient. The technical testing is intensively performed in two main parts, including signal conditioning and electrical stimulator part. The accuracy and reliability of the results are experimented all time according to specific specification of this constructed device. Finally, the function testing with some subjects will be expected too.

4.1 Technical testing and results

The technical testing of designed and constructed prototype is tested in order to evaluate the performances of device. Testing was performed in two main parts, including signal conditioning and electrical stimulator. This testing procedure can be performed as follow:

4.1.1 Stimulator testing

A wire-wrapped prototype of the electrical stimulator was implemented. Heat sinks were properly attached. Transformer provides a minimum isolation. All resistors are 1/4W-carbon with 1%-tolerance. The important parameters for testing stimulator consist of frequency, duration, and intensity of stimuli. These parameters are used for eliciting the response of H-reflex. Testing is shown as follow:

4.1.1.1 Rectangular pulse frequency adjustable 0.1 to 1.0 Hz

On the design and construction, the pulse-repetition is software controlled by the VIs, written by LabVIEW. This VI is based on the counter's function with DAQ-STC chip of board for generating pulse train as required. The VI provides to

adjust frequencies in range of 0.1 Hz to 1 Hz. The result of output is a TTL signal that responses to 0 V (low) and 5 V (high) in value. It is delivered toward the stimulator to impose the stimulation current. Figure 4.1 shows to result testing the counter and device to generate a continuous pulse train. Its output is available to the counter's OUT pin.

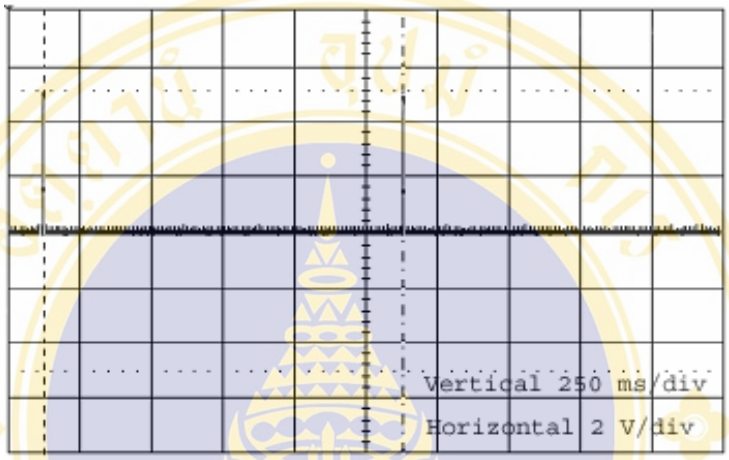

Figure 4.1 Obtained result of the rectangular pulse train at 1 Hz generated by DAQ board.

Table 4.1 Results of testing to generate the desired frequency.

Frequency (Hz)	Actual frequency (Hz)	Frequency read by oscilloscope (Hz)
0.1	0.098	0.101
0.2	0.200	0.200
0.3	0.298	0.301
0.4	0.400	0.400
0.5	0.500	0.500
0.6	0.600	0.600
0.7	0.699	0.701
0.8	0.800	0.800
0.9	0.898	0.901
1.0	1.000	1.000

Testing method includes:

A) Configure the device number, counter number, and desired frequency on the front panel of VI.

B) Connect the probe of oscilloscope CH1 to GPCTR0_OUT of SCB-100 connector block.

C) On the panel of oscilloscope, the output waveform is measured.

D) Measures the frequency on the panel of oscilloscope and read the actual frequency on the front panel of VI.

E) Change the frequency to the other steps, then, measure the frequencies again.

4.1.1.2 Rectangular pulse duration adjustable 0.1 to 1.0 ms

In the same method to pulse frequency, the pulse duration is handled by the VI. Referring the equation 3.3 previously, this is an algorithm for controlling the pulse-duration as required. The pulse duration is in range of 0.1 ms to 1.0 ms. The pulse result determined the frequency and duration is passed to an external device (optocoupler) for driving switching circuit. The results can be shown in Figure 4.2 and Table 4.2.

Testing method is as follow:

A) Configure the device number, counter number, and desired duration on the front panel of VI.

B) Connect the probe of oscilloscope to pin 4 of optocoupler.

C) On the panel of oscilloscope, the output waveform is monitored.

D) Measures the duration on the panel of oscilloscope read the actual frequency on the front panel of VI.

E) Change the duration to the other steps.

F) Read the duration of the pulse on the oscilloscope screen.

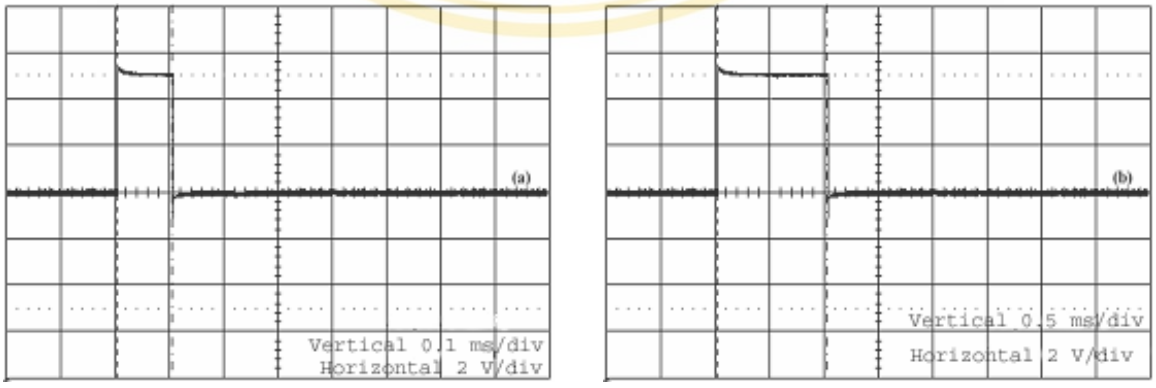

Figure 4.2 The output pulse of optocoupler (a) at 0.1 ms and (b) at 1.0 ms.

Table 4.2 Results of measure the output pulse duration.

Duration (ms)	Actual duration (ms)	Duration read by oscilloscope (ms)
0.1	0.10	0.10
0.2	0.20	0.20
0.3	0.30	0.30
0.4	0.40	0.40
0.5	0.50	0.50
0.6	0.60	0.60
0.7	0.70	0.70
0.8	0.80	0.80
0.9	0.90	0.90
1.0	1.00	1.00

4.1.1.3 Intensity of stimulation

In this thesis, the stimulation output is the positive-monophasic (rectangular pulse) constant current pulse and is adjustable from 1 mA to 20 mA. To evaluate the amplitude of stimulation limits without the restriction imposed by subject pain-threshold, a 10 kΩ load resistor R_{skin} was initially fixed. Referring to Figure3.2 the measured transfer function of the circuit, defined as the amplitude of the load current against the tunable-regulated voltage, can be shown in Figure 4.3, for stimulation rates of 0.1 Hz and 1.0 Hz. The waveform of the oscillation at the secondary of transformer, at maximum-current condition, is shown in Figure 4.4. Frequency and amplitude are 390 $V_{peak\text{-}to\text{-}peak}$ and 218 Hz, respectively.

Testing method:

- Connect the resistance load 10 kΩ to terminal output.
- Detect the output by the probe of oscilloscope.
- Vary the amplitude of the load current against the regulated voltage from 1 mA to 20 mA.
- During varied the amplitude, read and recoded.

Tests were performed at different stimulation ratings. The waveform of the voltage across load resistor at I_{skin} = 20 mA is shown in Figure 4.5, for the duration of 0.1 ms and 1.0 ms, respectively. Measured pulse transition is shorter than 30 μs that makes the circuit suitable to relatively high stimulation rates.

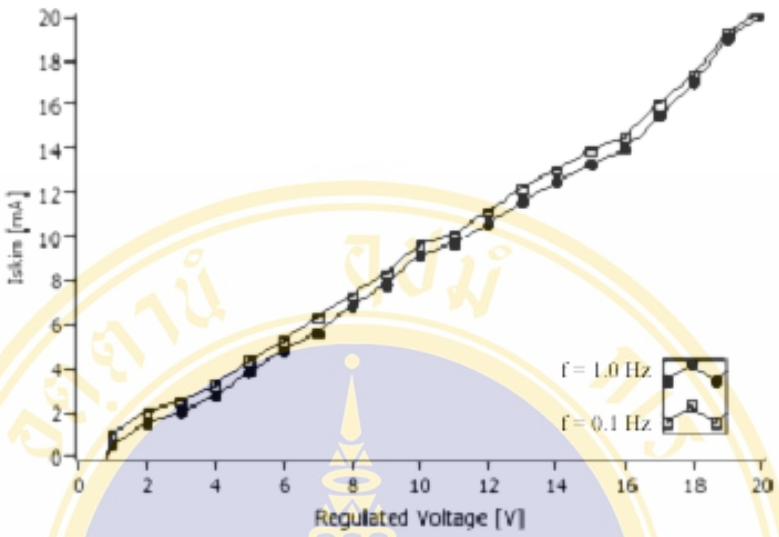

Figure 4.3 Measured amplitude of skin current (I_{skin}) as function of regulated voltage.

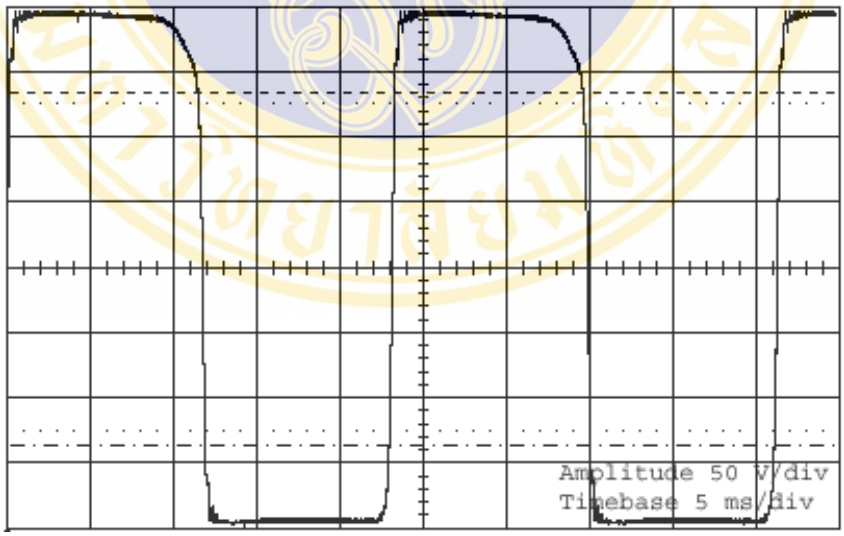

Figure 4.4 Oscillation at secondary of transformer at condition of maximum current (I_{skin} = 20 mA).

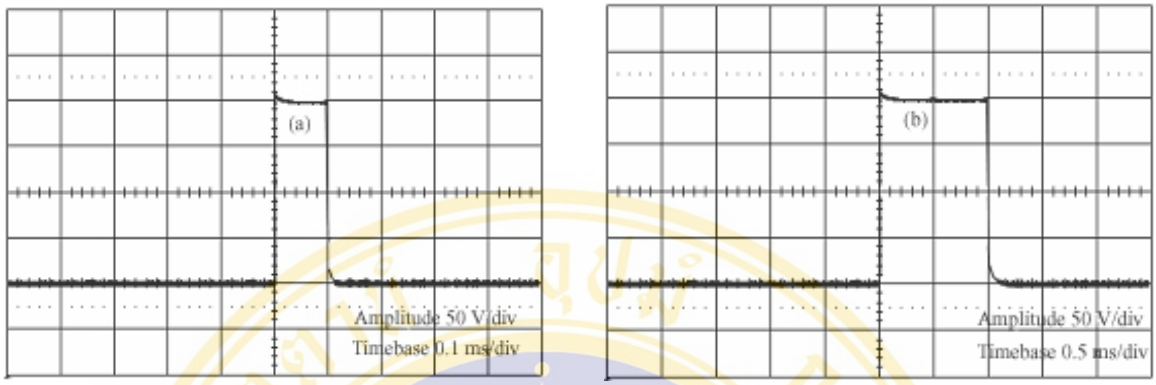

Figure 4.5 Voltage across load resistor at I_{skin} 20 mA for (a) pulse duration of 0.1 ms and (b) pulse duration of 1.0 ms. Measured pulse transitions shorter than 30 μs make the circuit suitable to relatively high stimulation rates.

4.1.2 Signal conditioning testing

Testing was performed in two main parts in each procedure of data acquisition as amplifier part and filtering part. The procedure of these testing is as follow:

4.1.2.1 Amplifier testing

Amplifier part is demonstrated in features of bioelectrical amplifier of the constructed device. This will examine overall of the amplifier modules of system for electrical signal of detection and measuring, by performance in three main parts as follow:

(A) Input impedance testing (Figure 4.6)

Input impedance (Z_{in}) part is total internal resistance of inputs preamplifier which is the first important stage for preparing signal (31 53). Z_{in} was tested in a resistance value (reactance) of each input channel of input amplifier into the constructed signal conditioning. Testing is as follow:

1) Connection signal generated into input amplifiers circuit of each channel with function generator (HP 33120A), by using a dual channel digital oscilloscope (TDS 210) and a digital multimeter tester (DMM Fluke 75 series), as connection and measuring at point A and B as shown in Figure 4.6.

2) Adjusted frequency signal of function generator at the same frequency and input voltages, by using to 10 Hz and 10 mVp-p.

3) Adjusted of the decade resistor (Rs) was given point B, signal equal to 1/2 of point A and equal to Rb, Rs =Rb//Rp, Rb = Zin.

4) Read resistance values from the decade resistor.

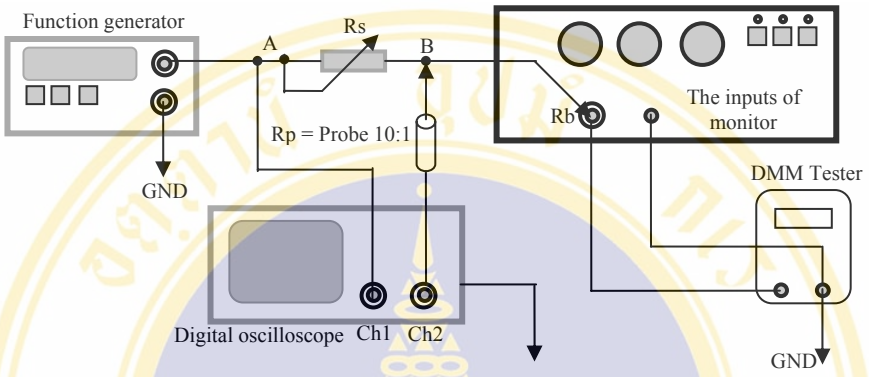

Figure 4.6 Input impedance (Zin) amplifier testing of system monitor.

The input impedance testing was measured as a resistance value of the decade resistor of each input channel by using digital multimeter. The resistance of Rb is equal to 10.58 MΩ. In summary, the input impedance Zin was calculated from Rb, by using adjustment Rs = Rb, a given point B signal equal to ½ of point A signal. TDS 210 oscilloscope, using a probe tester at Ch2 input measured signals at point A and B. The probe of oscilloscope had internal impedance (Rp) in order of 20 MΩ, which also can be calculated from Rs = Rp//Rb = (RpxRb)/(Rp+Rb) and Rb = (RsxRp)/(Rp-Rs). When Rs is decade resistor, Rp and Rb are determined as input impedance of oscilloscope probes and input impedance (Zin) in each channel. When Zin of input channel is measured Rs, resulting in Rs = 10.58 MΩ. Zin can be attenuated as:

$$Zin = Rb = Rs // Rp$$

$$Zin = (10.58x20) / (10.58 + 20)$$

$$Zin = 22.462\ M\Omega$$

In the inherent property of the high gain differential amplifier is the limitation in input impedance (biological amplifier). The minimum acceptable ratio of amplifier input impedances are 10 times the electrode impedance. At this ratio, it is possible to have some electrode current flow. Electrode impedance, it is desirable that the paste or jelly used

with electrode resulted in skin-to-electrode impedance of 5-10 kΩ or less, measured at 50 Hz. The input impedance over the working frequency range shall be no less than 500 kΩ to 10 MΩ between any single patient electrode and ground (55, 56). If the impedances are set too higher, million to one, the static noise and ambient pickup begin to occur.

B) Common mode rejection ratio (CMRR) of differential amplifier testing

Common mode rejection (CMR) part is ratio expression while common mode rejection ratio (CMRR) is logarithm of that ratio. The CMRR is termed of the absolute value of ratio of the differential gain (Ad) divided by using the common mode gain (Ac), CMRR was defined as $|Ad / Ac|$ and in 20 log of dB unit (31, 54, 57).

$$\text{Due to CMRR} = 20 \log Ad / Ac \quad \text{(dB)}$$

where Ad is gain of differential mode input signal and Ac is gain of common mode input signal.

- Differential mode gain with input signal testing (Ad).

The Ad testing is shown in Figure 4.7 as:

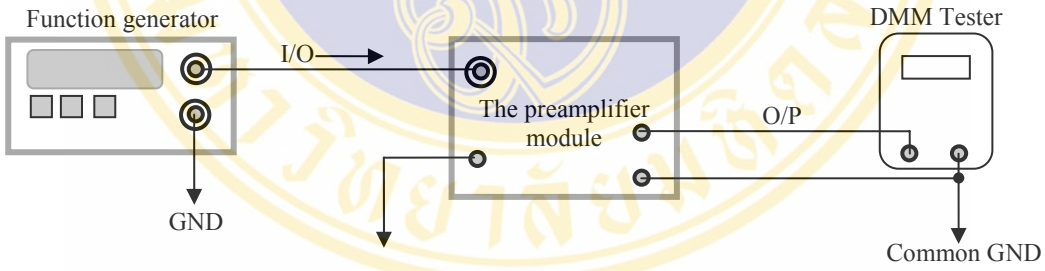

Figure 4.7 Ad testing and how connecting to the constructed device.

1) Connected the input signal supplied from function generator into preamplifier circuit in system of the constructed device, by using a digital multimeter tester.

2) Applied the input voltage from 10 mV up to the voltage that the output not saturated and then fixed it.

3) Adjusted the frequency to cover the range of signal detect from function generator (0.5 to 1500 Hz).

4) Read calculated and recorded the output voltage (Vo) to Ad, as shown in data Table 4.3 below.

Table 4.3 Results of testing the differential mode gain (Ad), by using Vi = 10 mV.

Function Gen. (Hz)	Ad of preamp. testing	
	Vo (mV)	Ad (Vo/Vi)
0.5	303	30.3
1	301	30.1
5	300	30.0
10	300	30.0
50	303	30.3
100	303	30.3
200	305	30.5
500	305	30.5
700	307	30.7
1000	307	30.7
1200	307	30.7
1500	310	31.0

- Common mode gain of input signal testing (Ac).

The common mode gain (Ac) of testing is shown in Figure 4.8 as follow:

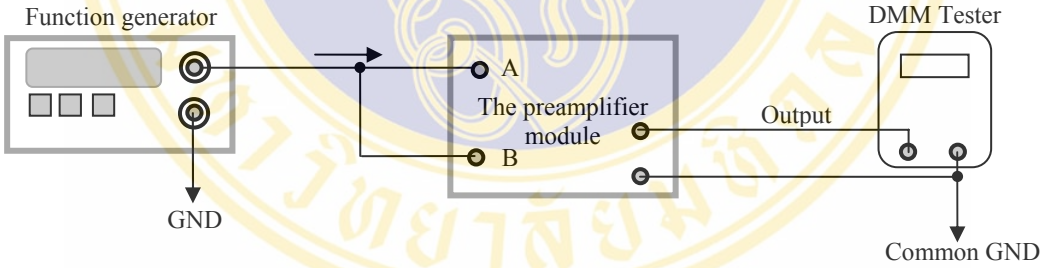

Figure 4.8 Ac testing and how connecting to device.

1) Connect the function generator to preamplifier circuit.

2) Applied 10 mVp-p output signals from function generator into input amplifier at point A and B.

3) Adjusted the frequency to cover the range of signal detect (0.5 to 1500 Hz), as the same frequency in Ad, by using Ac = Vo/Vi.

4) Read calculated and recorded the output voltage (Vo) to Ac, as shown data in Table 4.4 below.

Table 4.4 Results of testing the common mode gain (Ac), by using Vi = 10 Vp-p.

Function Gen. (Hz)	Ac of preamp. testing	
	Vo (mV)	Ac (Vo/Vi)
0.5	2	0.00020
1	2	0.00020
5	2	0.00020
10	2.2	0.00022
50	2.4	0.00024
100	2.6	0.00026
200	2.6	0.00026
500	2.8	0.00028
700	2.8	0.00028
1000	3	0.00030
1200	3	0.00030
1500	3	0.00030

Table 4.5 Results of calculation of CMRR (dB) from data in Table 4.3 and 4.4.

Function Gen. (Hz)	Preamplifier testing		
	Ad	Ac	CMRR
0.5	30.3	0.00020	103.61
1	30.1	0.00020	103.55
5	30.0	0.00020	103.52
10	30.0	0.00022	102.69
50	30.3	0.00024	102.02
100	30.3	0.00026	101.33
200	30.5	0.00026	101.39
500	30.5	0.00028	100.74
700	30.7	0.00028	100.80
1000	30.7	0.00030	100.20
1200	30.7	0.00030	100.20
1500	31.0	0.00030	100.28
		average	101.96

Ad and Ac in Table 4.3 and 4.4 can be used to calculate of the CMRR as shown in Table 4.5. For example calculation, at frequency 10 Hz, Ad = 30 and Ac = 0.00024 (CMRR=20log Ad/Ac). Thus, CMRR = 20 log Ad/Ac = 20 log 30/0.00024 = 101.938 dB. It was found that CMRR varied from 100 to 104 dB, averaged CMRR to 102 dB with the

range of specific specification (≥ 100 dB) at frequency response of signal requirements of detection. This is sufficient for amplifier system in system required of this device.

C) Amplifier gain testing

The amplifier gain testing of the constructed device was determined by using a small signal of function generator (1 mV peak) through amplifier of system with detection and measuring. The amplifier gain of system included gain to x10, x100, x1000(1k), which as it are needed of instrument. Also, the procedures of amplifier gain testing are as follows:

1) Applied 1 mV peak sine waveform function generator, to amplifier by adjusted the frequency cover the range of the signal detection in each frequency response of amplifier system.

2) Detected the output signal by using a probe of oscilloscope, adjusted the amplifier gain.

3) Read and recorded output voltages, on oscilloscope as shown data in Table 4.6 below.

4) Repeat steps 2 and 3 for each amplifier gain.

Table 4.6 Testing of amplifier gain by using function generator, Vi = 1 mV.

Function Gen. (Hz)	Vo of gain amplification of amplifier system		
	Gain x10 (mV)	Gain x100 (mV)	Gain x1k (V)
0.5	10.02	100.01	1.028
5	10.04	100.00	1.025
10	10.08	100.02	1.015
25	10.10	100.10	1.010
50	10.00	100.15	1.006
100	10.03	100.05	1.002
250	9.96	99.95	0.997
500	9.86	99.86	0.994
1k	9.80	99.79	0.988
10k	9.80	99.69	0.980
AVG	9.97	99.96	1.004
% error	0.30	0.04	0.40

4.1.2.2 Filter part testing

- Low pass filter testing.

The low pass filters are used to filter noise high frequency affected to the system and is also used as an anti-alias filter. For measuring reflex response of the system, it operates in a range of 10 kHz. The procedures of low pass filter testing are as following:

1) Applied sine wave signal is fixed an input voltage to 1 V of low pass filter circuit testing of the constructed device, as the bandwidth of low pass filter circuit.

2) Adjusted the frequency to cover the range for filtering from function generator and observed the frequency cut-off on screen of an oscilloscope to measuring.

3) Read calculated and recorded, output voltage (Vo), by using the gain in dB, Gain = 20 log Vo/Vi (-dB). The results testing of low pass filter at cut-off frequency of 10 kHz is shown data in Table 4.7 below.

Table 4.7 Results of the response gain in dB of low pass filter testing.

Low pass filter testing		
Frequency (Hz)	Vo (V)	Gain (-dB)
10	1.00	0.000
100	1.00	0.000
500	1.00	0.000
800	1.00	0.000
1000	1.00	0.000
2000	1.00	0.000
3000	1.00	0.000
4000	1.00	0.000
5000	1.00	0.000
6000	0.96	-0.354
7000	0.96	-0.354
8000	0.94	-0.537
9000	0.74	-2.615
10000	0.70	-3.098
12000	0.50	-6.020
15000	0.24	-12.396
20000	0.12	-18.416
30000	0.06	-24.437

- Notch filters testing (Band-reject filter at 50 Hz).

The notch filter or band reject filter is used to eliminate HUM at 50 Hz in system. The results testing of notch filter are shown in Table 4.8. The procedures are used in cut-off frequency at 50 Hz, when as following:

1) Applied 10 V sine wave signal from function generator, to system of notch filter circuit.

2) Adjusted the frequency to cover the range of notch filter and observed the cut-off frequency on the oscilloscope panel.

3) Read, calculated and recorded voltage output, by using the gain in dB, Gain = 20 log Vo/Vi (-dB). The results of notch filter testing in system are shown data in Table 4.8 below.

Table 4.8 Results of notch filter testing, Vi = 1 V.

Notch filter testing		
Frequency (Hz)	Vo (mV)	Gain (-dB)
10	1.00	0.0
20	0.98	-0.2
30	0.90	-0.9
40	0.82	-1.7
42	0.72	-2.9
44	0.67	-3.5
46	0.46	-6.7
48	0.12	-18.4
50	0.01	-40.0
52	0.13	-17.7
54	0.48	-6.3
56	0.68	-3.3
58	0.72	-2.9
60	0.84	-1.5
70	0.88	-1.1
80	0.90	-0.9
90	0.96	-0.4
100	1.00	0.0

4.1.2.3 Leakage current testing

The following leakage current tests were performed on input leads of amplifier in system for patient safety. Testing was performed by using the Electrical Safety Analyzer instrument (30, 32, 35). When performing this test was factor the instrument deducted. In addition to, the leakage current testing is accordance with standard IEC 601-1 BF (30, 35, 58). The leakage current testing was achieved by using Electrical Safety Analyzer Bio-Tek model 270 instrument, Inc., as follows:

1) Classic leakage current testing, at power ON condition, was done with neutral grounded and open neutral method as shown in Table 4.7 below. From Table 4.7, the leakage current of this testing is less than 10 μA and then it safe to use with patients according to standard IEC 601-1 BF (30, 31, 32, 35, 58).

2) Leakage current testing of leads without patient lead cable, at power ON condition, was done with open neutral method. The results of measurement are shown in Table 4.9 below. For the leakage current testing of leads with patient lead cable is attached, the results of measurement are also shown in Table 4.10.

Table 4.9 Leakage current testing by neutral grounded and open neutral method.

Conditions	Leakage current (μA)	
	Neutral grounded	Open neutral
A. Normal polarity-Grounded	0.23	0.24
B. Normal polarity-Ungrounded	>25	3.8
C. Reverse polarity-Grounded	0.4	0.25
D. Reverse polarity-Ungrounded	>250	4.1

Table 4.10 Leakage current testing of leads without patient lead cable and with patient lead cable.

Conditions	Leakage current (μA)							
	Without leads				With leads			
	R1	R2	G	All	R1	R2	G	All
A. Normal polarity-Grounded	7	7	7.5	8	9	9.5	11	12
B. Normal polarity-Ungrounded	7	7	7.5	8	9	9.5	11	12
C. Reverse polarity-Grounded	7	7	7.5	8	9	9.5	11	12
D. Reverse polarity-Ungrounded	7	7	7.5	8	9	9.5	11	12

4.1.3 Data acquisition testing

The testing of data acquisition is concerned to obtain an analog signal prepared for human computer interfacing. There are two major parts for data acquisition testing, including DAQ board testing for the computer recognition and processing, and LabVIEW program testing for displaying and recording the measured response. The procedures of these testing are as follow:

A) DAQ hardware testing

Before the DAQ hardware is tested, it is necessary to consider analog input specifications. These specifications give information on both the capabilities and the accuracy of the DAQ product. Basic specification is achieved to configure analog input channel. It can launch the DAQ Channel Wizard from the DAQ Solution Wizard, accessed by selecting Tool»Measurement & Automatic Explorer and clicking Data Neighborhood, to configure the channels. The DAQ Channel Wizard helps to define the physical quantities which are measuring on each DAQ hardware channel. It queries for information about the physical quantity being measured, the sensor or actuator being used, and the associated DAQ hardware. The procedures of the analog input channel configuration are as follow:

1) Click the DAQ Solutions button in the LabVIEW dialog box to launch the DAQ Solution Wizard.

2) When the Welcome to the DAQ Solution Wizard dialog box appears, click the Go to DAQ Channel Wizard button.

3) Select the Data Neighborhood category from Tools » Measurement & Automation Explorer. Right-click Data Neighborhood and selects Create New from the shortcut menu to configure a new channel. In the Create New dialog box select Virtual Channel and click the Finish button.

4) Select Analog Input as the channel type to configure and click Next button. Then, type a channel name and channel description in the appropriate text boxes.

5) Select the type of sensor. In this test, the type of sensor is chosen as voltage which is defined the units and range of controlling signal. The voltage type is in volts unit and in range of -5.0 to +5.0 volts.

6) Define the sensor scales the signal from the physical units to the hardware units. The default setting is no scaling.

7) Select data acquisition device and channel setting that will read signal. The data acquisition device is chosen as AT-MIO-64E-3 multifunction DAQ board for Windows. Prior channel setting of DAQ device is ACH0 for reading signal that is in mode of differential measurement.

The new configuration is listed under Data Neighborhood. To test DAQ hardware in interactive environment, right-click on the configured channel name in the configuration tree and select Test. The results of DAQ hardware testing is illustrated in Figure 4.9.

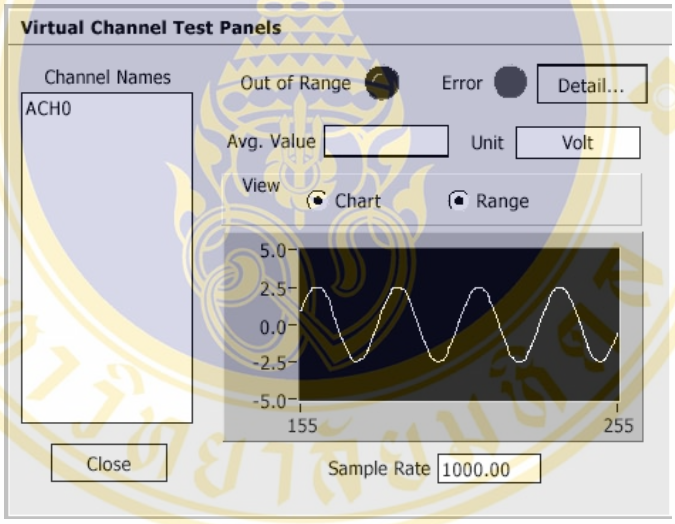

Figure 4.9 The DAQ hardware testing that read a sine waveform generated by function generator on channel ACH0.

B) LabVIEW program testing

LabVIEW is written as a VIs to send the appropriate commands to control the data acquisition of signal. Displaying waveform continuously, analyzing some parameter, and options for either saving or opening data are tested to ensure the accuracy and capabilities of processing signal. Furthermore, digital filter without errors of phase shift is demonstrated to provide an option for reducing noises pickup from stray signals. The procedures of testing are as follow:

- Acquiring and displaying data part testing

On the condition of acquiring H-reflex signal, controlling data acquisition with digital triggering is demonstrated, since the acquired signal want to receive data in a range desired relative to the stimulus event. In this testing, the VI written retrieves the specified amount of data from one input channel, defined previously, each time a digital start occur. It shows to trigger an acquisition multiple times while avoiding the overhead of configuration and buffer allocation each time. Use the front panel and block diagram in the following illustration to get started testing.

1) On front panel referred to Figure 3.19 previously, configure the device number (1), channel (0), counter (0), durations, and frequencies.
2) Select the New Acquire function by clicking the button for acquiring data in the real time.
3) Make the appropriate I/O connections, connect sine signal supplied from function generator to the input channel on the I/O connector as configured previously, ACH0 for analog input and PFI0/TRIG1 for trigger signal.
4) Adjust the timebase and position as suited. A result of testing can be shown in Figure 4.10 below.

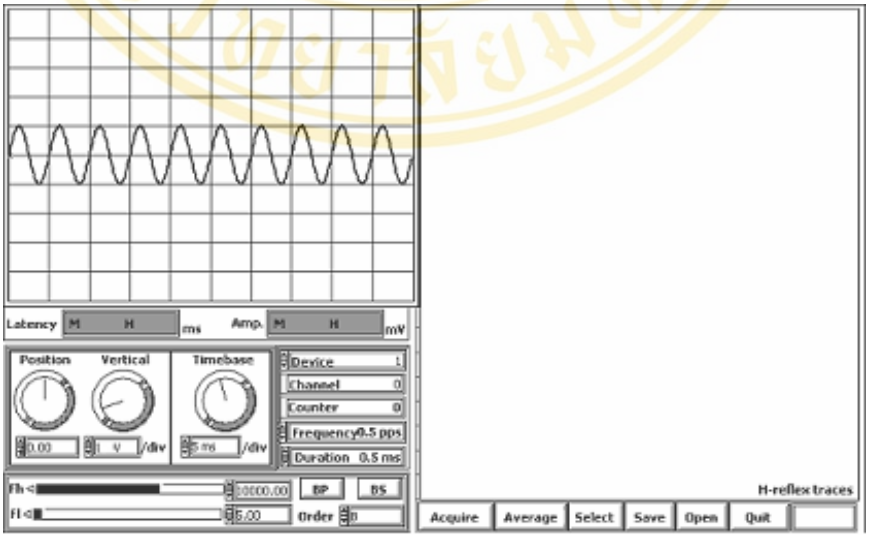

Figure 4.10 Front Panel of acquiring data testing with the original sine signal, 1 V at 200 Hz.

- Analyzing part testing

The analysis of acquired signal is an important heart of diagnosing obtained states. In this testing, it is a generic data analyze that permits partitioning of a segment of data on-the-fly without having to run and rerun the program numerous times. A Cursor Display was used to manually identify a segment of data for analysis. The segment of signal to be analyzed was first identified by moving the cursors. Using Attribute Nodes to configure Cursor Display, the cursors automatically read the x-axis (time) and y-axis (amplitude) coordinates of a segment to be analyzed. When the "Analyze Segment" button is turned "ON", the values on selected segment can be identified both x-axis (time) and y-axis (amplitude) by cursors, and then to be read into Numeric Indicators. Array Max & Min, Array Size, and Mean functions can be used, by moving the cursor 0 and 1, for indicating the statistical values of the selected data.

- Saving and opening part testing

In this testing, the VI is written to demonstrate (1) acquiring and saving the data in binary format and (2) reading the previously stored data file. The original random data is built as an array of double-precision floating-points number between 0 and 1 with using the data of 50 samples. For loop Function is used to create an array of data, the array of storing data is shown on left Waveform Graph in Figure 4.11a. When the data is saved completely, the saved data can be opened and read the existing file stored previously in binary form. The procedures of opening the data file are illustrated on the right front panel in Figure 4.11b. The result of the opened data is the same data to the saved data.

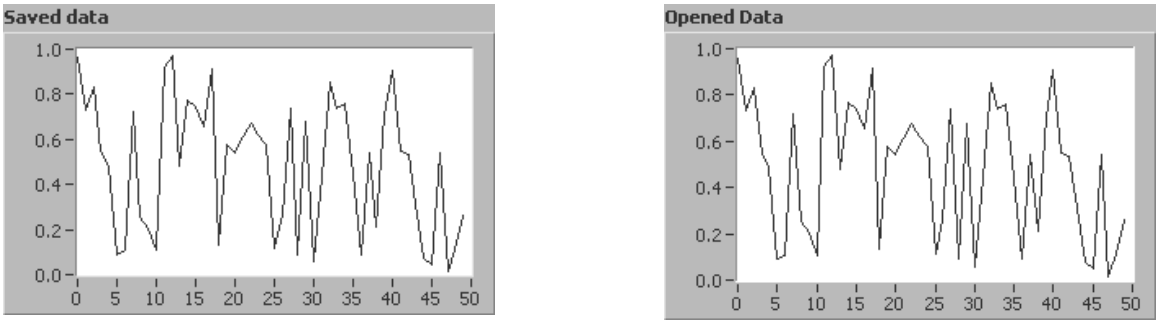

(a) (b)

Figure 4.11 (a) Front panels of the saved data and (b) opened data file testing.

- Digital filter testing

In this testing, the VI combines a sine wave generated by the Sine Pattern VI with high-frequency noise. (The high-frequency noise is obtained by high-pass filtering uniform white noise with a Butterworth filter.) The combined signal is then band-pass filtered by another Butterworth filter to extract the sine wave. Note in this testing that two Butterworth filters are separated by a Reverse 1D Array function. Digital filtering causes a phase shift (a constant error) and may be connected by reversing polarity of the signal using the Reverse 1D Array function and passing it through the filter again. The front panel is shown in Figure 4.12. On the front panel, Five Digital Controls are used to define the "Sampling Frequency", "Order", and "Low and High Frequency Cuttoffs", respectively. 10 cycles of sine wave are generated as a raw data input that there are 1000 samples. Because of the Butterworth filter is a type of indefinite impulse response (IIR) filter which its output depends on the current and past input values as well as the past output values, a transient appears at its output each time the VI is called. This transient can be eliminated after the first call to the VI by setting its init/cont control to a TRUE value.

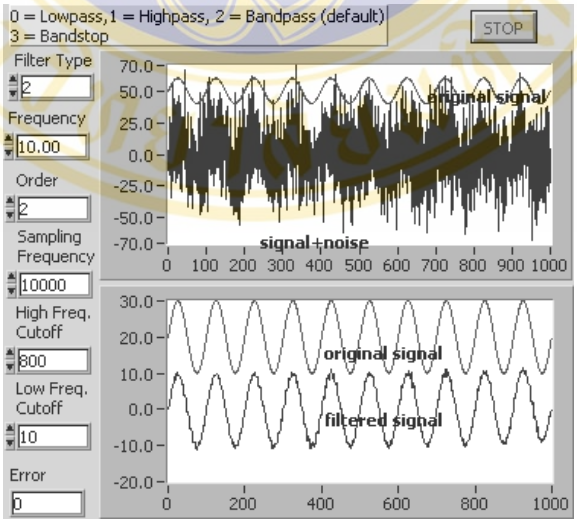

Figure 4.12 Front panel of digital filter testing. This demonstrates as a digital band-pass filter with default low- and high-frequency cutoffs of 10 Hz and 800 Hz, respectively. While the default condition is a low-pass, high-pass, and band-stop options are also available.

4.2 Functional testing and results

The operational system test of each functions are achieved on the constructed device, by powering in normally, and in operation system itself. The functional testing was applied with electrical signals that would normally receive to feign normal operating modes and loaded with normal operational loads. This testing is unification of the functional working test and uses some specifications to apply the set of demonstrations that will prove correct operation of the circuit system. Moreover, the testing is a simple one but serves to show the way in which system part can be worked in functional tests, devised by measuring input and output signals. The functional test can be simulated at the suitable point in the circuit to test particular parts of the circuit. In addition to, the simplest this functional test is to perform the continuity check such as the checking of whether the electrical path of the constructed device is correct.

4.2.1 Noise level testing.

The procedure of noise level test checks for the level of interference to test the receiving signal at input amplifier detection. Three input resistors (3×5 kΩ from EEG Instrumentation Standard, 1977) are illustrated in Figure 4.13.

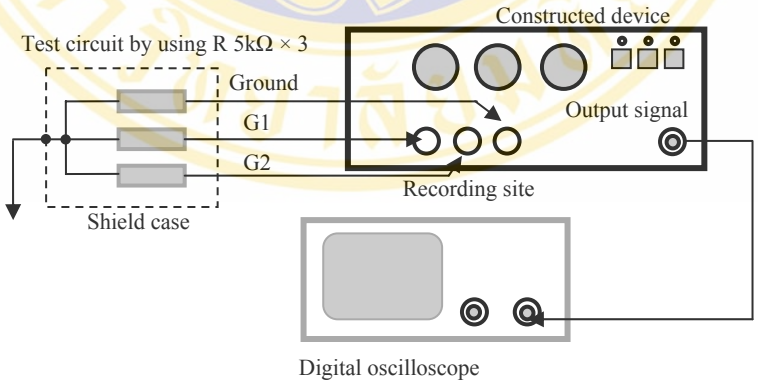

Figure 4.13 Connection of the amplifier noise test setup.

They were shown that waveform measuring and printout noise referred to input of amplifier of the constructed instrument. The noise testing of this instrument was demonstrated to noise signal of the input voltage through of the amplifier system by measuring on screen of oscilloscope, before pass into the signal processing part by

monitoring on the personal computer. On panel of oscilloscope, the measured noise signal of this setup to 2.20 mV was obtained. Therefore, the equivalent input noises were 2.20μV_{p-p}.

4.2.2 The function testing with external signal

This function testing is achieved by using an external signal from function generator. In testing, ability in classification of instrument, by applying a fundamental 50 mVp-p sine wave (voltage fixed) through resistor divider attenuation input voltage 1 mVp-p into this device. Then, the output signal is passed into interfacing computer by a connector block. This probation was checked to output display and signal processing of monitors by measuring the amplitude, latency, and occurrences of shape. The results of testing are shown in Table 4.11 and it used the classification of this testing is shown in Figure 4.14.

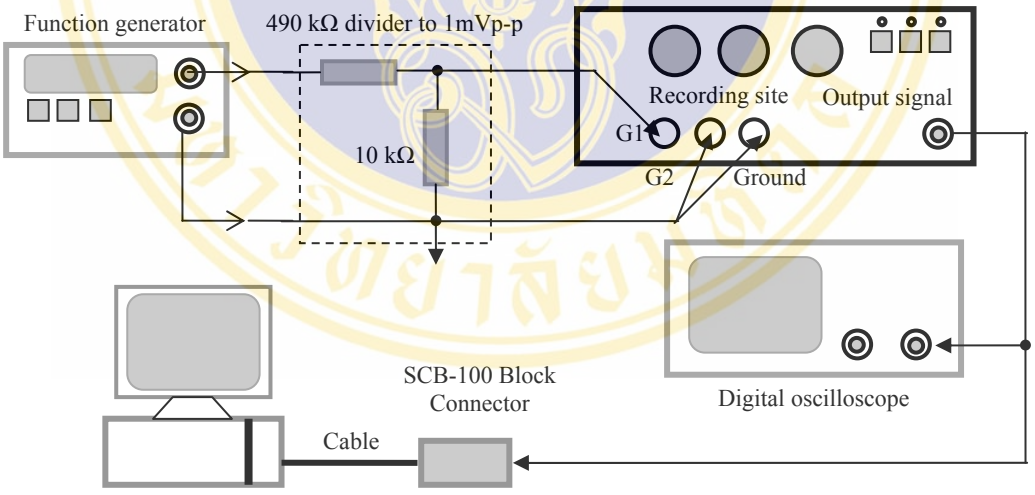

Figure 4.14 Connection of amplifier gains in the classification test setup with function generator.

Table 4.11 Results of the functional testing of system with the external signal from function generator, by fixing to 1 mVp-p, adjustment frequency to cover range, using TSD 210 oscilloscope testing to measure mean amplitude (Vo) versus to measure on PC computer.

Frequency Condition (Hz)	The function testing of mean amplitude (Vo) on oscilloscope					
	Gx10 (mV)		G x100 (mV)		Gain x1k (V)	
	Read Vo	%Error	Read Vo	%Error	Read Vo	%Error
1	10.00	0.00	100.00	0.00	1.00	0.00
10	10.00	0.00	100.00	0.00	1.00	0.00
20	9.90	1.00	99.00	1.00	0.98	2.00
100	9.90	1.00	99.00	1.00	0.98	2.00
250	10.00	0.00	100.00	0.00	1.00	0.00
500	10.00	0.00	100.00	0.00	1.00	0.00
1k	10.00	0.00	100.00	0.00	1.00	0.00
2k	9.90	1.00	100.00	0.00	1.00	0.00
5k	9.90	1.00	99.00	1.00	0.99	1.00
8k	9.90	1.00	98.00	2.00	0.98	2.00
AVG	9.95	0.50	99.50	0.50	0.99	0.70

Frequency Condition (Hz)	The function testing of mean amplitude (Vo) on computer display					
	Gx10 (mV)		G x100 (mV)		Gain x1k (V)	
	Read Vo	%Error	Read Vo	%Error	Read Vo	%Error
1	10.00	0.00	100.00	0.00	1.00	0.00
10	10.00	0.00	100.00	0.00	1.00	0.00
20	9.90	1.00	99.00	1.00	0.98	2.00
100	9.90	1.00	99.00	1.00	0.98	2.00
250	10.00	0.00	100.00	0.00	1.00	0.00
500	10.00	0.00	100.00	0.00	1.00	0.00
1k	10.00	0.00	100.00	0.00	1.00	0.00
2k	10.00	0.00	100.00	0.00	1.00	0.00
5k	9.90	1.00	99.00	1.00	0.99	1.00
8k	9.90	1.00	99.00	1.00	0.98	2.00
AVG	9.96	0.40	99.60	0.40	0.99	0.70

4.3 The functional testing with subject

Nine normal subjects and seven abnormal subjects were asked to test for H-reflex. In 9 normal subjects, they consist of 4 men and 5 women. They were examined for displaying the occurrence of H-reflex, and measuring the latency and amplitude both M-wave and H-reflex in the gastrocnemius-soleus muscle.

After setting the DAQ device to differential input the timebase was set to 5 ms/div with amplitude of 1 mV/div and the counter was switched to external triggering. After the triggering level was adjusted the stimulator output was turned off. An amplifier sensitivity of 200-1000 μV/cm typically suffices for most responses. Digital filter settings commensurate with routine motor studies are recommended. The default is band-pass filter with cut-off frequency in range from 5 Hz to 10 kHz. The simulator was set to give monophasic square wave stimuli at 0.5 pulse/sec and 0.5 ms duration. The stimulus intensity is gradually increased until a response (H-reflex) with a latency approximating 30 ms is detected. The current level is increased in small increments until a motor response (M-wave) is just noted. One should then optimize the H-reflex by decreasing or minimally increasing the current intensity until the H-reflex amplitude is minimized. Several responses are observed at this stimulus level to ensure a reproducible and stable response. The latency is then recorded to the initial departure of the H-reflex from the baseline. This is typically, although not always, a positive deflection. A characteristic appearance of the H-reflex is a triphasic initially positive potential. However, it is not unusual to observe an initially negative H-reflex.

For the H-reflex latency, it is found to correlate highly with both age and leg length. A regression equation may used to predict the optimal H-reflex latency. The values tested in subjects are compared with the predicted normal values from equations. One is the technique of Braddom and Johnson which represents a well-standardize method for obtaining H-reflex latencies. The predicted normal value can be calculated by using the following formulas, Equation 4.1 and 4.2 are referred in reference (67) and (4), respectively:

$$\textit{H-reflex latency (ms)} = 9.14 + 0.46(\textit{leg length}^{1}\ \textit{in cm}) + 0.1(\textit{age in year}) \quad \ldots(4.1)$$

$$H\text{-}reflex\ latency^{2}\ (ms) = 3.013 + 0.146(height\ in\ cm) \quad \ldots(4.2)$$

- *leg length*[1] is the length from the stimulation site to the top of the medial malleolus.
- *H-reflex latency*[2]: the normal upper limit of the H-reflex latency is 2SD above the predicted value (2SD = 3.1).

The predicted normal value in equation 4.2 is based on leg length and age, and in equation 4.2 is based on height. Results for measuring H-reflex are shown in Table 4.12 to Table 4.29. Table 4.13 to 4.21 shows the results of measurement for nine normal subjects. Table 4.22 to 4.28 shows the results of measurement for seven abnormal subjects. For the shape and occurrence of H-reflex in each subject are shown in Figure 4.15 to 4.30. In addition to, the recruitment curve of H-reflex is illustrated.

Table 4.12 Information of subjects.

Normal				
# subject	Age (year)	Height (cm)	Leg Length (cm)	
			Right	Left
1	28	169	33.0	33.0
2	27	171	35.0	35.0
3	26	170	33.5	33.5
4	27	171	34.0	34.0
5	25	158	33.0	33.0
6	25	160	33.0	33.0
7	25	160	32.5	32.5
8	25	161	33.0	33.0
9	25	162	33.0	33.0
Abnormal				
1	56	165	32.5	32.5
2	64	166	33.0	33.0
3	62	164	32.0	32.0
4	53	168	33.0	33.0
5	48	173	34.0	34.0
6	53	165	33.0	33.0
7	52	176	35.5	35.5

Table 4.13 Results of measurement for the normal subject1 (male).

#test	stimulus (mA)	M amplitude (mV)		H amplitude (mV)		H latency (ms)	
		right	left	right	left	right	left
1	5	-	-	0.92	1.08	26.52	26.24
	7	2.10	2.03	1.97	1.95	26.04	26.24
	9	6.13	6.22	1.77	1.86	27.32	28.26
	11	6.15	6.00	0.40	1.07	30.20	30.18
	13	6.24	6.27	-	-	-	-
2	5	0.49	0.48	0.95	1.08	26.20	25.98
	7	2.15	3.55	1.90	2.09	25.82	26.18
	9	6.15	6.26	1.70	1.82	27.06	28.72
	11	6.38	6.09	0.42	1.12	31.10	30.24
	13	5.94	6.27	-	-	-	-
					average	27.53	27.75

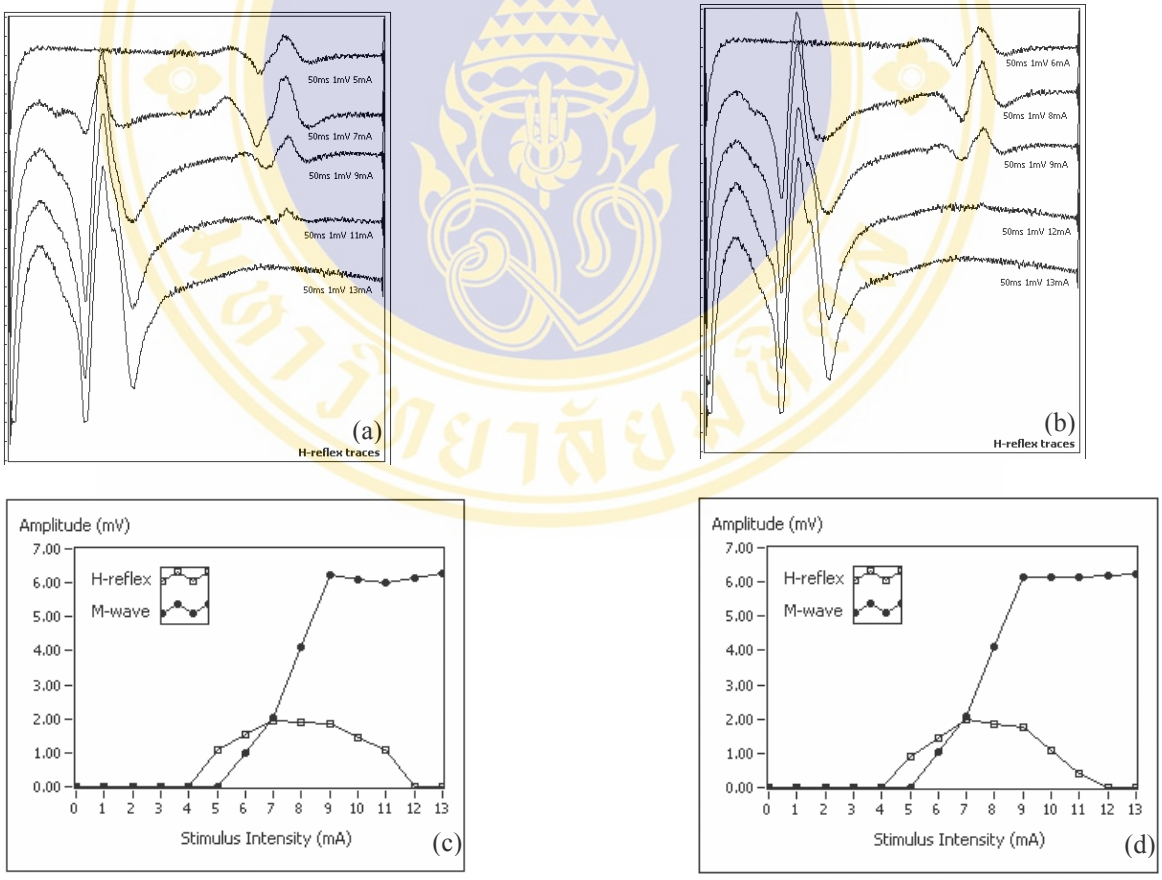

Figure 4.15 The occurrence results for (a) left leg and (b) right leg, along with M-wave and H-reflex recruitment curves for (c) left leg and (d) right leg in normal subject1.

Table 4.14 Results of measurement for the normal subject2 (male).

#test	stimulus (mA)	M amplitude (mV)		H amplitude (mV)		H latency (ms)	
		right	left	right	left	right	left
1	6	-	0.57	1.10	1.99	27.02	26.00
	8	4.83	3.55	2.30	2.08	26.02	26.18
	9	6.22	6.20	1.86	1.80	29.62	28.90
	12	5.88	6.00	0.95	0.80	30.52	31.76
	13	6.27	6.27	-	-	-	-
2	6	-	0.50	1.08	2.01	26.98	26.02
	8	4.80	3.50	2.28	2.10	26.02	26.20
	9	6.18	6.20	1.80	1.80	29.58	28.90
	12	5.92	5.88	0.98	0.78	30.54	31.76
	13	6.27	6.27	-	-	-	-
					average	28.29	28.22

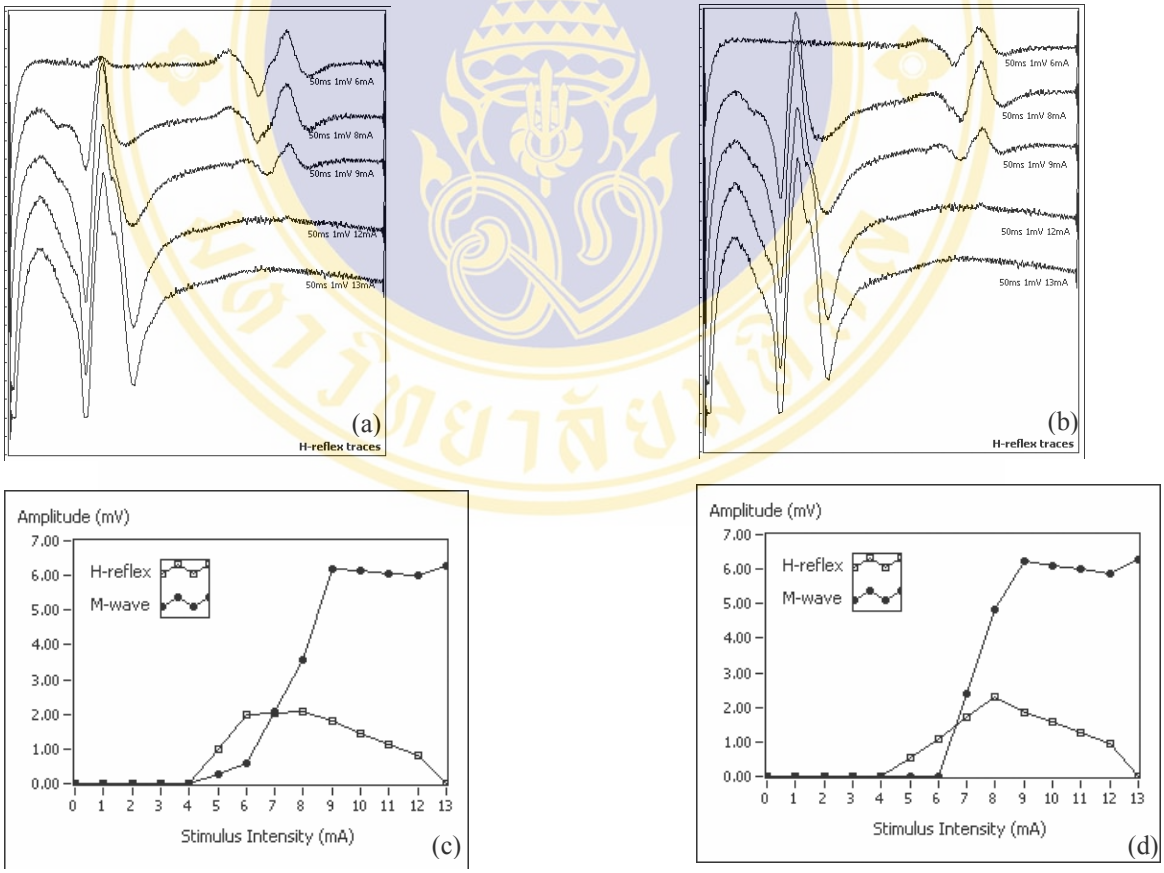

Figure 4.16 The occurrence results for (a) left leg and (b) right leg, along with M-wave and H-reflex recruitment curves for (c) left leg and (d) right leg in normal subject2.

Table 4.15 Results of measurement for the normal subject3 (male).

#test	stimulus (mA)	M amplitude (mV)		H amplitude (mV)		H latency (ms)	
		right	left	right	left	right	left
1	7	-	-	1.04	1.30	26.12	24.88
	9	1.46	1.30	0.98	1.68	27.76	30.94
	10	1.34	1.37	-	-	-	-
	12	1.76	1.85	-	-	-	-
	15	1.76	1.85	-	-	-	-
2	7	-	-	1.04	1.34	26.12	25.02
	9	-	1.32	1.10	1.58	27.40	30.90
	10	1.40	1.30	-	-	-	-
	12	1.76	1.85	-	-	-	-
	15	1.76	1.85	-	-	-	-
					average	26.85	27.93

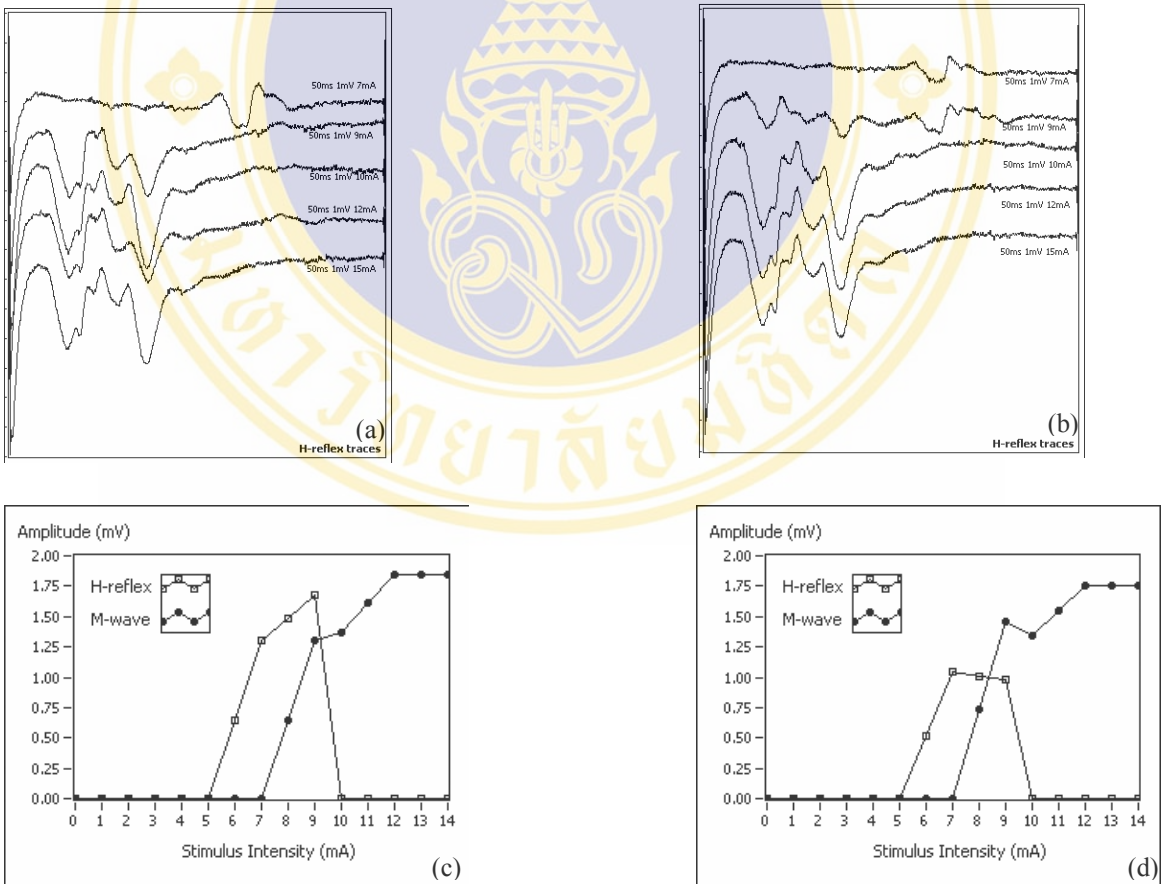

Figure 4.17 The occurrence results for (a) left leg and (b) right leg, along with M-wave and H-reflex recruitment curves for (c) left leg and (d) right leg in normal subject3.

Table 4.16 Results of measurement for the normal subject4 (male).

#test	stimulus (mA)	M amplitude (mV)		H amplitude (mV)		H latency (ms)	
		right	left	right	left	right	left
1	7	-	0.60	1.47	1.11	26.18	26.66
	9	1.40	1.52	1.34	1.64	27.76	31.78
	11	1.36	1.21	-	-	-	-
	13	1.68	1.21	-	-	-	-
	14	1.68	1.21	-	-	-	-
2	7	-	0.58	1.47	1.08	26.18	26.68
	9	1.38	1.50	1.32	1.60	27.74	31.80
	11	1.36	1.21	-	-	-	-
	13	1.68	1.21	-	-	-	-
	14	1.68	1.21	-	-	-	-
					average	26.97	29.23

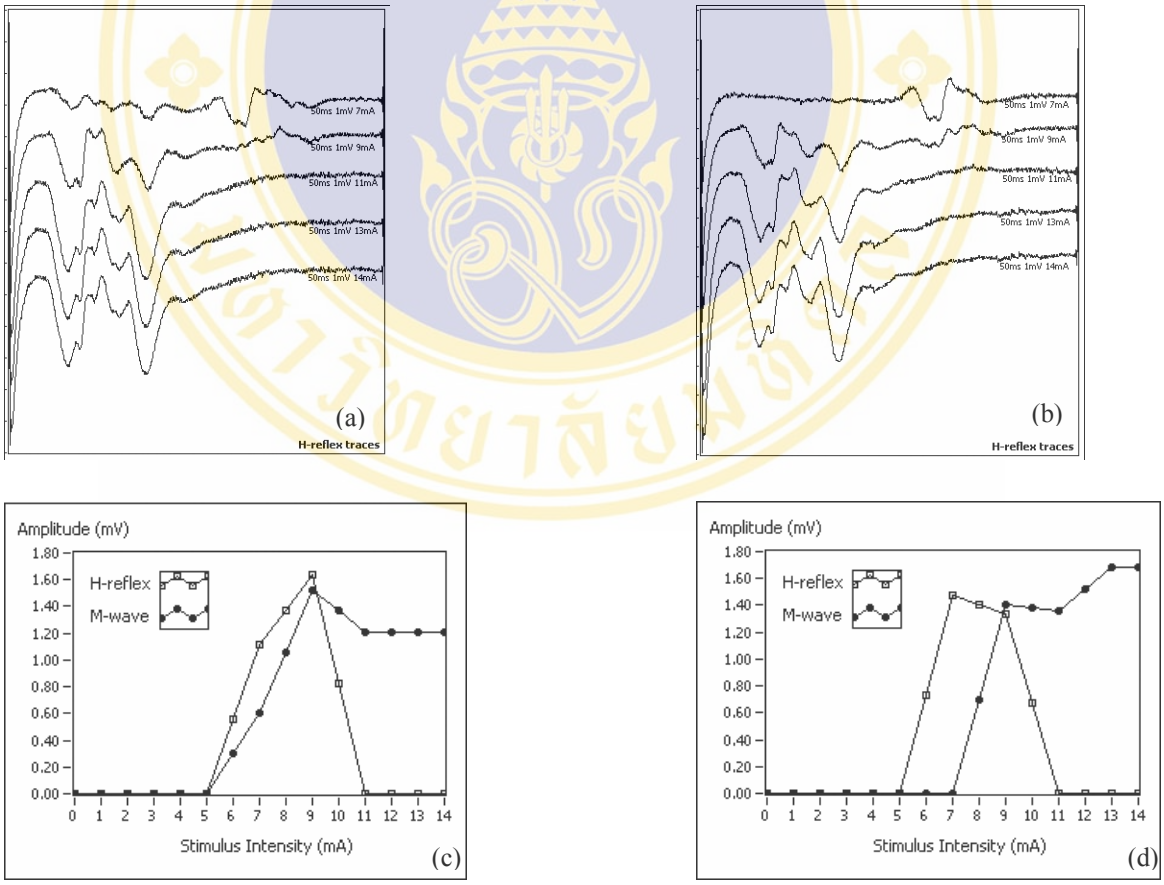

Figure 4.18 The occurrence results for (a) left leg and (b) right leg, along with M-wave and H-reflex recruitment curves for (c) left leg and (d) right leg in normal subject4.

Table 4.17 Results of measurement for the normal subject5 (female).

#test	stimulus (mA)	M amplitude (mV)		H amplitude (mV)		H latency (ms)	
		right	left	right	left	right	left
1	5	0.15	0.16	1.75	0.25	24.20	25.00
	7	0.96	1.11	2.72	2.17	24.46	24.04
	9	2.84	3.44	0.91	0.64	24.46	25.74
	10	3.10	3.46	0.65	0.50	24.50	25.74
	12	3.55	3.48	-	-	-	-
2	5	0.14	0.14	1.74	0.23	24.18	25.02
	7	0.95	1.09	2.70	2.15	24.44	24.08
	9	2.84	3.28	0.91	0.60	24.46	25.76
	10	3.10	3.48	0.65	0.50	24.50	25.76
	12	3.45	3.48	-	-	-	-
					average	24.40	25.19

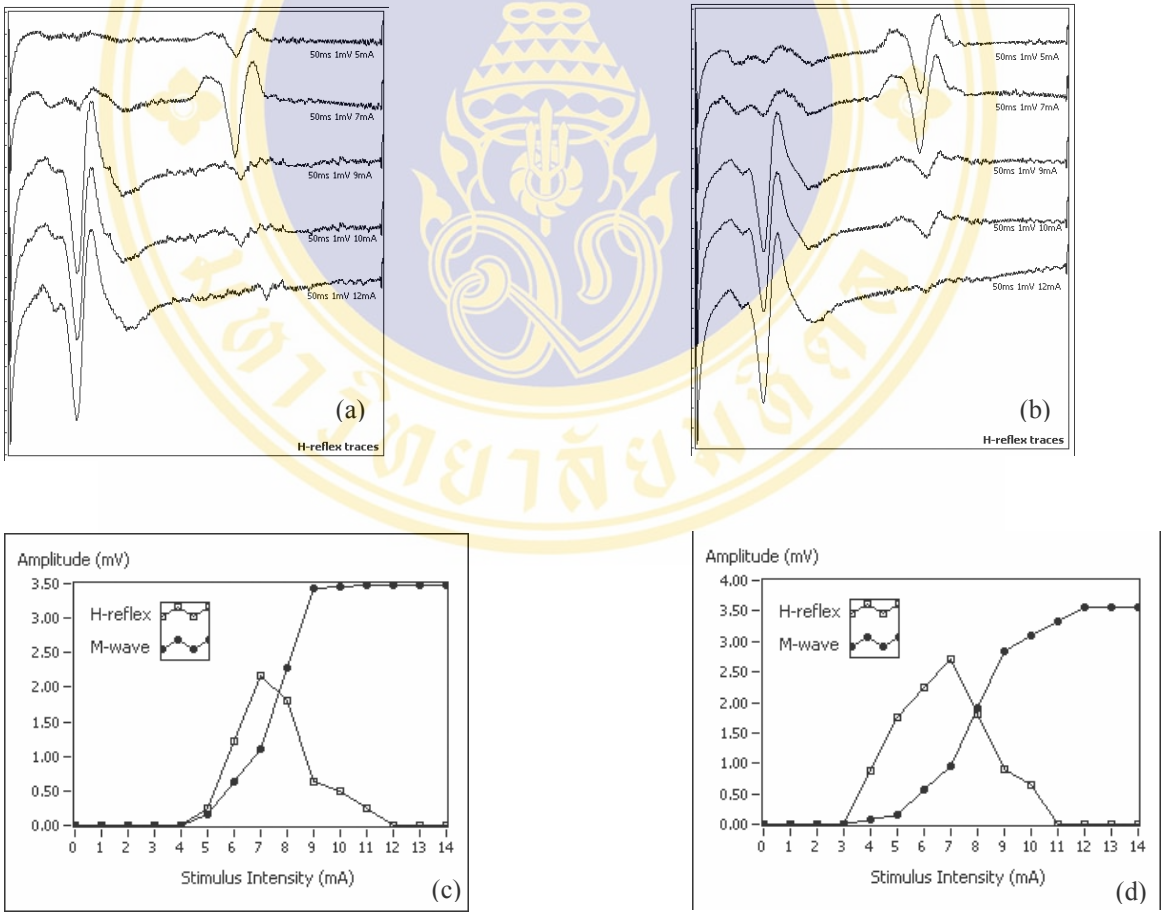

Figure 4.19 The occurrence results for (a) left leg and (b) right leg, along with M-wave and H-reflex recruitment curves for (c) left leg and (d) right leg in normal subject5.

Table 4.18 Results of measurement for the normal subject6 (female).

#test	stimulus (mA)	M amplitude (mV)		H amplitude (mV)		H latency (ms)	
		right	left	right	left	right	left
1	6	-	-	0.68	0.68	29.30	28.26
	8	0.50	0.65	2.41	2.50	27.24	29.22
	10	1.74	2.60	2.08	1.86	28.32	29.00
	12	3.55	3.35	1.38	1.28	30.24	29.98
	14	3.97	3.97	1.52	1.00	30.54	30.32
2	6	0.50	-	0.68	0.68	29.28	28.26
	8	0.45	0.67	2.38	2.48	27.20	29.20
	10	1.78	2.65	2.10	1.84	28.34	29.00
	12	3.58	3.40	1.40	1.25	30.20	30.00
	14	3.90	3.97	1.50	0.98	30.56	30.30
					average	29.12	29.35

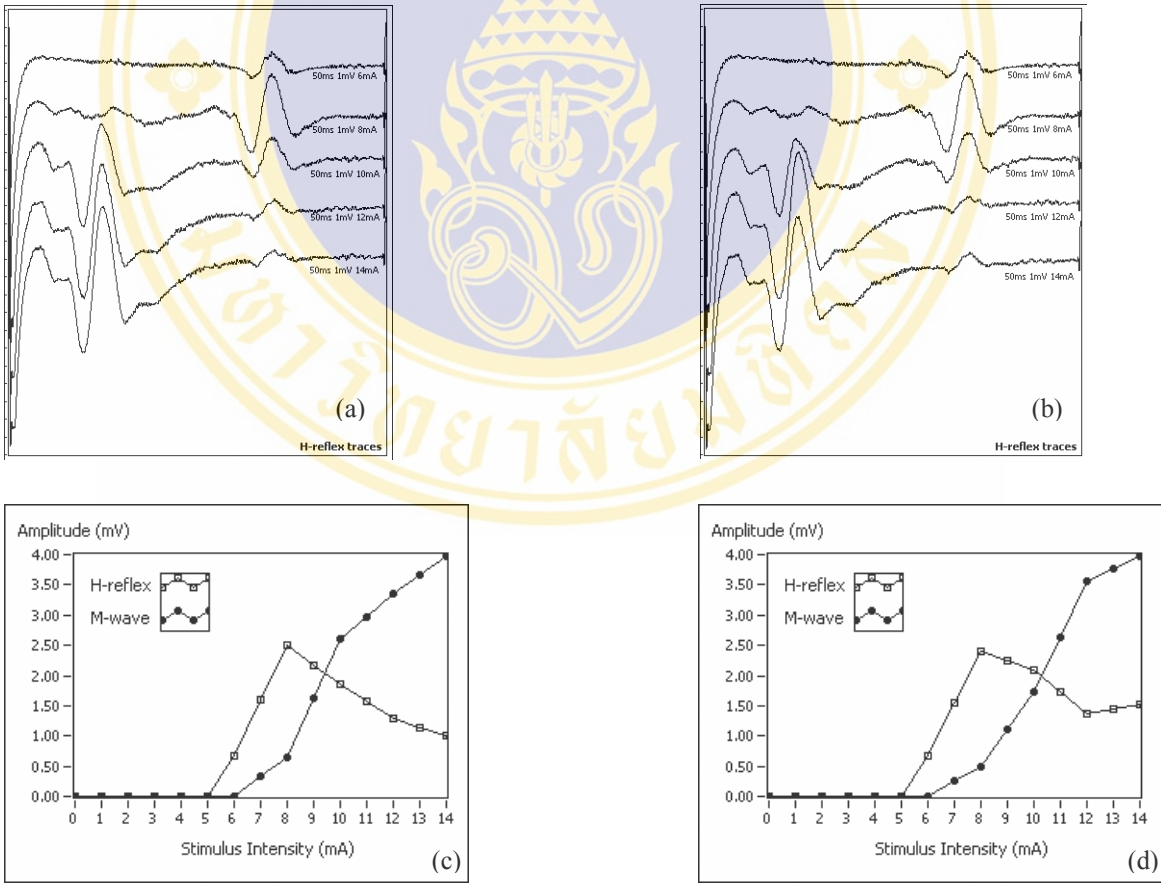

Figure 4.20 The occurrence results for (a) left leg and (b) right leg, along with M-wave and H-reflex recruitment curves for (c) left leg and (d) right leg in normal subject6.

Table 4.19 Results of measurement for the normal subject7 (female).

#test	stimulus (mA)	M amplitude (mV)		H amplitude (mV)		H latency (ms)	
		right	left	right	left	right	left
1	5	-	0.12	0.83	0.97	25.28	25.70
	7	0.84	1.76	1.63	1.18	25.70	25.14
	9	4.22	2.98	0.78	0.91	28.60	26.38
	10	4.63	3.63	-	-	-	-
	12	4.63	4.55	-	-	-	-
2	5	-	0.12	0.83	0.97	25.28	25.70
	7	0.86	1.80	1.60	1.14	25.86	25.14
	9	4.22	2.98	0.78	0.91	28.60	26.40
	10	4.63	3.65	-	-	-	-
	12	4.63	4.55	-	-	-	-
					average	26.55	25.74

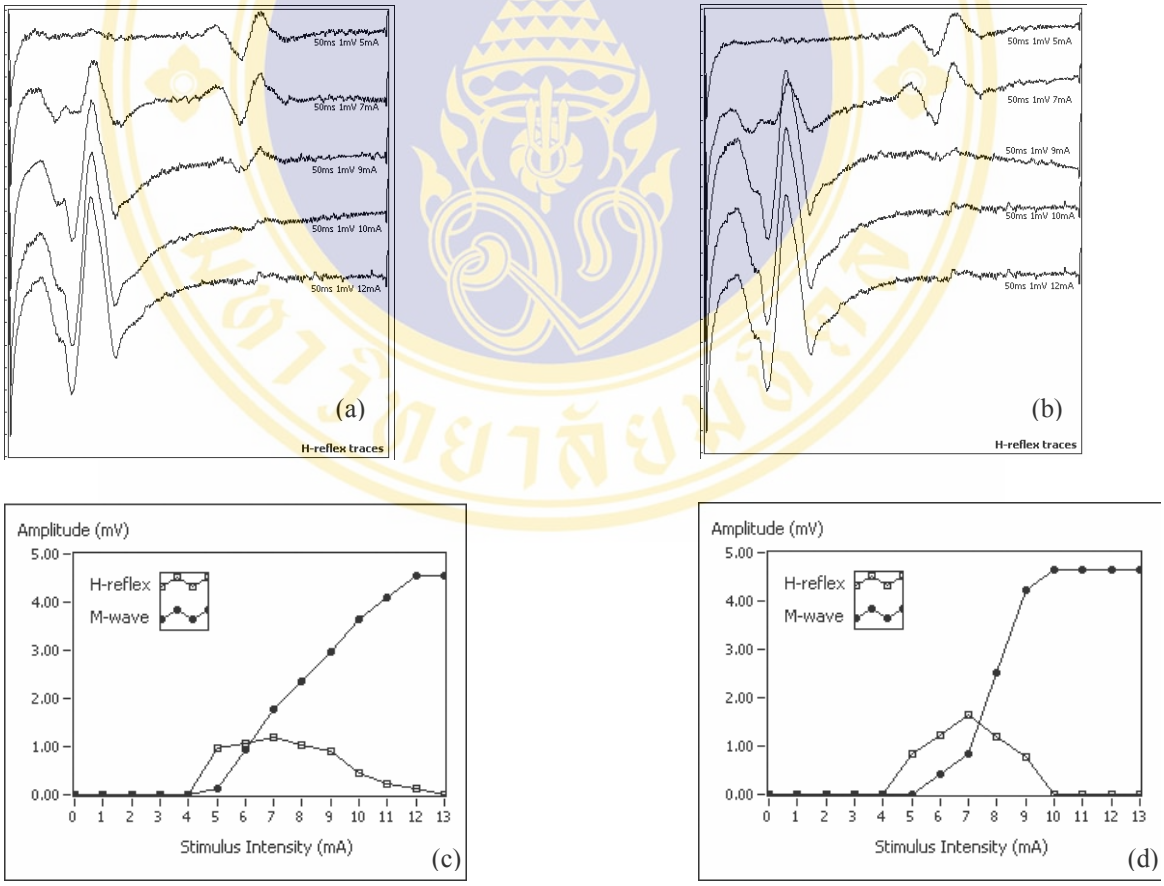

Figure 4.21 The occurrence results for (a) left leg and (b) right leg, along with M-wave and H-reflex recruitment curves for (c) left leg and (d) right leg in normal subject7.

Table 4.20 Results of measurement for the normal subject8 (female).

#test	stimulus (mA)	M amplitude (mV)		H amplitude (mV)		H latency (ms)	
		right	left	right	left	right	left
1	5	0.57	-	1.01	0.50	27.50	25.70
	7	2.73	2.24	1.16	1.23	26.74	27.16
	9	2.92	2.82	1.10	0.94	28.50	27.16
	11	3.55	2.90	0.68	-	30.52	-
	13	3.60	2.90	-	-	-	-
2	5	0.53	-	0.99	0.52	27.48	25.68
	7	2.73	2.26	1.16	1.20	26.76	27.14
	9	2.90	2.80	1.08	0.92	28.50	27.16
	11	3.55	2.93	0.60	-	30.50	-
	13	3.60	2.93	-	-	-	-
					average	28.35	26.67

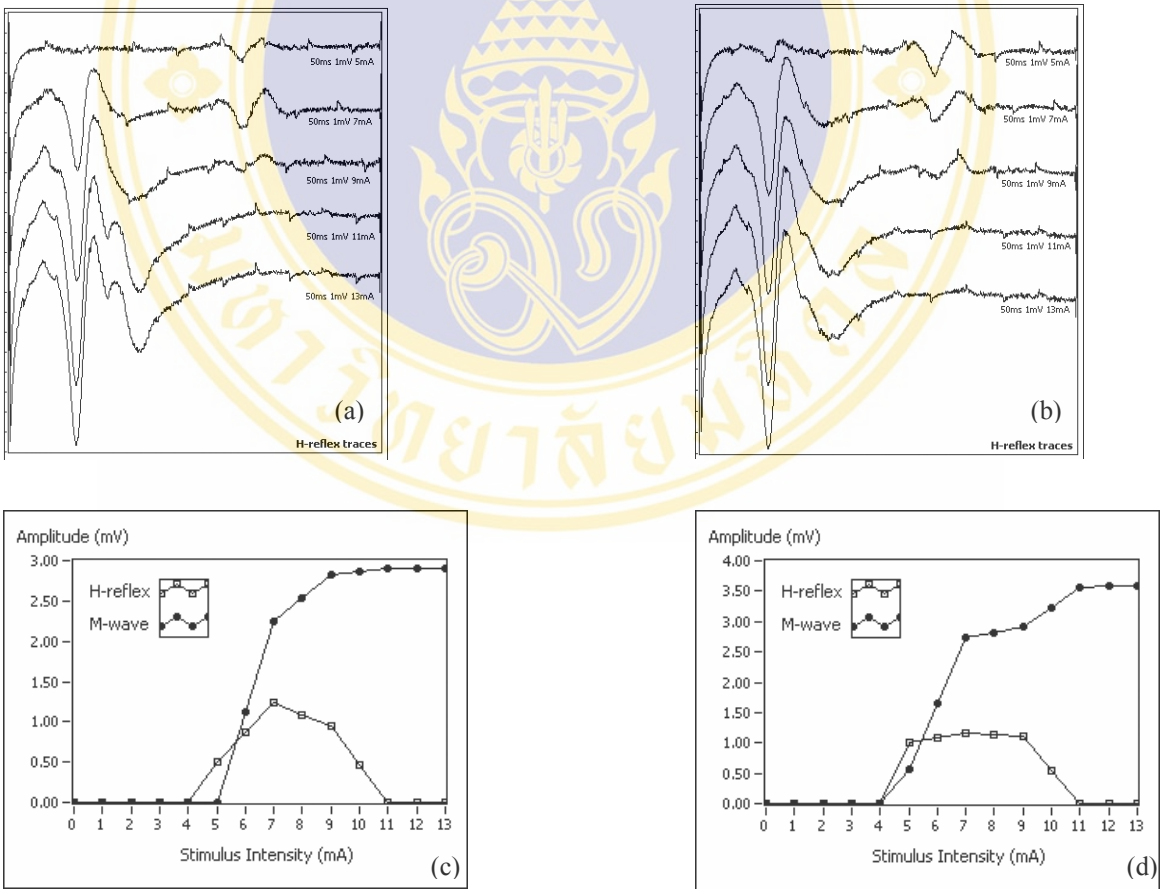

Figure 4.22 The occurrence results for (a) left leg and (b) right leg, along with M-wave and H-reflex recruitment curves for (c) left leg and (d) right leg in normal subject8.

Table 4.21 Results of measurement for the normal subject9 (female).

#test	stimulus (mA)	M amplitude (mV)		H amplitude (mV)		H latency (ms)	
		right	left	right	left	right	left
1	7	0.83	0.72	0.96	1.06	27.16	27.52
	9	2.98	3.31	1.53	1.53	27.16	27.86
	11	3.42	3.19	1.26	1.71	27.96	27.90
	13	3.61	4.34	0.98	1.01	27.96	28.04
	15	4.27	5.28	-	-	-	-
2	7	0.83	0.72	0.96	1.06	27.18	27.52
	9	2.96	3.30	1.55	1.55	27.18	27.86
	11	3.40	3.16	1.28	1.70	27.90	27.86
	13	3.61	4.30	0.96	0.98	27.90	28.02
	15	4.30	5.14	-	-	-	-
					average	27.55	27.82

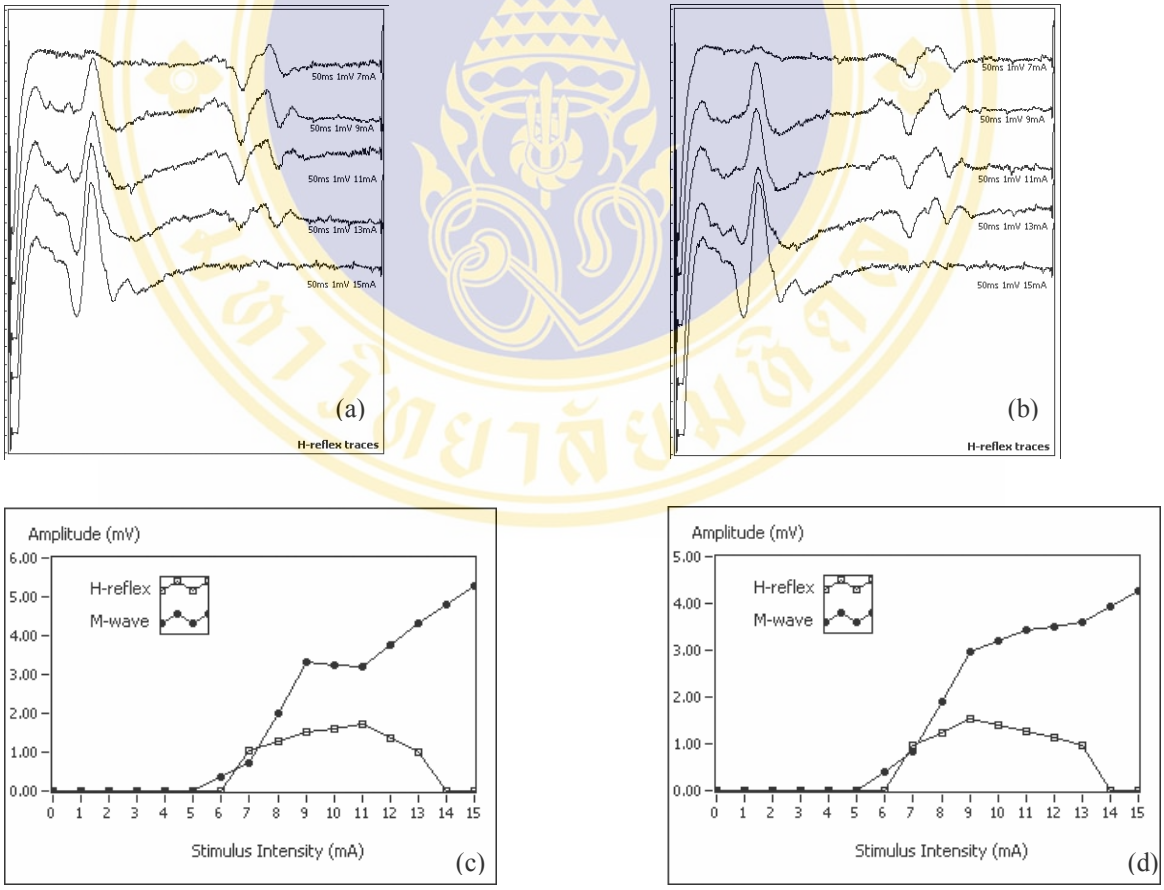

Figure 4.23 The occurrence results for (a) left leg and (b) right leg, along with M-wave and H-reflex recruitment curves for (c) left leg and (d) right leg in normal subject9.

Table 4.22 Results of measurement for abnormal subject1 (male).

#test	stimulus (mA)	M amplitude (mV)		H amplitude (mV)		H latency (ms)	
		right	left	right	left	right	left
1	6	-	0.52	0.52	0.21	29.96	31.76
	8	0.84	3.47	1.61	0.69	29.84	30.66
	10	1.04	4.20	2.37	1.42	29.96	31.90
	12	3.03	4.27	1.35	1.23	31.10	32.72
	14	3.51	4.54	-	0.50	-	33.34
2	6	-	2.83	0.47	0.86	30.24	31.62
	8	0.76	3.81	1.34	1.26	29.74	31.62
	10	1.36	4.12	2.04	1.46	27.36	31.62
	12	3.01	4.23	1.55	1.08	27.50	32.32
	14	4.79	4.52	-	0.50	-	32.32
					average	29.46	31.99

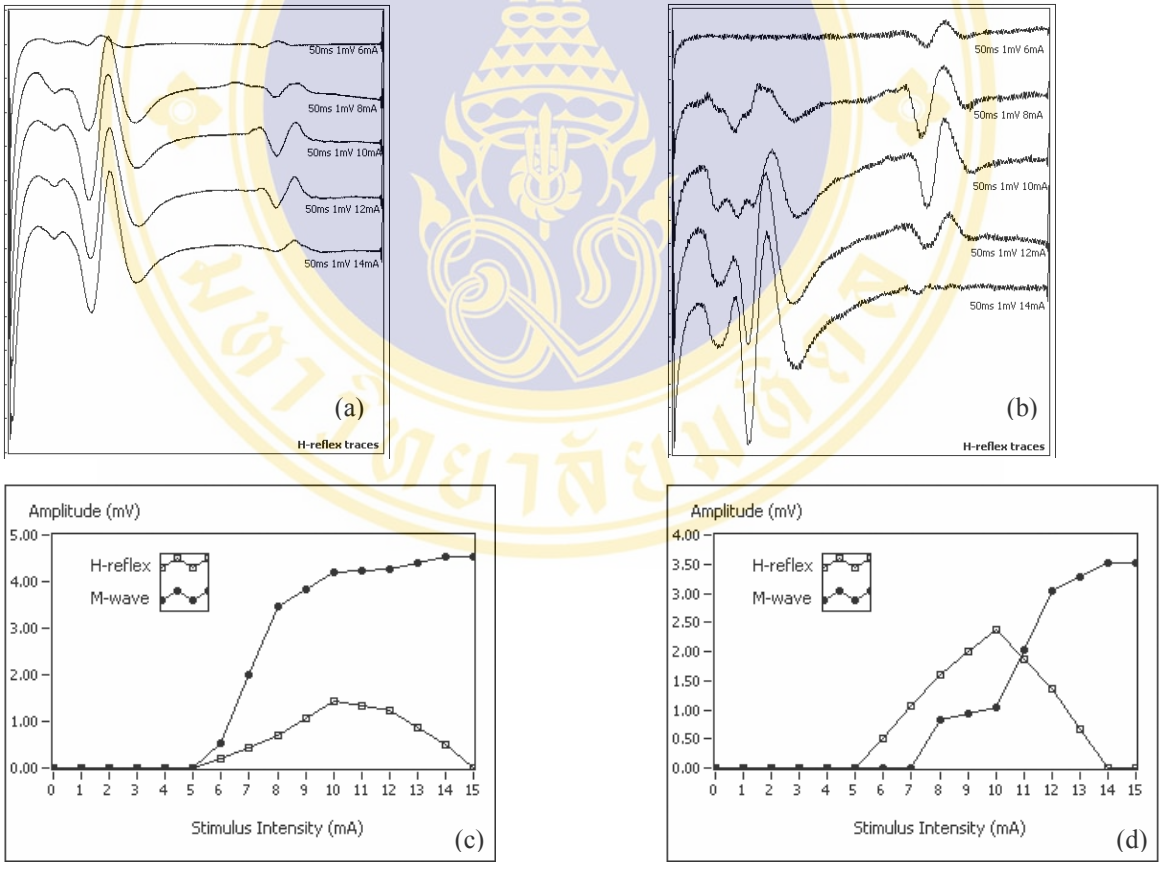

Figure 4.24 The occurrence results for (a) left leg (abnormal) and (b) right leg, along with M-wave and H-reflex recruitment curves for (c) left leg (abnormal) and (d) right leg in patient1.

Table 4.23 Results of measurement for abnormal subject2 (male).

#test	stimulus (mA)	M amplitude (mV)		H amplitude (mV)		H latency (ms)	
		right	left	right	left	right	left
1	7	0.51	0.42	0.23	-	33.34	-
	9	1.00	3.08	0.12	0.29	35.52	33.80
	11	0.71	3.13	-	0.27	-	33.82
	13	0.71	3.13	-	-	-	-
	15	0.71	3.13	-	-	-	-
2	7	0.48	0.45	0.25	-	33.40	-
	9	1.06	3.08	0.10	0.20	35.60	33.86
	11	1.08	3.13	-	0.20	-	33.86
	13	1.08	3.20	-	-	-	-
	15	1.08	3.23	-	-	-	-
					average	34.47	33.84

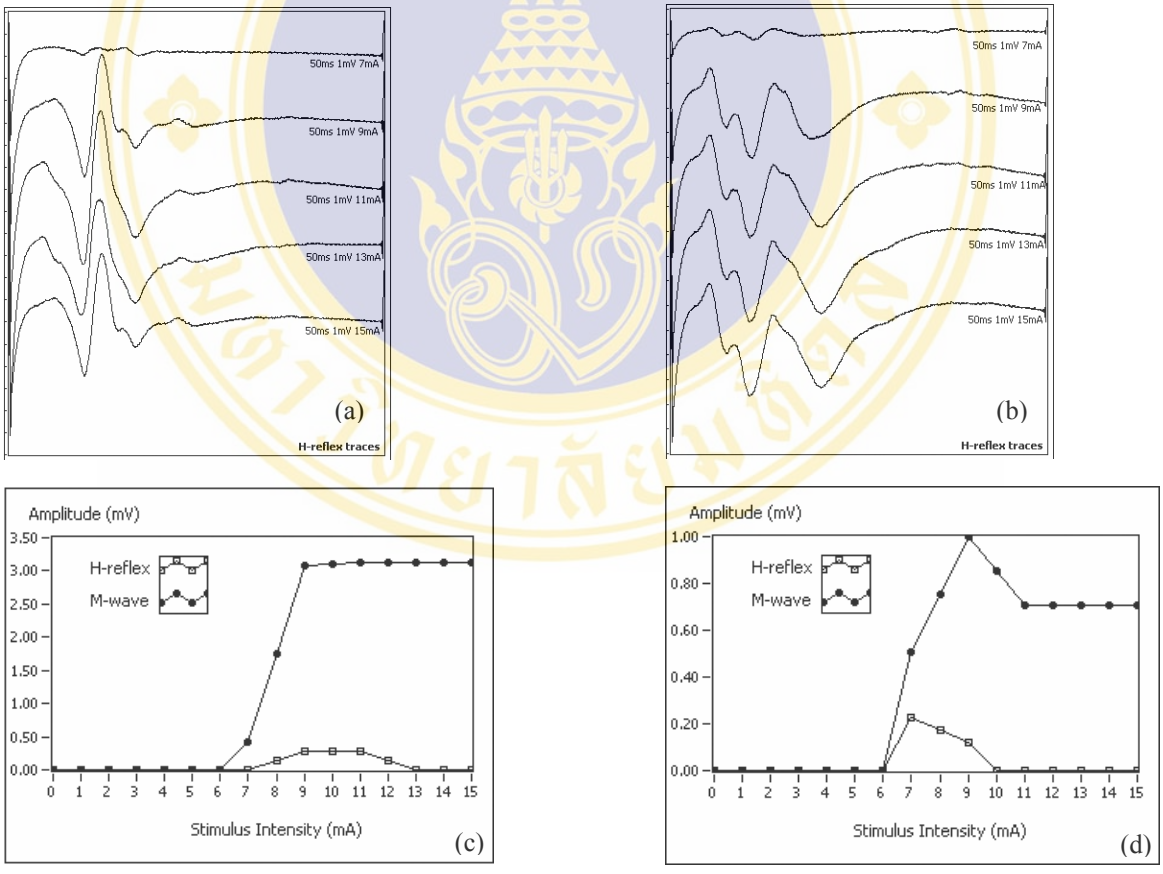

Figure 4.25 The occurrence results for (a) left leg (abnormal) and (b) right leg, along with M-wave and H-reflex recruitment curves for (c) left leg (abnormal) and (d) right leg in patient2.

Table 4.24 Results of measurement for abnormal subject3 (male).

#test	stimulus (mA)	M amplitude (mV)		H amplitude (mV)		H latency (ms)	
		right	left	right	left	right	left
1	7	-	-	0.72	0.50	29.04	28.34
	9	0.36	0.68	0.80	1.15	31.44	29.14
	11	1.00	1.92	1.23	0.88	31.34	34.24
	13	1.24	1.59	0.79	0.60	33.82	35.76
	15	1.24	1.96	-	-	-	-
2	7	-	-	0.62	0.68	29.28	30.18
	9	0.74	1.84	0.95	1.15	31.20	29.28
	11	1.09	1.80	0.81	0.99	31.40	34.16
	13	1.16	2.01	0.62	0.50	33.80	35.60
	15	1.16	2.01	-	-	-	-
					average	31.42	32.09

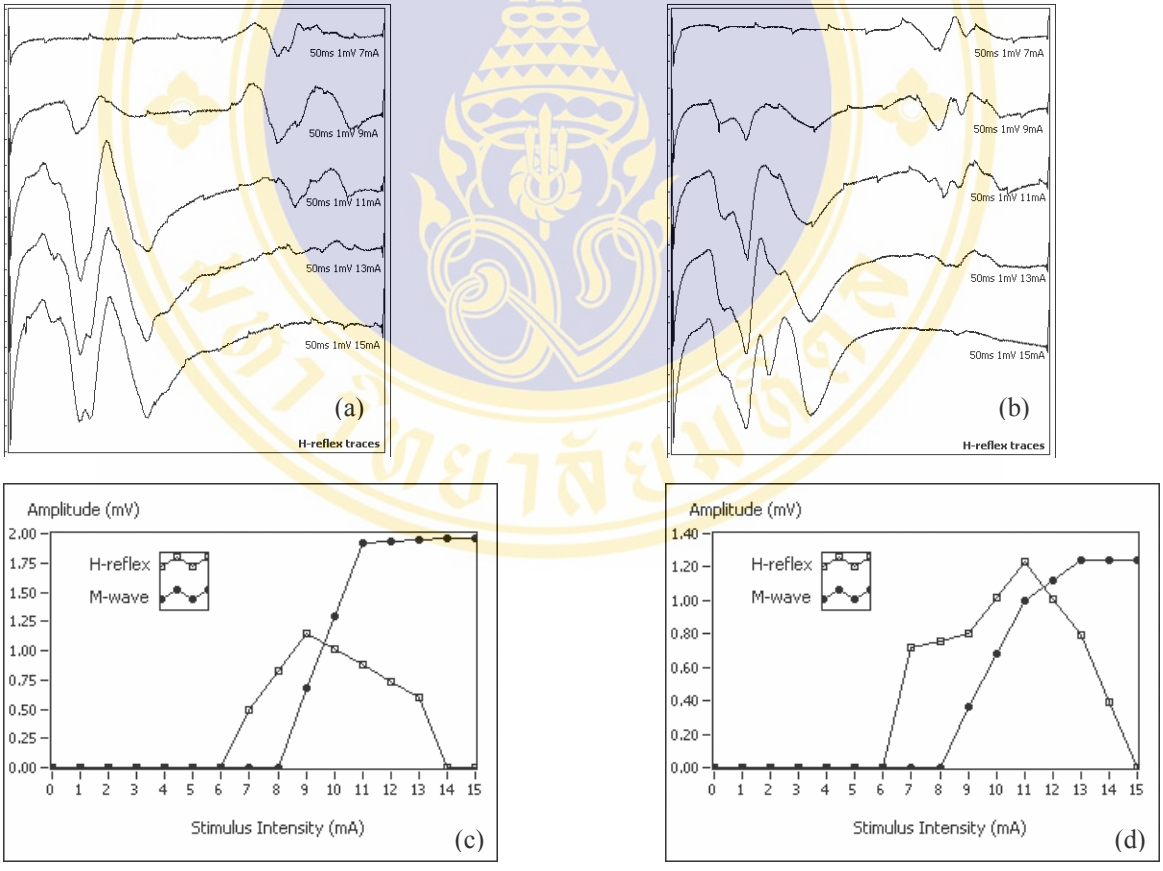

Figure 4.26 The occurrence results for (a) left leg and (b) right leg (abnormal), along with M-wave and H-reflex recruitment curves for (c) left leg and (d) right leg (abnormal) in patient3.

Table 4.25 Results of measurement for abnormal subject4 (male).

#test	stimulus (mA)	M amplitude (mV)		H amplitude (mV)		H latency (ms)	
		right	left	right	left	right	left
1	7	-	0.30	1.13	0.10	29.96	29.56
	9	1.00	1.13	1.80	1.27	31.08	27.62
	11	2.64	3.04	1.19	1.51	34.52	27.12
	13	2.70	4.12	1.08	1.27	33.78	27.12
	15	2.70	4.55	0.48	1.17	33.80	27.76
2	7	-	0.25	1.38	0.26	29.96	29.96
	9	1.44	1.20	1.84	1.44	33.00	27.48
	11	2.33	3.43	1.47	1.41	33.00	27.50
	13	2.68	4.35	1.10	1.27	33.82	27.50
	15	2.68	4.71	-	1.17	-	27.22
					average	32.55	27.88

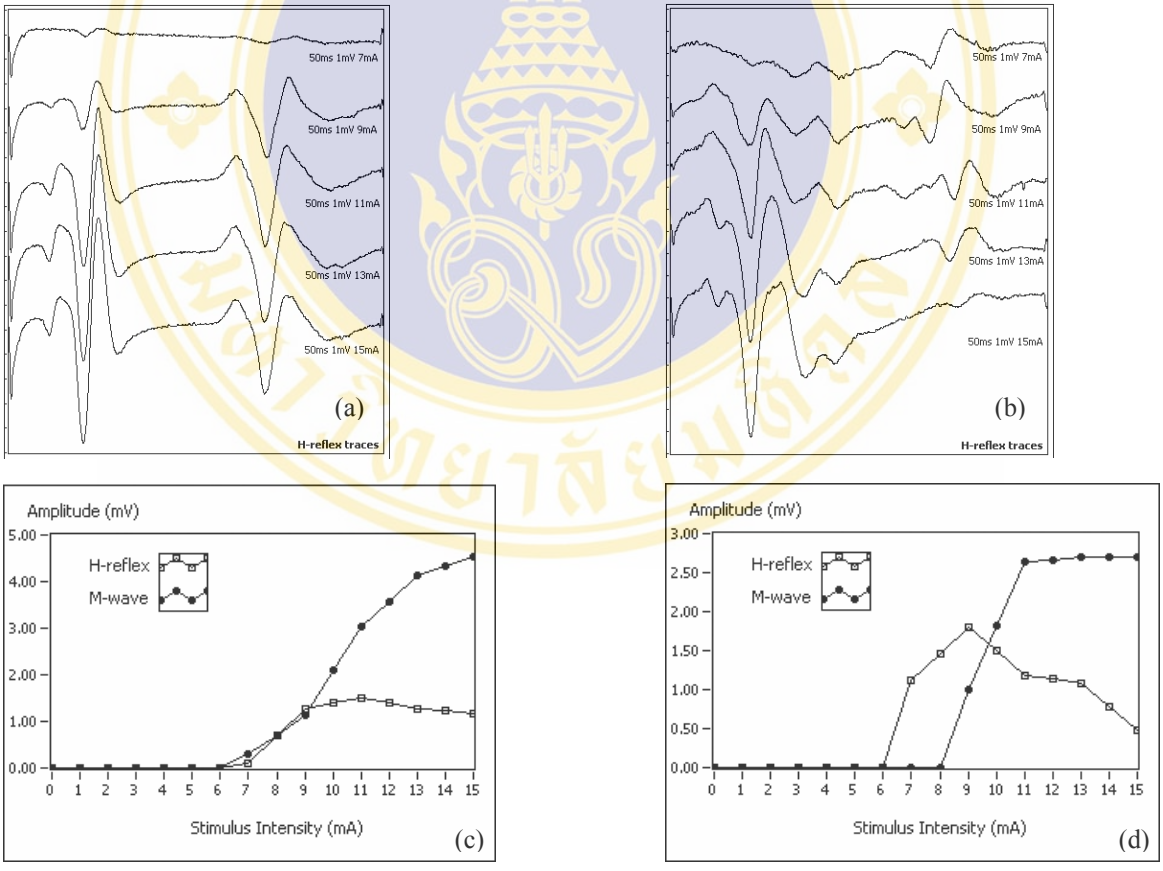

Figure 4.27 The occurrence results for (a) left leg and (b) right leg (abnormal), along with M-wave and H-reflex recruitment curves for (c) left leg and (d) right leg (abnormal) in patient4.

Table 4.26 Results of measurement for abnormal subject5 (male).

#test	stimulus (mA)	M amplitude (mV)		H amplitude (mV)		H latency (ms)	
		right	left	right	left	right	left
1	7	0.29	0.80	0.82	0.30	29.04	30.80
	9	1.48	1.83	2.19	0.74	29.04	29.80
	11	1.85	2.17	1.21	0.50	30.30	32.48
	13	2.88	2.84	0.80	-	33.96	-
	15	2.90	3.04	0.27	-	33.96	-
2	7	0.37	0.80	1.31	-	29.10	-
	9	1.37	1.75	1.70	0.97	29.72	30.08
	11	1.93	2.20	0.95	0.79	30.10	30.08
	13	2.43	2.68	0.23	0.70	33.54	30.18
	15	3.23	3.10	0.10	-	34.00	-
					average	31.28	30.57

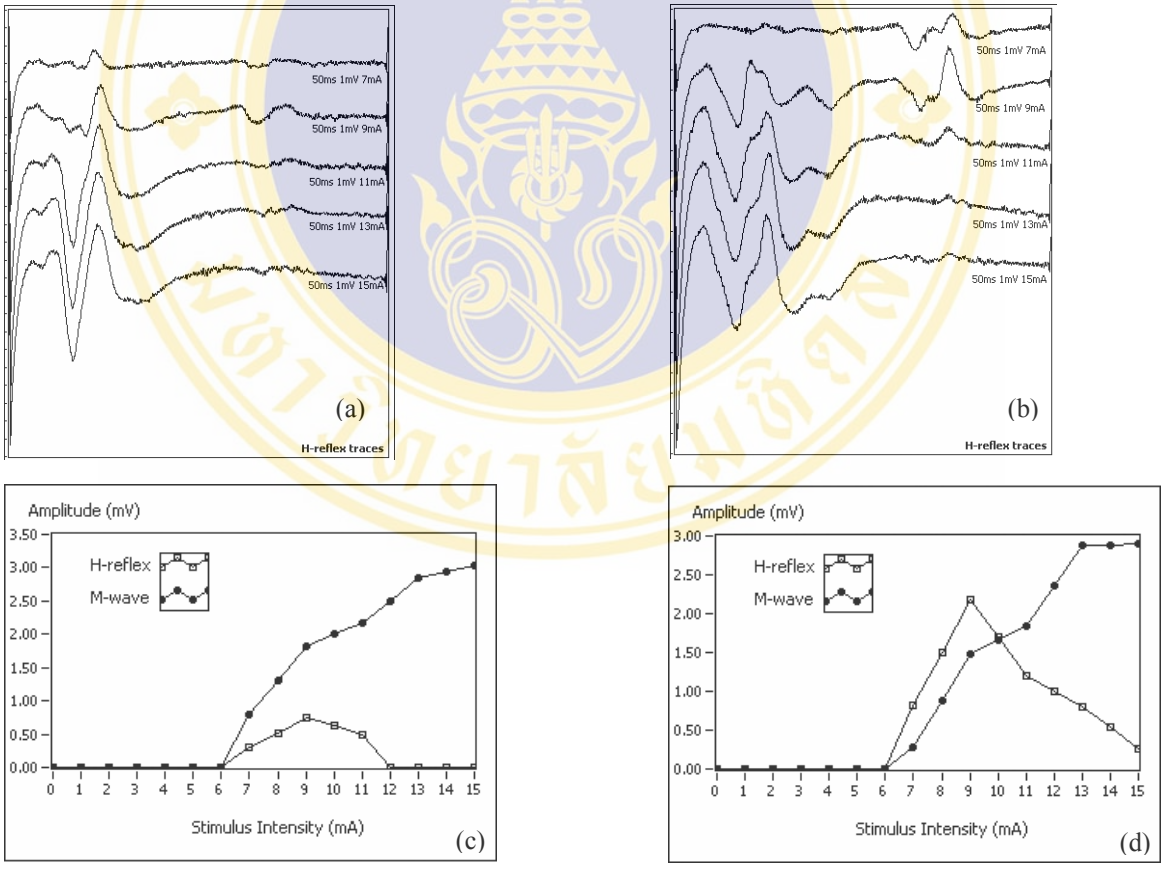

Figure 4.28 The occurrence results for (a) left leg and (b) right leg (abnormal), along with M-wave and H-reflex recruitment curves for (c) left leg and (d) right leg (abnormal) in patient5.

Table 4.27 Results of measurement for abnormal subject6 (male).

#test	stimulus (mA)	M amplitude (mV)		H amplitude (mV)		H latency (ms)	
		right	left	right	left	right	left
1	7	-	0.78	0.72	-	27.00	-
	9	0.60	1.30	0.83	0.72	27.00	28.46
	11	1.48	2.18	1.04	0.66	30.80	29.38
	13	1.90	3.47	0.50	0.59	31.00	29.38
	15	1.90	3.87	-	-	-	-
2	7	-	1.20	1.24	-	26.52	-
	9	0.48	1.52	0.81	0.94	26.42	27.48
	11	1.14	2.58	0.77	0.81	28.06	27.90
	13	1.84	3.75	0.69	0.55	29.46	30.07
	15	1.84	3.80	-	-	-	-
					average	28.28	28.78

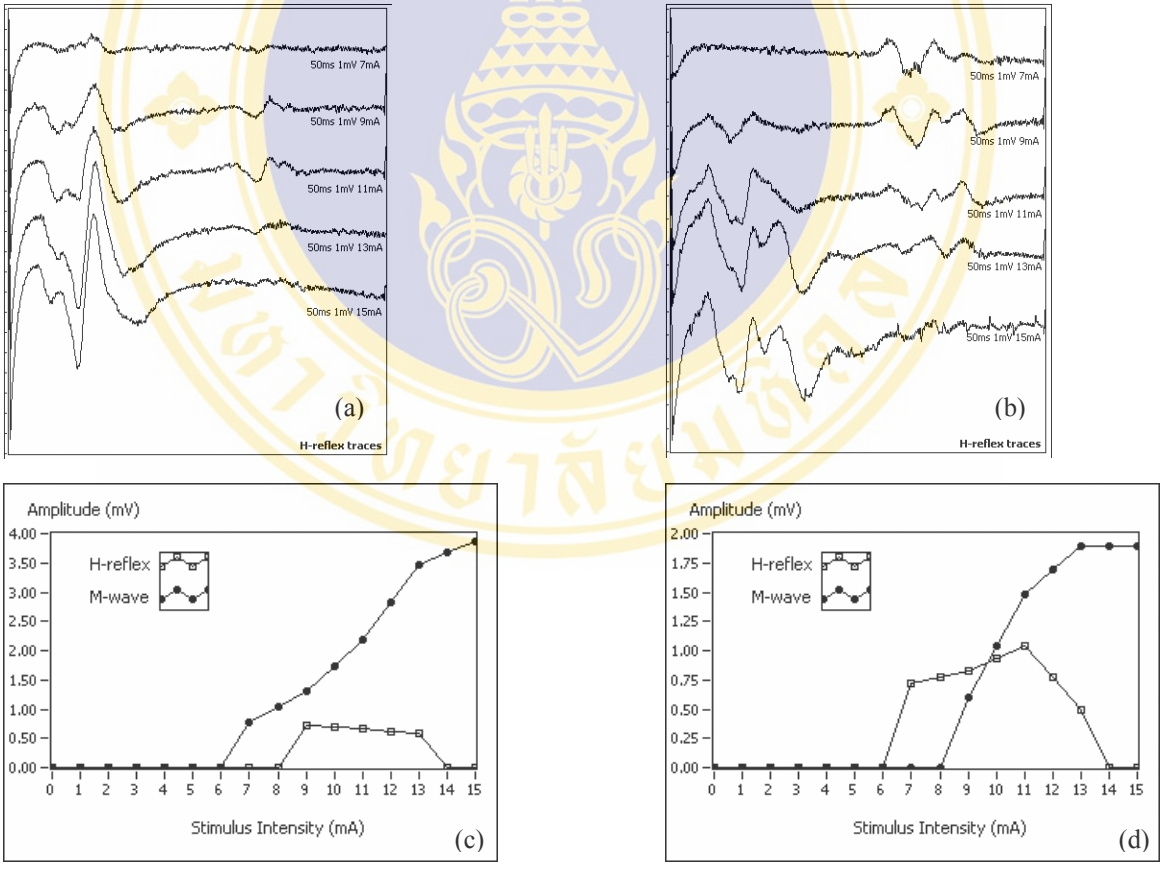

Figure 4.29 The occurrence results for (a) left leg and (b) right leg (abnormal), along with M-wave and H-reflex recruitment curves for (c) left leg and (d) right leg (abnormal) in patient 6.

Table 4.28 Results of measurement for abnormal subject7 (male).

#test	stimulus (mA)	M amplitude (mV)		H amplitude (mV)		H latency (ms)	
		right	left	right	left	right	left
1	7	-	0.65	0.20	-	32.42	-
	9	0.46	1.28	0.16	-	33.14	-
	11	0.97	1.39	-	-	-	-
	13	1.12	2.15	-	-	-	-
	15	1.22	2.19	-	-	-	-
2	7	-	0.70	0.30	-	32.52	-
	9	0.89	1.50	0.10	-	32.52	-
	11	1.02	1.99	-	-	-	-
	13	1.16	2.07	-	-	-	-
	15	1.61	2.12	-	-	-	-
					average	32.65	

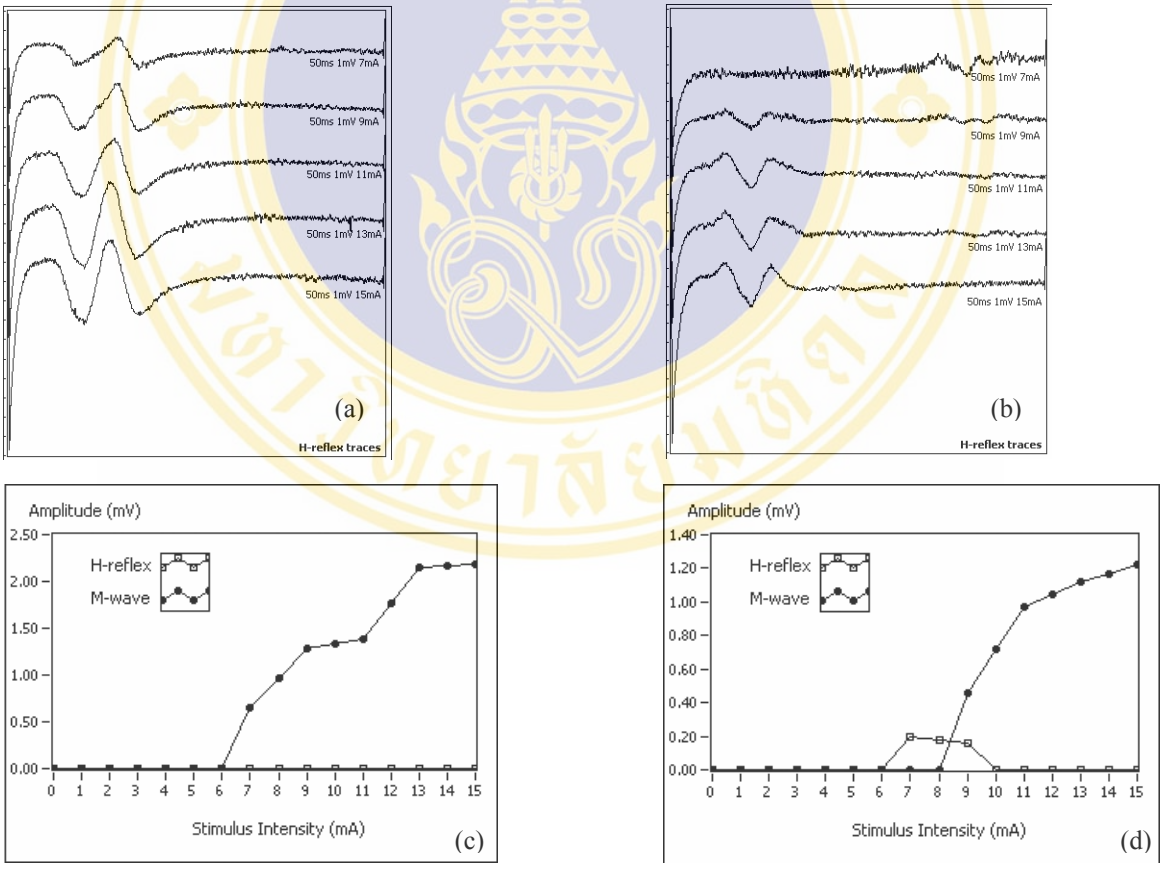

Figure 4.30 The occurrence results for (a) left leg and (b) right leg (abnormal), along with M-wave and H-reflex recruitment curves for (c) left leg and (d) right leg (abnormal) in patient7.

Table 4.29 below shows the latencies of subject compared with the predicted normal H-reflex latency together with the maximal M-wave, the maximal H-reflex, and the percentage in the ratio of H_{max}/M_{max}.

Table 4.29 Results of latency in each subject compared with the predicted normal value that is calculated from formula 4.1 and 4.2.

#subject	M_{max} amp. (mV)		H_{max} amp. (mV)		$H_{predict}$ (4.1) lat. (ms)	$H_{predict}$ (4.2) lat. (ms)	$H_{average}$ lat. (ms)		% H_{max}/M_{max}	
	R	L	R	L			R	L	R	L
Normal										
1	6.38	6.27	1.97	2.09	27.12	27.69	27.53	27.75	30.88	33.33
2	6.27	6.27	2.30	2.10	27.94	27.98	28.29	28.22	36.68	33.49
3	1.76	1.85	1.10	1.68	27.15	27.83	26.85	27.93	62.50	90.81
4	1.68	1.52	1.47	1.64	27.48	27.98	26.97	29.23	87.50	92.68
5	3.55	3.48	2.72	2.17	26.82	26.08	24.40	25.19	76.62	62.36
6	3.97	3.97	2.41	2.50	26.82	26.37	29.12	29.35	60.71	62.36
7	4.63	4.55	1.63	1.18	26.59	26.37	26.55	25.74	35.21	25.93
8	3.60	2.93	1.16	1.23	26.82	26.52	28.35	26.67	32.22	41.98
9	4.30	5.28	1.55	1.71	26.82	26.66	27.55	27.82	36.05	32.39
Abnormal										
1	3.51	4.54	2.37	1.46	29.69	27.10	29.46	31.99	67.52	32.16
2	1.08	3.23	0.25	0.29	30.49	27.25	34.47	33.84	23.15	8.98
3	1.24	2.01	1.23	1.15	30.06	26.96	31.42	32.09	99.19	57.21
4	2.70	4.71	1.84	1.51	29.62	27.54	32.55	27.88	68.15	32.06
5	3.23	3.10	2.19	0.97	29.58	28.27	31.28	30.57	67.80	31.29
6	1.90	3.87	1.24	0.94	29.16	27.10	28.28	28.78	65.26	24.29
7	1.61	2.19	0.00	0.00	30.67	28.71	32.65	0.00	0	0

Table 4.30 Results in consistency of the H-reflex latency on each side and side-to-side difference.

#subject	$H_{average}$ latency (ms)		Side-to-side Difference (ms)
	Right	Left	
1	27.53	27.75	0.22
2	28.29	28.22	0.07
3	26.85	27.93	1.08
4	26.97	29.23	2.26
5	24.40	25.19	0.79
6	29.12	29.35	0.23
7	26.55	25.74	0.81
8	28.35	26.67	1.68
9	27.55	27.82	0.27

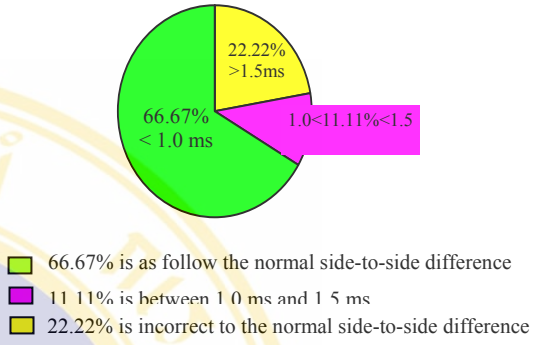

The standard side-to-side difference for normal population should be less than 1.5 ms or less than 1.0 ms in some investigators. For the results of side-to-side difference, 66% is as follow the normal side-to-side difference, 11% is between 1.0 ms and 1.5 ms, and 22% is incorrect to the normal side-to-side.

Table 4.31 Results in consistency of the H-reflex latency on each side and side-to-side difference.

#subject	$H_{average}$ latency (ms)		Side-to-side Difference (ms)
	Right	Left	
1	29.46	31.99	2.53
2	34.47	33.84	0.63
3	31.42	32.09	0.67
4	32.55	27.88	4.67
5	31.28	30.57	0.71
6	28.28	28.78	0.50
7	32.65	xx	xx

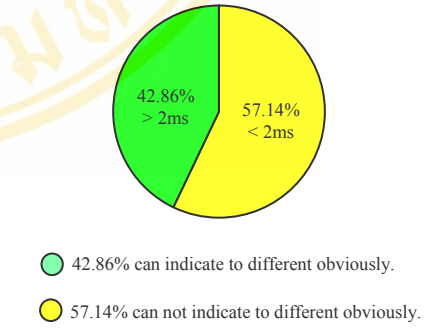

This table shows consistency of the H-reflex latency on each side of abnormal subject. Subject7 can not be found the H-reflex on the left, compared with the right.

CHAPTER V
DISCUSSION

The major goal of the study was to design and construct an H-reflex detectable instrument as well as the developed LabVIEW program for acquiring the H-reflex, which used as a clinical tool and provides a noninvasive method of monitoring the integrity and functionality of central nervous system, particularly the information concerning with the monosynaptic reflex pathway. Furthermore, the instrument might be a quick clinical evaluation for peripheral nerve dysfunction. The discussion of the results from designed and constructed instrument along with the recording program for eliciting and acquiring the H-reflex activity are presented in two parts as follow:

5.1 The design and construction

The design, the provision, and the construction of materials in both of the electrical stimulator and data acquisition system are discussed. Not only that, any deficiency in function or operation is mentioned including the modification and adjustment for suitable use. Moreover, the discussion on an external feature of the monitor and the low cost of the research are presented.

5.1.1 The stimulator system parts

For this part, the discussion to result and reason in the design and construction of parameters of stimulator system together with the protection system are mentioned. The important parameters in stimulator system consist of the frequency, duration, and intensity of stimulation. In designing the frequencies and durations as such required, the timing VI program is selected to use. Owing to it can easily control and can also produce accurate and highly stable time delay or oscillation. It is also reliable, easily applied, and inexpensive. It requires rather low power consumption. Functionally, it operates as an astable multivibrator that can produces rectangular pulse continuously by programming counter software. It is written as a VI that generates a continuous pulse train on the OUT pin of the chosen counter, default is counter 0. This

VI works with the DAQ device that has a DAQ-STC counter timer chip. The instructions are necessary to consider consisting of the device number of board, the counter number, input/output connection, and pulse polarity. When VI is run, the continuous pulse train with desired frequency and duration are generated on the OUT pin of the chosen counter. The actual parameters outputs may differ from desired inputs because the pulse is obtained by dividing down a timebase by a whole number. It may be that exact desired frequency cannot be obtained. The output at OUT pin is a trigger signal for the synchronization of data acquisition process relative to the stimulus event, and is used for controlling a pulse current as desired on the stimulator.

For the intensity of stimulation, the type of power output is constant current which generate the peak power at 200 Vdc load maximal 10 kΩ and keep the current level constantly while stimulating regardless load impedance. It helps to guarantee a preset current intensity when the delivered current changes with the characteristic of the electrode/skin load and it is more appropriate than other commercially available stimulators handling over voltage pulse. In addition, it is an alternative and simple constant-current stimulator employing only conventional high-voltage components while featuring good controllability of stimulation parameters such as amplitude, duration, and frequency of the pulsed current. Its small number of components makes it attractive for low-cost application.

When high voltage comes in contact with human subjects, safety must be of primary concern. The design and construction incorporate many safety features intended to protect the subject from harmful electrical shock: isolation and protection techniques. All power supplies are transformer coupled and isolated from mains power supplies via an isolation transformer hardwired to the power cord. The stimulator chassis is hardwired to ground earth and leakage between any lead to ground is less than 10 μA, in accordance with hospital equipment safety standards (61). This prevents the subject from being dangerously shocked if he or she touches a grounded appliance while being stimulated or in the unlikely event that a failure occurs and high-voltage power supplies are applied directly to the stimulating electrodes. The optical isolation (optocoupler) in the timing stage ensures subject safety even if dangerous voltages are applied to the inputs. Furthermore, the protection circuit with a

crowbar technique is used to prevent over voltage supplied in output stage for generating a pulse-current.

The power supply part uses rechargeable battery to supply of all system in constructed device for operation. These are used to internally isolated transformers and regulated circuit for power supply into battery charger circuit, which shielded and placed as far as possible from the input part and the acquiring part because of the electrical interferences.

5.1.2 The signal conditioning parts

The application of constructed device in signal conditioning circuitry is very advantages, essentially as noninvasive monitoring. This concept expands the function and enhances the performance of preparing signal before analog to digital conversion process. It reduces the complexity of the electrical and electronic circuits designed and improves an ability of measurement function. The system is simply due to its less sophistication. In acquiring of H-reflex response detected into a bioamplifier circuit, this part seems to work very well, however it is more convenient to use an IC instrumentation amplifier, such as AD524 or INA 110 (preamplifier), as a single chip instead of using many operational amplifiers (ICs), which are connected to make a complete circuit. The instrumentation amplifier on the single chip has many advantages, particularly requiring a few external components to be connected and reducing to external interference, resulting in increasing bioelectrical signal measurement and detection stability significantly (33, 55, 59, 60). For the next stage of signal conditioning circuitry before the sampler and the analog to digital conversion, the anti-aliasing filter in an analog butterworth filter is used to prevent the aliasing components from being sampled. It is mostly designed as a low-pass filter that besides to be used in preventing aliasing events, it is also used for eliminating high noise frequencies to be completely certain that the frequency content of the input signal is limited. The designed circuit is simpler to use and only a few items need be considered for proper operation and good efficiency. To minimize lowpass and notch frequency shift with temperature, silver mica, or polycarbonate, capacitors should be used with precision resistors. Notch depth depends on component match; therefore, 0.1 percent resistors and 1 percent capacitors are suggested to minimize the trimming needed for a 60 dB notch. To insure stability of the TL084, the power supplies should be bypassed

near the integrated circuit package with 0.01 μF disc capacitors. The signal conditioning circuitry is implemented in a shield case isolated from the stimulator part. This separation helps to prevent artifacts or unwanted frequencies generated from the transformer of the stimulator which may affects the accuracy of the instrumentation amplifier or analog-to-digital converter in the input part (32, 54, 57, 60, 62).

5.1.3 The analog to digital (ADC) and digital to analog (DAC) parts

Both ADC and DAC is a plug-in data acquisition (DAQ) device of National Instruments Corporation which is a board to be sat in a slot in a slot in a computer's motherboard. This plug-in DAQ device of National Instruments Corporation offers a wide variety of ADC and DAC modules for a number of platforms, here uses Windows. The structure of this board uses E Series technology to deliver high performance and reliable data acquisition capabilities for a wide range of applications. These E Series DAQ devices feature analog and digital triggering capability, as well as two 12-bit analog outputs, two 24-bit 20 MHz counter/timers, and eight digital Input/Output (I/O) lines. Depending on computer hard drive these devices can stream data to disk at rates up to 500 kS/s. The I/O connector for this board (AT-MIO-64E-3) has 100 pins that can connect to 100-pin accessories with the shielded cable of SCB-100 connector block. The SCB-100 is used as a shielded I/O connector blocks for rugged, very low noise signal termination. The analog input and output of board are is software configurable that make it easy to handle, debug, and develop the measurement when an error occurs. For input mode of measurement, it can also be software configurable. The configuration with differential input mode of board is appropriate because of the signal source is supplied by a battery-powered device that has an isolated ground-reference point (floating source) and meet any of the following conditions:

- The input signal is low level (less than 1 V).
- The leads connecting the signal to the DAQ board are greater than 3 m.
- The input signal requires a separate ground-reference point or return signal.
- The signal leads travel through noisy environments.

The following the differential signal connection resulting to reduce picked-up noise and increase common-mode noise rejection. The differential signal connection

also allows input signals to float within the common-mode limits of the programmable gain instrumentation amplifier (PGIA).

In using output mode of DAQ board, it is software configurable to generate an analog output for controlling an external stimulator circuit and providing a digital trigger signal. The DAQ board has a counter chip, DAQ-STC chip, which provides a high precision timing with the resolution of 24 bit. With high resolution of counter chip, the generated analog output is available to control the external circuit. Furthermore, the DAQ-STC provides a very flexible interface for connecting timing signals to external circuitry, by using the RTSI bus for interconnecting timing signals between boards and the programmable function input (PFI) pins on the I/O connector for connecting to external circuitry.

5.1.4 The cost estimation

The cost evaluation of this instrument is appraised only on the components and materials used in the stimulator and signal conditioning system because of these instruments are designed and constructed to apply the accessory and DAQ board existed. The cost of any technology in the construction and designing cost, the experiment and modification which is very important and rather expensive not included. Moreover, this evaluation is an estimation of only the laboratory prototype system. If the estimation is appraised in the commercial prototype, the entire production cost must be higher than this laboratory prototype but it is also still reasonable.

Cost of the stimulator part is listed as follow.

1) Bipolar stimulating electrode part	4,500 baht
2) Electrical components	5,650 baht

Cost of the signal conditioning part is listed as follow.

1) Electrodes	6,850 baht
2) Analog components	4,400 baht

Cost of the power supply part is listed as follow.

1) Battery part	1,500 baht
2) Battery charger part	500 baht
Cost of cage and other accessories etc.	2,200 baht

Then, the total cost estimation of this prototype is 25,600 baht.

Using only conventional standard components, which are inexpensive and commonly available, make it attractive for low cost applications. When it is compared to commercial device, the cost of this prototype is rather cheaper than the commercial device for the same part while featuring good capabilities.

5.2 Discussion of the test and results in constructed device

Several considerations in the technical and functional testing are discussed interestingly, including an error and accuracy of the parameter setting. The operative function and durability of prototype system are also presented.

5.2.1 The technical consideration of stimulator part

At present the construction is complete and printed circuit boards (PCBs) are being fabricated. The design and construction are planed to investigate the capabilities for evoking the H-reflex response. The implementations of previous parameters can be discussed as follow.

5.2.1.1 The adjustable frequency and duration part of stimulator

The frequency and duration of stimulation are imposed and controlled by a counter of DAQ board that is software configurable and programmable. With the precise resolution of 24 bit and minimum pulse duration of 10 ns in edge-detect mode by using a counter on DAQ board, generating an output pulse is available for precision timing. The output pulse derived from the counting capability respond to and output TTL signals; square-pulse signals that are 0 V (low) or 5 V (high) in value as configured. The one-shot pulse imposed by this counter has been input to the optocoupler. This will be available to isolate electrically the stimulator from the counter on DAQ board that enforces the pulse duration of load current. This pulse duration is necessary to amplify a sufficient current level to drive the switching circuit because the structure of switching circuit is formed by MOSFET transistor which it is adequately required a large current level. To obtain an enough current level, the push-pull arrangement with class AB amplification is employed. This amplification is well solution that tries to take the good points and minimize the problems of each in class A and B.

Specified intervals for pulse-width of the stimulation current is 0.1 ms $\leq T_{pulse} \leq$ 1.0 ms. Pulse-repetition is in ranges from 0.1 Hz to 1 Hz. Both are realized as follow

the clinical safety and requirement (32, 35). In addition, they are software programmable in other interval for investigating new conditions on the same content. The result of pulse duration is a short square-pulse signal that is similar to a twitch with a single electrical shock. An advantage of imposing the pulse current with software configuration is accuracy, easy and fast to handle and debug the errors occurred.

5.2.1.2 The power output part of stimulator

The power output of stimulation is designed to simplify in controlling while featuring good controllability of stimulation parameters such as amplitude, duration, and frequency of the pulsed current. By using the standard regulator circuit, an oscillator incorporated to a step-up transformer, and a common ac/dc conversion, the output control in the regulator stage is proportional to the peak-amplitude at the secondary of transformer that provides the necessary compliance voltage to generate the desired stimulation currents. On the present prototype, the desired stimulation current ranges from submaximum to subtheshold. It is difficult to determine specific values of these ranges, since depending on many factors of stimulation such as type of stimulating electrode, sort of output intensity, method of setting, etc. A good solution of these complication is determined the intensity of stimulation as the constant current type because it guarantees a preset current intensity when the delivered current changes with the characteristic of the electrode/skin load and it is more appropriate than other commercially available stimulators handing over voltage pulse (32, 35, 57, 63). Hence, the output voltage of regulator is sufficiently set up in ranges from 0 V to 20 V. This range is also available to be supplied by the battery source. As function of set up regulated voltage and the step-up transformer with a ratio of windings N_1 = 1:10, a high-voltage oscillation of 438 $V_{p\text{-}p}$ at maximum or approximately 210 V_{dc} after ac/dc conversion appears at its secondary. This high voltage is sufficiently supplied to demand in generating the intensity output of stimulation.

To ensure 0 V as the minimize dc-voltage in the voltage regulator stage diodes are serially connected to the output pin of regulator for dropping voltage. The driving stage built around a self-biased current mirror is formed by N-channel MOS transistors. The standard cascade configuration was selected by its simplicity while providing a high dynamic output-resistance (4, 41). As equation in 3.8 referred to

Chapter 3, the peak-amplitude of pulse stimulation depends on the compliance high voltage and a reference resistor. The acquired compliance high voltage and fixed reference resistor of current mirror determine the stimulus current through the skin, which is independent of load characteristic. At good approximation, adjusting the stimulation current by means of a variable resistor in voltage regulator compensates for the poor matching between discrete transistors in the current mirror. Upon assertion of push-pull driver, the switching circuit switches on the current mirror, so that a pulsed current is delivered by the stage.

The load represent to a maximum value of 10 kΩ that mimics the electrode/skin interface and the bulk resistance (63). On area of stimulation, the skin subject was abraded and an electrolyte gel applied to improve contact with the electrode leads. This improved contact is available to pass the intensity of stimulation as specified intervals for the amplitude of stimulation current.

5.2.2 The technical consideration of signal conditioning part

5.2.2.1 Input impedance of preamplifier part

The instrumentation amplifier AD524 IC chip is used as the first part of signal conditioning by selecting to become a buffer amplifier and preamplifier (44). The input impedance (Zin) testing of system was measured to Zin of the input preamplifier to 22.46 MΩ. By the modern amplifiers for medical usage have input impedance in range from 2 to 10 MΩ [32, 43, 57]. Any AC line voltage has associated with it an electric field. This field effect may be coupled into circuit by stray capacitance. One plate of stray capacitance referred in figure 14 is consisted of the entire length of the hot wire and the other plate is formed by the length of the wire connected between the 1 kΩ resistors. Air is the dielectric medium. The common value of stray capacitance may typically be 0.01 pF at 50 Hz (31, 33, 35, 60).

5.2.2.2 CMRR of preamplifier part

Referring to Table 4.3 in Chapter 4, when the frequency is increased CMRR of the differential amplifier will be decreased because of a non-linear function common mode voltage (31, 32). The CMRR is maximum at dc and low frequency and decreased at high frequency. When the low pass filter and the notch filter are added to the system of conditioning, CMR will reduce owing to imperfect matching of buffer preamplifier and input resistance of the input low pass filter. From Table 4.1 and 4.2,

if gain of preamplifier is decreased CMR will decrease too. Hence we are not able to build high CMR with high gain. The CMR of 100 to 120 dB is commonly specified for signal measurement. From the result, the CMRR of preamplifier is 103.61 dB at 0.5 Hz. This value is some what typical to house-hold IC. When the low pass filter and the notch filter are added at the rear, CMRR is decreased to 102.02 at 50 Hz. This value is impaired by the imperfect of the rear circuits. This is also a serious disadvantage of the instrumentation amplifier (IA). The straight forward method of improvement the CMRR of preamplifier is to select another specific IA having high CMRR (110 dB for AD524 and 120 dB for INA 110). The imperfect matching resistance in the input low pass and notch filters can be improved if the accuracy of precise resistor is within 1% or better.

5.2.2.3 Amplifier gain of signal conditioning part

Referring to Table 4.4 in chapter 4, the amplifier gain of system have % error of signal amplifies to 1.20% at medial range of system. The reduction of amplifier gain is attenuated to signal amplification by using divided circuit. The result of % error tested incorporates to reduce CMRR of amplifier which effects from the filter unit. The imperfect matching resistance in the input filters can be improved if the accuracy of precise resistor is within 1% or better.

5.2.2.4 Frequency response of system amplifier

On the responses detection and monitoring of this constructed device, there are desirable to band limit this amplifier to the band of frequency contained in the reflex potentials for attenuating the higher and lower frequencies in order to maximize and minimize the signal-to-noise ratio. This is the amplitude ration of the energy in the wanted signal to the energy in the noise signal. The characteristics of the H-reflex signal of monitoring are well established that its amplitude is stochastic in nature and can be represented reasonably. The frequency response of this amplifier is constructed in the range of 0.5 Hz to 10 kHz, as follow the requirement of H-reflex monitor specification (31, 32). For the discussion of the electrical noise characteristics may be issued from various sources (64) such as:

- Inherent noise in the electronics components in the detection and monitoring equipment: All electronics equipment generates electrical noise. This noise cannot be eliminated; it can only be reduced by using high

quality electronic components, intelligent circuit design and construction techniques.

- Ambient noise: This noise originates from sources of electromagnetic radiation, such as electrical power wires, radio and television transmission, fluorescent lamps, etc. In fact, any electromagnetic device generates and may contribute noise. The surfaces of our bodies are constantly inundated with electric-magnetic radiation and it is virtually impossible to avoid exposure to it on the surface of the earth. The dominant concern for ambient noise arises from the 50 Hz-radiation from power sources by using notch filter of system designed. This notch filter with the circuit twin-T-notch filter 50 Hz are designed which its begin to deduct the noise in range of 48 to 52 Hz and fully deduct at the frequency cut-off at 50 Hz. Results and testing are shown in Table 4.6 and its graph is shown in appendix A.3.
- Motion artifacts: There are two major sources of motion artifact, one from the electrode/skin interfaces, and the other from movement of the cable connecting the electrode to the amplifier. Both can be essentially reduced by proper design of the electronic circuits.

5.2.2.4 Leakage current of constructed device

The chassis leakage current tested the constructed device as less than 10 μA that is acceptable and safe to use with patient according to standard IEC 601-1 BF (30, 65).

5.2.3 The technical consideration of data acquisition part

As follow testing the DAQ hardware and LabVIEW progrom previously, the abilities and efficiencies of acquiring, monitoring, and recording the input signal are well acceptable as specification needed. The DAQ hardware is so reliable because it is a standard device to assure the good criterion from National Instruments Company. So, the accuracy of DAQ part is depended on four contents those are the configuration of DAQ board, good preparation of signal conditioning circuitry, I/O connections, and sending appropriate instructions for processing in each function. Upon simulations for testing DAQ board referred to Fig. 4.9 in previous chapter, the DAQ board can well be appropriate for measuring. Nevertheless, the measurement error of DAQ board may be occurred. There are two causes for inaccuracies in the DAQ board, including gain and

offset. For best results of the solution, use a well-calibrated MIO board so that offsets can be ignored. Eliminate offset error by grounding one channel on the SCB-100 board and measuring the voltage. This value, the offset of the board, can then be subtracted by software from all other readings.

The instructions is written by LabVIEW are called virtual instruments (VIs). They are available for acquiring, displaying, analyzing, and recording the data. The VIs provides a generic data acquisition that permits partitioning of a segment of data on-the-fly without having to run and rerun the program numerous times. In technical consideration of acquiring data, The VI is written to obtain the data continuously with using a technique of circular buffering method and triggering method. The circular buffering method is appropriate for viewing, processing, or logging portions of data as it is being acquired similar to continuous data acquisition. Furthermore, the triggered acquisition provides two key advantages here. First, it time-references the input signal relative to the trigger event. Second, the user can capture the signal only in the region of interest and thus, conserve hardware memory (66). With timed acquisition, a hardware clock is used to control the acquisition rate for fast and accurate timing. The VI uses the Intermediate VIs to perform a buffered acquisition, where LabVIEW stores data in an intermediate memory buffer during acquisition. Data are retrieved from that buffer and displayed on the graph. For E-series DAQ boards, the trigger signal is connected to PFI/TRIG1 pins. From the result in Figure 4.10, the acquired signal is accuracy when it is compared with original signal that is simulated by software program.

Because of the signal is available in the digital form, it is simple to handle the signal for analyzing as desired. The functions of LabVIEW provide many capabilities in processing signal. The signal is obtained to analyze in many ways that is consisted of digital filtering for eliminating unwanted signal out of original signal, a segment technique for selecting the interval of interested signal, averaging signal for minimizing the data of signal, and peak detection technique for identifying the peak amplitude and location of measuring signal. A problem found to use the common filtering technique is a phase shift of signal. This problem is software solved by reversing polarity of the signal using the Reverse 1D Array function and passing it through the filter again. In averaging signal, it is programmed to acquire the data in

many times into While Loop function. Each times of iteration, data is stored and delivered by Shift register function. The present data and previous data are recalled for averaging signal. The segmental and peak detection of signal are achieved to increase the efficient and accuracy in measuring. Considering a notice in using peak detection technique is a configuration of width parameter control. This parameter can effectively reduce the noise in the input signal while finding the peaks. The minimum value is three; using this value results in no noise reduction. Using a width value larger than three implicitly smoothes the data.

5.2.4 The functional consideration of the constructed device.

In the functional testing of constructed device was used an external signal supplied by the function generator. The functional test of signal amplification with the function generator was shown in Table 4.11, as average percentage error of signal amplification by system is varied from 0.40 % to 0.70 % (AVG 0.55%). The results of this testing was read error by an average of 0.55 % that is acceptable as the purpose of design.

5.3 Discussion of the test and results of subjects

The H-reflex electromyograms for each test of subject were illustrated in Fig 4.15 – 4.30. The associated recruitment curves were plotted together in each figure too. The curves have been normalized with respect to the maximum M response for each data set. The results are in agreement with results obtained by other references in the field and verify the correct operation of the system. Considering the theoretical background with focus on the H-reflex of gastrocnemius-soleus muscle it expected three distinctive waveforms each showing a characteristic formation when applying an electrical current.

First, the stimulus artifact which is the potential recorded at the time that the stimulus is applied. It includes the electrical or shock artifact which is a potential due to the volume-conducted electrical stimulus. The artifact usually precedes the activity of interest. Regarding from Figure 4.15 to 4.30 there are either artifacts in H-reflex EMG of normal subjects and abnormal subjects. Mostly, the Figure 4.15-4.30 shows the steadily background activity of the gastrocnemius varying between 0.2 and -0.2 mV. There are regions with high activity, followed by regions with low activity and

vice versa. In addition to end-plate activity or random potentials, the base activity is also dependent on the posture and the movement performed with the specific muscles. Contraction of the gastrocnemicus leads to a slight increase in the base activity, relaxation of the joint causes a loss in activity.

Secondly, the results of each subject confirmed the emerging of the M-wave (Figure 4.15a, b to 4.30a, b) resulting from the direct stimulation of the muscle. The M-wave is a compound action potential evoked from the muscle by the electrical stimulus directly activating the motor axons. It evokes regularly with sporadic repeated stimuli at low rates.

Third, the H-reflex emerged mostly in normal subjects as shown in Figure 4.15-4.23 and issued rarely in abnormal subjects as shown in Figure 4.24-4.30. As predicted there is the reflexive response evoked by stimulation of the Ia-fibers in most subjects. The H-wave occurs with an average delay between 25-30 ms after the M-wave owing to its resulting signals that travel to the spinal cord, across a synapse, and back again to the muscle. The H-wave in this experiment occurs with a delay in each subject as shown in Table 4.13-4.29. The shape of the H-wave is quite reduced owing to some methodological and practical reasons.

For the consideration of results, there are many possible causes for the rare measuring of H-reflexes. The H-wave becomes weaker as the stimulus increases so that the M-wave becomes larger while the H-wave progressively declines. This inverse relation evolves through the propagating action potential in the motor axons towards the cell body (antidromical conduction). This way, reflexively evoked action potential is cancelled so that there is only the M-wave (besides the artifact). Other factors may have influenced the rare yield of H-waves: The amount of the electrode paste is difficult to specify and may have an influence on the conductance of the surface electrodes. Moreover it is difficult to find the right position on the leg both with stimulating electrodes and with the recording electrodes. There are also decisive differences regarding hairy parts and plain parts dependent on the surface of the skin of the lower leg. Finally some setup encountered difficulties with the acquisition of data. Comparing the effective stored and acquired data with the measured amount of data sets contained in the electromyogram, it states that some measurements that couldn’t be stored likely be H-reflexes. As we had overcome these problems, it was

already late and we were encountering a lack in time to repeat all measurements again. Generally, we suggest applying lower stimulus since the threshold for activation of the Ia-fibers is lower than the threshold for motor axons. Therefore, at low stimulus intensity a pure H-reflex can be evoked.

The shapes of the recruitment curves suggest a possible diagnostic process for understanding of nerve phenomena. Such curves are loci of peak response amplitudes versus stimulation intensity and vary in character as a function of muscle temperature, state of contraction, age, etc. Nevertheless, typical curves do exist for a control position, half-way through stance, and half-way through swing. For results in here, the recruitment curve is illustrated only in the control position, as shown in Figure 4.15c, d - 4.30c, d. As these results, they confirmed to relate between the amplitude of H- or M-wave and the stimulation level as theoretically. The result of decreased H-reflex amplitude in recruitment curve is a result of collisions between action potentials carried via the sensory fibers (orthodromically) and action potential traveling antidromically along the motor fibers.

5.4 Suggestion

In the study on the design and construction of this instrument, the difficult and time consuming steps are the design, construction, and improving circuit of each system as well as writing program. The system controlled of all test seems to function very well when perform testing with the stable signal simulation and controlled conditions but seems to be unsatisfied when the system are obtained from the volunteers who produce motion artifact and interference on require other. Therefore, developments in the future, the system design should be improved to recognize and reject these artifacts and other noises as much as possible to increase the reliability of the construction instrument.

CHAPTER VI
CONCLUSION

The prototype of the H-reflex detectable instrument and the recording program are presented. The H-reflex detectable instrument provides two main parts, including the electrical stimulator for evoking the H-reflex and the signal conditioning circuitry for preparing signal. The instrument is incorporated into a computer based on reflex data acquisition system. The LabVIEW program is written as a virtual instrument (VI) for sending and controlling the appropriate commands to control acquirement, display and record of the H-reflex.

A simple constant-current stimulator based on standard high voltage components was designed and constructed. It comprises a voltage-regulator that supplies an oscillator built across the primary of a step-up transformer, whose secondary powers, after rectification, the high voltage to a switched current-mirror in the driving stage. As such a voltage is proportional to the stimulus current, which stand-by consumption is basically limited to the ac/dc conversion that supplies the voltage-regulator. Adjusting the regulated voltage controls current intensity, whereas an optically coupled timing circuit sets the pulse-width. A prototype with readily available components generates currents of amplitude and pulse-width within intervals $0 \leq I_{skin} \leq 20$ mA and 0.1 ms $\leq T_{pulse} \leq$ 1.0 ms, respectively, for stimulation rates from 0.1 Hz to 1.0 Hz. Although the circuit was originally devised to muscular stimulation through surface electrodes and sized for a maximum electrode/skin resistance of 10 kΩ, the proposed topology can be applied to other ranges of stimulators. The use of a step-up transformer with an increased ratio of windings and components with higher voltage specifications would accommodate larger values of stimulus current and skin resistance. The small number of components and low consumption make the stimulator available for portable applications.

The data acquisition consisted of signal conditioning circuitry, accessories, and LabVIEW program was developed for the acquisition of H-reflex activity following

the delivery of a stimulation pulse at popliteal fossa. Recording electrodes, signal conditioning circuitry, and accessories are achieved to prepare the signal appropriately for the digital process. The data are first collected, then amplified and conditioned, and then passed on to a computer for digital conversion and ultimate used by LabVIEW program. The surface recording electrodes measure voltage output from a gastrocnemius-soleus muscle. As such, the small direct and reflex action potential are amplified and conditioned before converting to digital signal for a personal computer. For this case, the H-reflex is initially amplified by a preamplifier and again by a select of gain amplifier. The second-order Butterworth filter is designed and constructed to offer low-pass filtering option. This filter is also used as an anti-alias filter which prevents the aliasing components from being sampled. Then, LabVIEW is used as the software filtering again. The digital filtering using a butterworth filter without phase shift was built as a subvirtual instrument (subVI) to offer band-pass option. After the reflex is completely amplified and conditioned, hardware interface devices are used to acquire this reflex and pass it on to a computer for digital conversion by an A-to-D board. Then, the reflex has been digitized, and it is ready to be accessed by LabVIEW functions.

The H-reflex detectable instrument and the recording program were tested together and demonstrated to be capable of eliciting and measuring both direct motor nerve (M-wave) and H-reflex responses by electrical stimulation of the posterior tibial nerve at the popliteal fossa. The simple parameters including latency, amplitude, and H/M ratio of H-reflex can be used to demonstrate the differences of reflex activity between a sound side and the affected side of a subject with concerned conditions, and to investigate how difference waveform morphologies. In addition, patterns in opposite site in the same subject can be related to the underlying physiological variable. With the simpler detectable instrument, the H-reflex test will be used widely for clinical application in monosynaptic arc reflex studies. The total cost of prototype construction is approximately 25,600 baht, much lower than a commercial H-reflex device having the same capabilities. From the laboratory tested this instrument, technical testing and function testing, the reliability and durability of this instrument is rather satisfactory and acceptable. Hence, after improving the motion and noise

artifacts rejection, this instrument is expected to function effectively in the actual operating condition.

REFERENCES

1. Roger M. Enoka. Neuromechanical Basis of Kinesiology. Human Kinetics Books Champaign. Lllinois, 1988; 175-179.
2. Jun Kimura. Electrodiagnosis in Diseases of Nerve and Muscle: Principles and Practice. F.A. Davis Company, Philadephia, 1989; 118-122.
3. Bhagwan T. Shahani and DiDier Cros. Neurophysiologic Testing in Spasticity. The Practical Management of Spasticity in Children and Adults. M. B. Glenn and J. Whyte, Lea&Febiger, Philadelphia, 1990.
4. Shin J. Oh. Principles of Clinical Electromyography: Case Studies. Williams&Wilkins, 1987; 6-7, 23, 35-44.
5. Eric RK, James HS, and Thomas MJ. Principle of Neural Science. 4 th ed. Health Profession Division. McGraw-Hill. 1991;36 731-735.
6. Michael J. Aminoff. Electromyography in Clinical Practice: Clinical and Electrodiagnostic Aspects of Neuromuscular disease. 3rd ed. Churchill Livingstone, San Francisco, 1990.
7. Meier-Ewert K, Gleitsmann K, and Reiter F. Acoutic jaw reflex in man: Its relationship to other brain-stem and microreflexs. Electroencephalogr. Clin. Neurophysiology, 1974; 36:629-637.
8. Vejbaesya C. Electromyography. Faculty of Siriraj Medicine. Bangkok, 1987; 118-122.
9. Mark A. Segraves. Stimulation of the Tibial Nerve. Evanston, 2001.
10. Ward T. A model of Hoffmann Reflex. Proceeding of EMBS Inter. Conference, Chicago IL, July 23-28, 2000; 1905-1908.
11. Stephen J. Dorgan. Uncoupled Oscillator Model of The Hoffmann Reflex. Proceeding of Inter Conf. of IEEE Eng. In Medicine and Biology Society, Vol. 20, No 6, 1998; 3112-3115.
12. Jader De Lima and Andriano S. Corderio. A Low-cost Neurostimulator with Accurate Pulsed-Current Control. IEEE Trans. On Biomedical Eng., Vol. 49, No 5, May 2002; 497-500.

13. Jader De Lima and Andriano S. Corderio. A Simple Constant-Current Neural Stimulator with Accurate Pulsed-Amplitude Control. Proceeding of IEEE/EMBS Inter. Conf., Istanbul, Turkey, October 25-28, 2001.
14. Jun Kimura. Electrodiagnosis in Diseases of Nerve and Muscle. F.A. Davis Com., Philadephia, 1990.
15. Robinson AJ and Mackler LS. Clinical Electrophysiology: Electrotheraph and Electrophysiology testing. 2nd edition, Williams & wilkins. Maryland. 1995.
16. ADInstrument Ltd. Human Electromyography. Application Note an313a, February 1998; 1-4.
17. ADInstrument Ltd. Principles of Nerve Stimulation. Application Note alb17c, April 2002.
18. Sabbahi M.A. The Use of Topical Anesthesia in the Rehabilitation of Patients with Spasticity. Neurotruma and Related Issue, vol. 2, eds. M. E. Miner and K.A. Wanker, 1987; 65-79.
19. McDonough A.L. LabVIEW: Data Acquisition & Analysis for the movement sciences. Prentice-Hall, Inc., New Jersey, 2001.
20. Rajesh S. Vaidya. Tips and Techniques in DAQ Triggering. Application Note 129, National Instruments, Oct. 1998; 1-18.
21. Halar EM, Brozovich FV, et. all. H-reflex latency in uremic neuropathy: Correlation with NCV and clinical finding. Arch. Phys. Med. Rehabil., 1979; 60: 174-177.
22. Schmisheimer RJ, Bour LJ, and et. all. Flexor carpi radialis H-reflex in polyneuropathy: Relations to conduction velocities of the median nerve and the soleus H-reflex latency. J. Neurol. Neurosurg. Psychiatry, 1987; 50: 447-452.
23. Wager EW and Buerger AA. A linear relationship between H-reflex latency and sensory conduction velocity in diabetic neuropathy. Neurology, 1974; 24: 711-714.
24. Troni W. Analysis of conduction velocity in the H pathway. Part 1. Methodology and result in normal subjects. J. Neurol. Sci., 1981; 51: 223-233.
25. Troni W. Analysis of conduction velocity in the H pathway. Part 2. An electrophysiological study in diabetic polyneuropathy. J. Neurol. Sci., 1981; 51: 235-246.

26. Vecchierinl MF and Gulheneuc P. Electrophysiological study of the peripheral nervous system in chidren: Changes in proximal and distal conduction velocities from birth to age 5 years. J. Neurol. Neurosurg. Psychiatry, 1979; 42: 753-759.

27. Eccles JC. The inhibitory control of spinal reflex action. Electroencephalogr. Clin. Neurophysiology, 1967; (Suppl. 25):20-34

28. Deschuytere J and Rosselle N. Diagnostic use of monosynaptic reflexes in L5 and S1 root compression. In JE. Desmedt (ed): New Developments in Electromyography and Clinical Neurophysiology, Vol 3, Karger, Basel, 1973; 360-366.

29. Schmisheimer RJ, Kemp B, and et. all. Flexor carpi radialis H-reflex in lesion of the sixth and seventh cervical nerve roots. J. Neurol. Neurosurg. Psychiatry, 1985; 48:445-449.

30. AAMI standards and Recommended Practices, Biomedical Equipment 4th ed. USA: Arlington, Virg, 1993.

31. Bronzino JD. The Biomedical Engineering Handbook. USA: A CRC Handbook Published in Cooperation with IEEE Press, CRC Press, Inc., 1995; 788-789, 802-866, 1185-1195, 1357-1366.

32. Webster JG. Medical Instrumentation, Application and Design. 2nd ed. USA: Boston, Houghton Mifflin, 1992; 1: 1-55, 3: 112-149, 4: 150-187, 5: 227-263, 6: 288-342.

33. Diefenderfer JA and Holton BE. Principles of Electronic Instrumentation. 3rd ed. Sauders golden sumburst series, Saunders College Publishing by Harcount Brace&Company, 1994; 5: 92-99, 6: 101-117, 9: 183-213, 11: 235-259, 12: 261-297, 14: 357.

34. Fernandez M, Pallas-Areney R. Electrode Contact Noise in Surface Biopotential Measurements. USA: Proceedings of the Annual International Conference of the IEEE Engineering in Mecdicine an Biology Society, 1992; 2: 123-124.

35. Aston R. Principles of Biomedical Instrumentation and Measurement. USA: Pennsylvania State Univ., Wilkes-Barre, Merrill Publishing Company, 1990; 1: 3-11, 2: 49-56, 3:59-75, 4:89-97, 5: 135-165, 6: 177-217, 13: 395-417.

36. Supakitamonphane C. A study on the design and construction EMG and heart rate monitors for mental stress detection and management. Biomedical Instrumentation, Mahidol Univ., Thailand, 2000.
37. Rosenthal L. Inductively tuned astable multivibrator. IEEE Trans. Circuits Syst., vol. CAS-27, Oct. 1980; 963-964
38. Harada K and Zhao G. Controlled power interface between solar cells and AC source. IEEE Trans. Power Electronics, vol. 8, Oct. 1993; 654-662
39. Ramakant A. Op-amps and Linear integrated circuits. 2nd ed. Prentice Hall, Inc., Englewood Cliffs, New Jersey, 1988; 8: 296-306, 10: 387-397.
40. Prasert S. A study on the design and construction of the equipment for electromyography, nerve conduction velocity and somatosensory evoked potentials. Biomedical Instrumentation, Mahidol Univ., Thailand, 1994.
41. Johns D. and Martin K. Analog Integrated Circuit Design. John Wiley & Sons, 1997.
42. Dumrongghanvitaya S. A Study on the Design and Construction of Cardiac Monitor in ICU. [M.Sc. Thesis in Biomedical instrument], Bangkok: Faculty of Graduate Studies, Mahidol Univ., 1979.
43. Perenze SE. A Laboratory Approach Using the Microcomputer for Instrumentation Data Analysis and Control. Prentice Hall International Edition, 1993; 2:46-79, 4:80-95, 6:96-101, 3:102-125, 17:222-227, 18:232-241.
44. Burr-Brown. Integrated Circuits Data Book: Linear Products. Burr-Brown Corporation, Arizona, USA, 1994; 2-1 to 2-57.
45. Feinberg BN. Applied Clinical Engineering. New Jersey: Englewood-Cliffs, Prentice-Hall, 1986.
46. PMI Databook. Precision Analog Integrated Circuit. Precition Monolithic Inc., 1988.
47. Berlin HM. Design of Op-Amp Circuits, with Experiments. Indiana: Harward W. Sams&Co., Inc., 1980.
48. National Semiconductor Corporation, Linear Databook 3, USA: California, Santa Clara, 1988.
49. Brooks C. Microelectronics: Device and Applications. West Virginia, National Education Corporations, 1985.

50. Carr JJ. Electronic Devices Glencoe tech series. McGraw-Hill International Edition, USA: New York printed Singapore, 1993.
51. Taborikova H and Sax DS. Conditioning of H-reflexes by a preceding subthreshold H reflex stimulus, 1969; Brain 92:203-227.
52. Crago P, Chizeck H, Neuman M, and Hambrecht F. Sensors for use with function neuromuscular simulation. IEEE Trans. Biomed. Eng., vol. BME-33, Jan. 1986.
53. Basmajian JV. Biofeedback Principles and Practice for Clinicians", 3rd ed., Maryland USA: Williams & Wilkins Baltimore, 1989; 1: 1-4, 4: 38-48, 30: 323-341.
54. Cromwell, Lesile, et al. Biomedical Instrument and Measurements", 2nd ed., USA, New Jersey, Englewood-Cliffs, Prentice-Hall, 1980.
55. Apaiwongse T. A study on the Design and Construction of ICU Bedside Monitor. M.Sc. Thesis in Biomedical Instrumentation, Bangkok: Faculty of Graduate Studies, Mahidol University, 1990; 6:125-201.
56. Geddes LA. Electrodes and Measurement of Bioelectric events. USA: New York, London, Sydney, and Toronto Wiley Interscience: a Division of John Wiley & Son, 1972.
57. Bahill AT. Bioengineering: Biomedical, Medical and Clinical Engineering. USA: New Jersey, Englewood-Cliffs, Carnegie-Mellon Univ., Prentice-Hall, 1981; 2:46-75, 5: 255-294, 6: 295-299.
58. Webster JG, et al. Encyclopedia of medical devices and instrumentation. USA: Wiley & Sons, 1988; 20-130, 195-222, 232-245, 727-771, 1002-1061, 1111-1126.
59. EDN Asia. The Design Magazine of the Electronics Industry in Asia. Design Feature: A Cahners Asia Ltd., Publication, 1998; 48-55.
60. Pallas-Areny R and Webster JG. Composite Instrumentation Amplifier for Biopotential, J Ann biomed Eng, 1990; 18: 251-262.
61. NFPA 99 Standard for Health Care Facilities, Dallas, TX: NFPA, 1993.
62. Gravenstein JS and Paulus DV. Clinical Monitoring Practices. 2rd ed., USA: Philadelphia, J.B. Lippincott Company, 1987; 23-40, 216-221, 415-431.

63. Christopher JP and Clayton L Van Doren. A high voltage, constant current stimulator for electrocutaneous stimulation through small electrodes. IEEE Trans. on Biomed Eng.,vol 46, No. 8, Aug. 1999; 929-934.

64. De Luca CJ. Surface Electromyography Detection and Recording. USA: Neuromuscular Research Center, Boston University, 1996.

65. Gravenstien JS and Paulus DV. Clinical Monitoring Practice. 2rd ed., USA: Philadelphia, J.B. Lippincott Company, 1987; 23-40, 216-221, 415-431.

66. Vaidya RS. Tips and Techniques in DAQ Triggering. Application Note 129, National Instruments, Oct., 1998; 1-18.

67. Daniel D, Electrodiagnostic Medicine, Hanling & Belfas, Philadelphia, 1995.

APPENDIX A

Appendix A1: Graph of low pass filters testing**.**

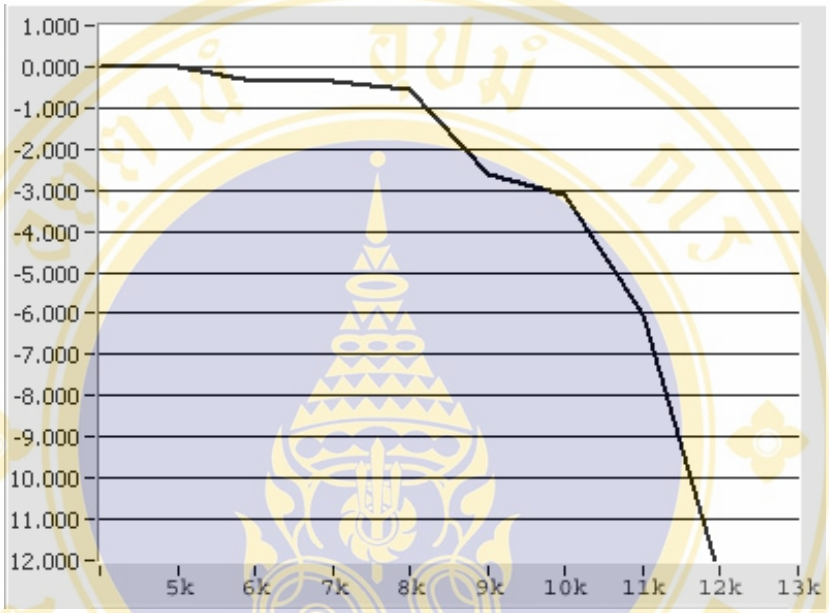

Appendix A2: Graph of notch filters testing.

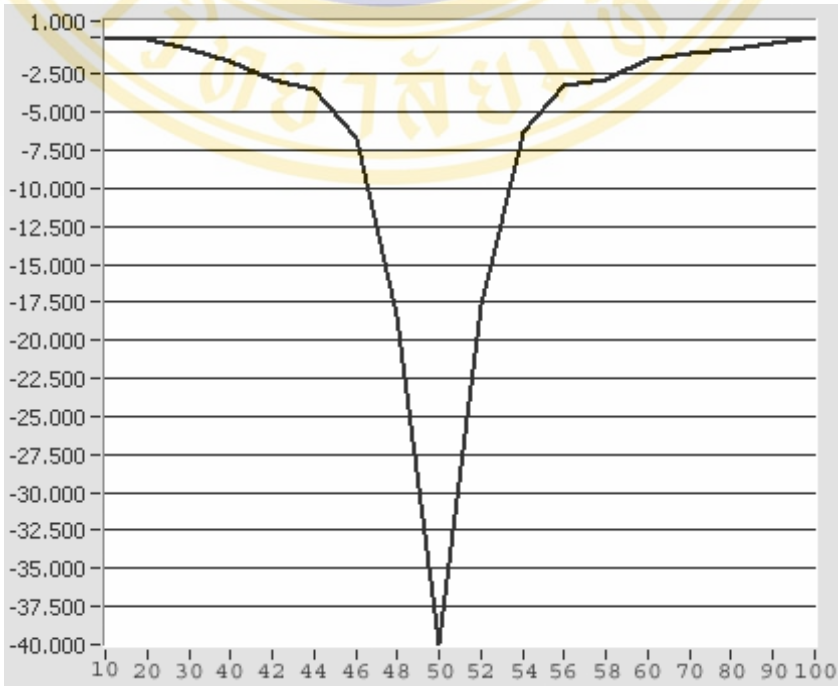

BIOGRAPHY

NAME	MR. Jiratn Tang-a-phan
DATE OF BIRTH	20 December 1977.
PLACE OF BIRTH	Suphanburi, Thailand
INSTITUTIONS ATTENDED	Srinakharinvirot University, 1996-2000 Bachelor of Engineering (Electrical Engineering) Mahidol University, 2001-2004 Master of Engineering (Biomedical Engineering)
POSITION & OFFICE	-
HOME ADDRESS	1338/3 Moo 6 T. U-Thong. A. U-Thong Suphanburi 72160 Tel. 035-551698, 01-8588654 E-mail : jitoday@gmail.com